Wojciech.Dulinski@ires.in2p3.fr

Détecteurs à semi-conducteurs

et leurs applications dans :

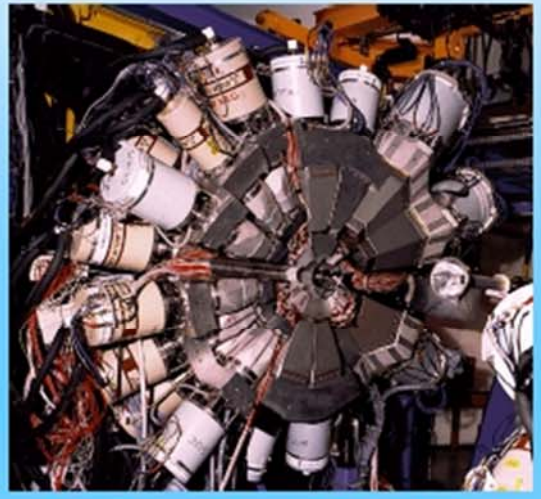

La Physique Nucléaire

L 'Astrophysique

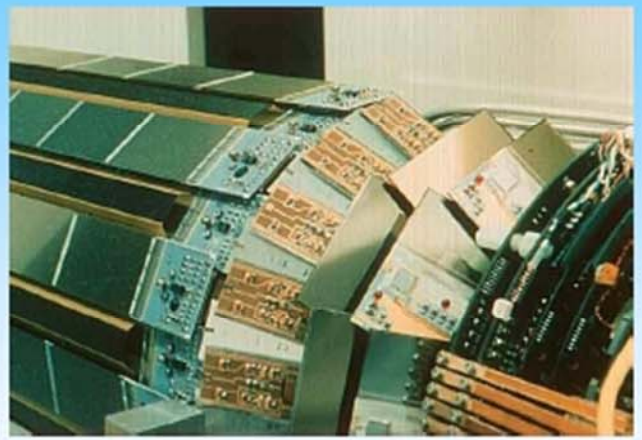

La Physique des Particules

L 'Imagerie médicale

Wojciech.Dulinski@ires.in2p3.fr

Détecteurs à semi-conducteurs

Sommaire

- Bibliographie
- Motivations expérimentales
- Détecteur à semi-conducteur générique
- Physique des semi-conducteurs
- Détecteurs à germanium
- Détecteurs à micropistes et pixels
- Effets de radiation: silicium-3D, diamant
- Électronique de lecture (notion)
- Autre types de détecteurs (SDD, CCD, DEPFET, a-Si)
- Développement: Ge segmenté, capteurs CMOS (MAPS), SiPM (SPAD)

Wojciech.Dulinski@ires.in2p3.fr

Références

1. A.S. Grove, *Physics and Technology of Semiconductor Devices, John Wiley* (1967)

2. S.M. Sze, *Physics of Semiconductor Devices, John Wiley* (1981)

3. S.M. Sze, *Semiconductor Devices, physics and technology, John Wiley* (1985)

4. S.M. Sze (editor), *Semiconductor Sensors, John Wiley* (1994)

5. W.R. Leo, *Techniques for Nuclear and Particle Physics Experiments, John Wiley* (1994)

6. G.F. Knoll, *Radiation Detection and Measurements, John Wiley* (1989)

7. G. Lutz, *Semiconductor Radiation Detectors (Device Physics), Springer-Verlag* (1999)

8. H. Spieler, *Semiconductor Detector Systems, Oxford University Press* (2005)

9. T.E. Schlesinger, R.B.James (editors), *Semiconductors for Room Temperature Nuclear Detector Applications, Academic Press* (1995)

10. A.J.P. Theuwissen, *Solid-State Imaging with Charge-Coupled Devices, Kluwer Academic Publishers* (1995)

11. C.J.S. Damerell, *Vertex Detectors: The State of the Art and Future Prospects, RAL-P-95-008* (1995)

Remerciement

Je remercie tous mes collègues et collaborateurs qui m 'ont inspiré pendant la préparation de ce cours. Vous trouvez ci-après leurs nom et adresse électronique (la liste certainement non exhaustive) pouvant être, aussi pour vous, une source inestimable d 'informations:

Pierre Delpierre (delpierre@cppm.in2p3.fr), Grzegorz Deptuch (deptuch@fnal.gov), Pierre Jarron (Pierre.Jarron@cern.ch), Harris Kagan (Harris.Kagan@cern.ch), Patrice Medina (patrice.medina@IReS.in2p3.fr), Michael Moll (Michael.Moll@cern.ch), Malgorzata Sowinska (m.sowinska@eurorad.com), Renato Turchetta (R.Turchetta@rl.ac.uk), Peter Weilhammer (Peter.Weilhammer@cern.ch)

Wojciech.Dulinski@ires.in2p3.fr

Physics motivation in nuclear physics experiments: γ spectroscopy

The great superiority of a germanium detectors in energy resolution, in connection with reasonably good efficiency, allows the separation of many closely spaced gamma-ray energies. Consequently, virtually all gamma-ray spectroscopy that involves complex energy spectra is now carried out with germanium systems.

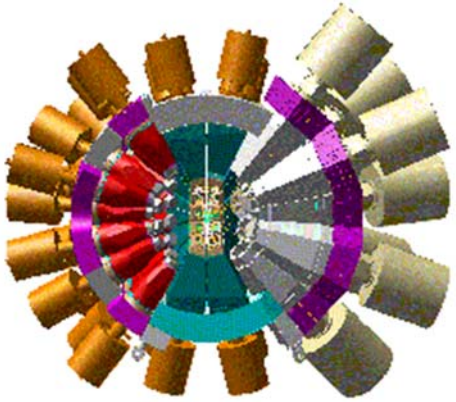

Example of modern experience in nuclear physics: EUROBALL

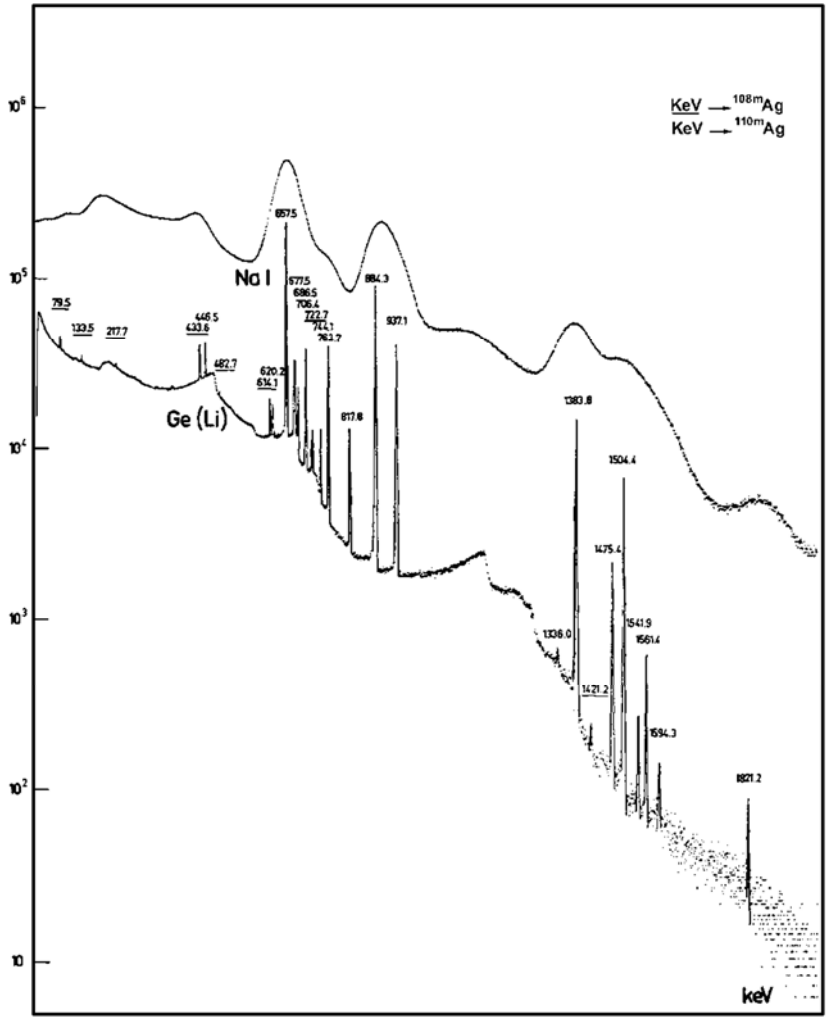

Comparative pulse height spectra recorded using a sodium iodide scintillator and a Ge(Li) detector (gamma radiation from ^{108}Ag and ^{110}Ag).

Wojciech.Dulinski@ires.in2p3.fr

Physics motivation in particle physics experiments: tracking

Vertex reconstruction is used for the following:

- lifetime
- quark mixing
- B-tagging
- top physics
- background suppression

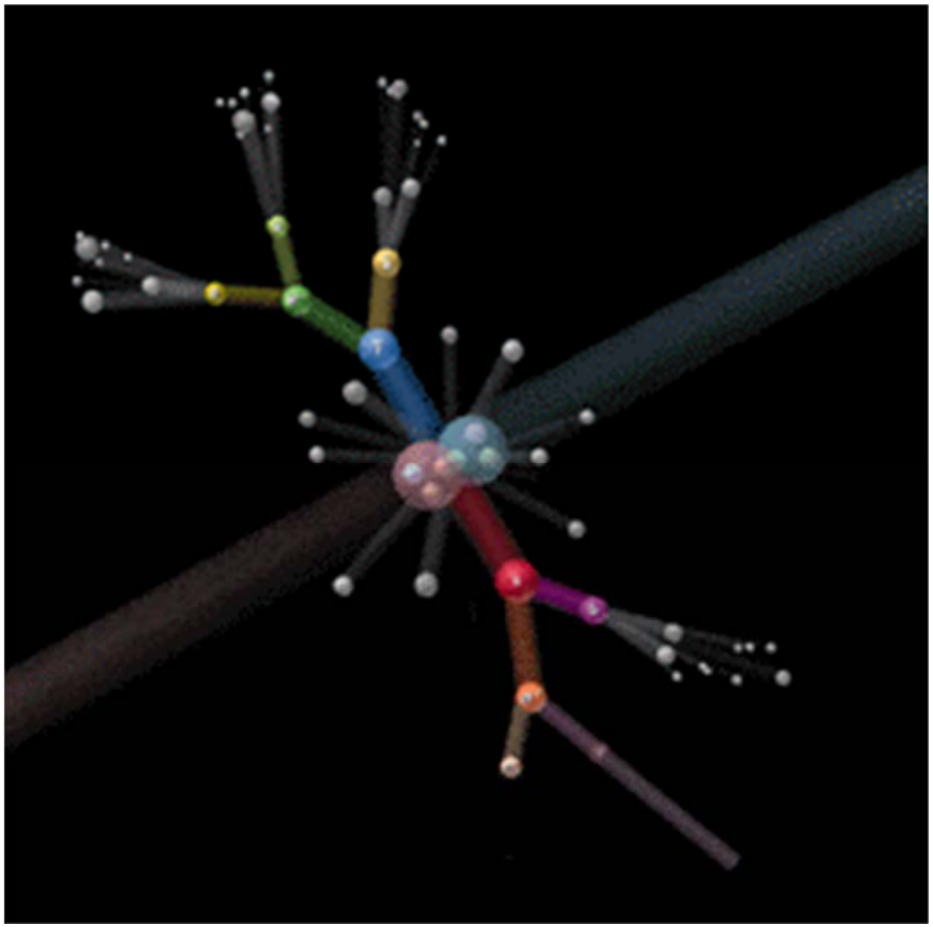

For this application, the spatial resolution is THE factor of merit!

Typical Tracking Detector Characteristics

Detector Type	Spatial Resolution
Drift Chambers	~100 μm
MSGC	~30 μm
Silicon Detectors	2-15 μm
Nuclear Emulsion	1 μm

Wojciech.Dulinski@ires.in2p3.fr

Vertex detector based on silicon detectors

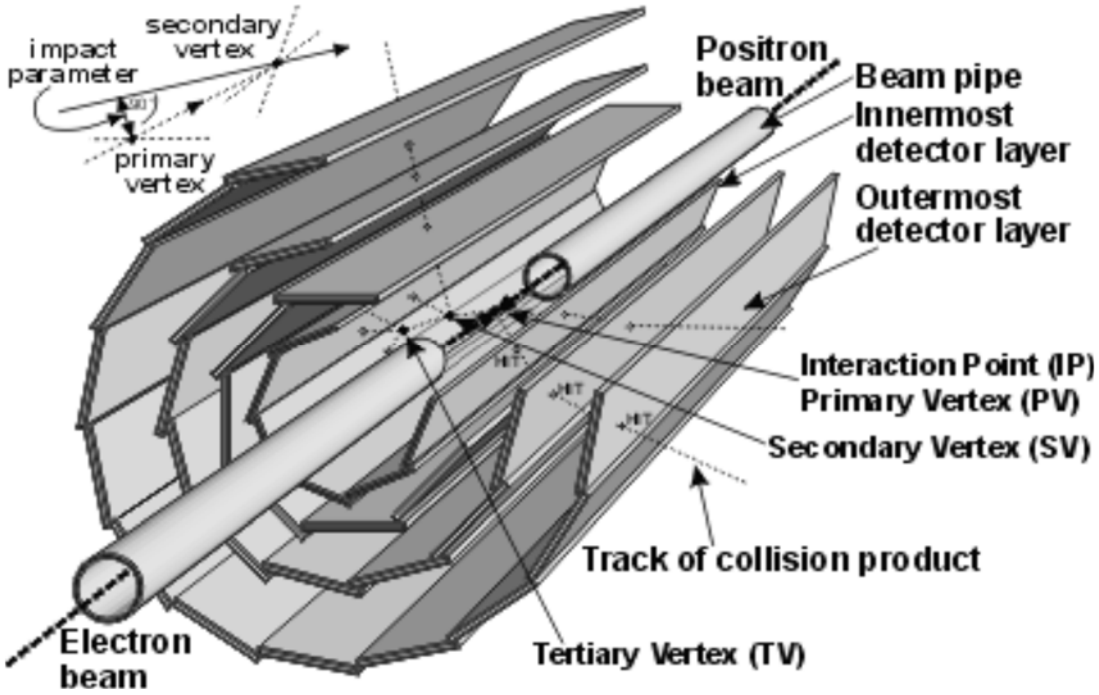

Was it there already??

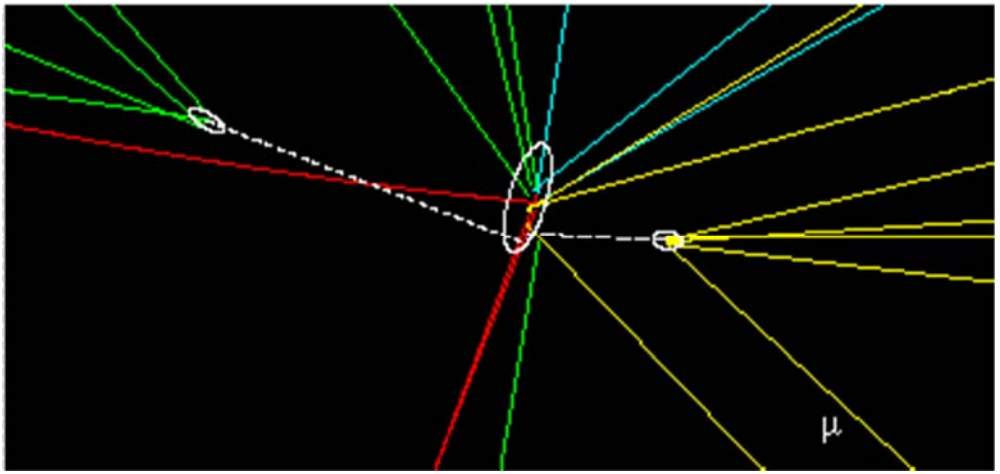

Event display shows a b candidate reconstructed in the ALEPH vertex detector.

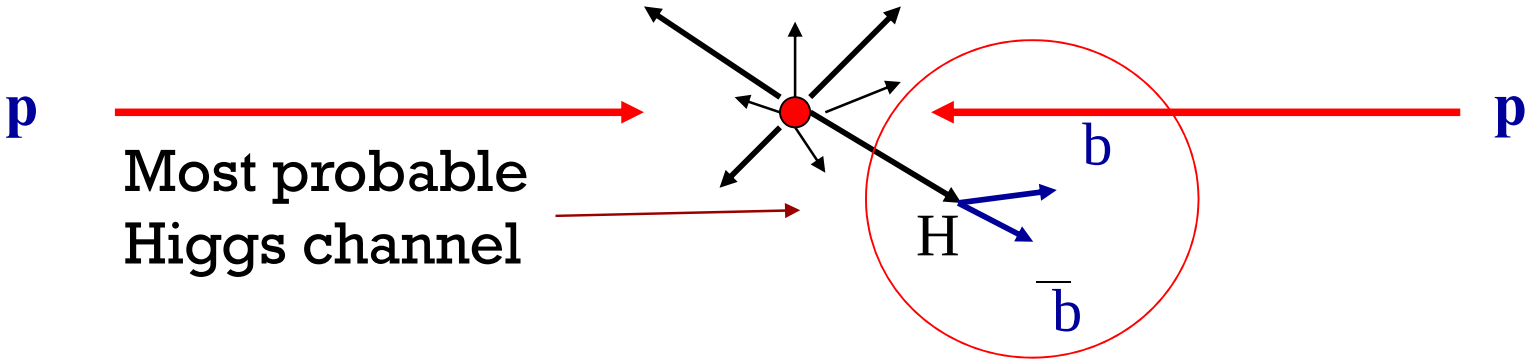

Wojciech.Dulinski@ires.in2p3.fr

Impact Parameter Resolution

Without Multiple Scattering

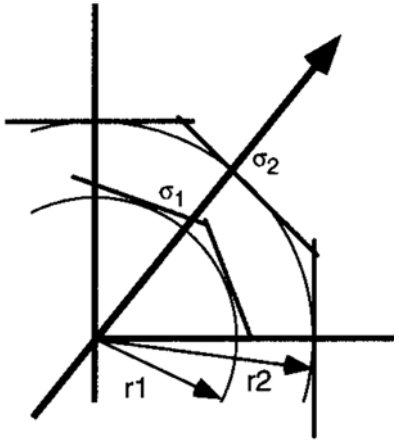

$$\sigma_I^{\,2} = \sigma_1^{\,2} + \frac{r_1^2}{(r_2^2 - r_1^2)}\sigma_2^{\,2}$$

So we want:

-small r_1, large r_2

-small σ_1, σ_2

With Multiple Scattering

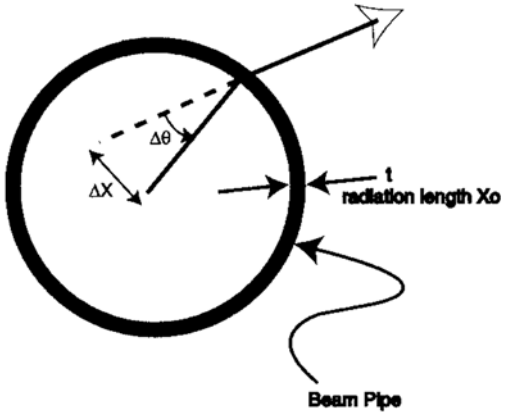

$$\Delta\theta \propto \frac{15}{P\beta}\sqrt{\frac{t}{X_0}}$$

$$\Delta X \propto \frac{r}{P\beta}\sqrt{\frac{t}{X_0}} \approx \frac{r}{P\beta}\sqrt{tZ^2\rho}$$

Background suppression

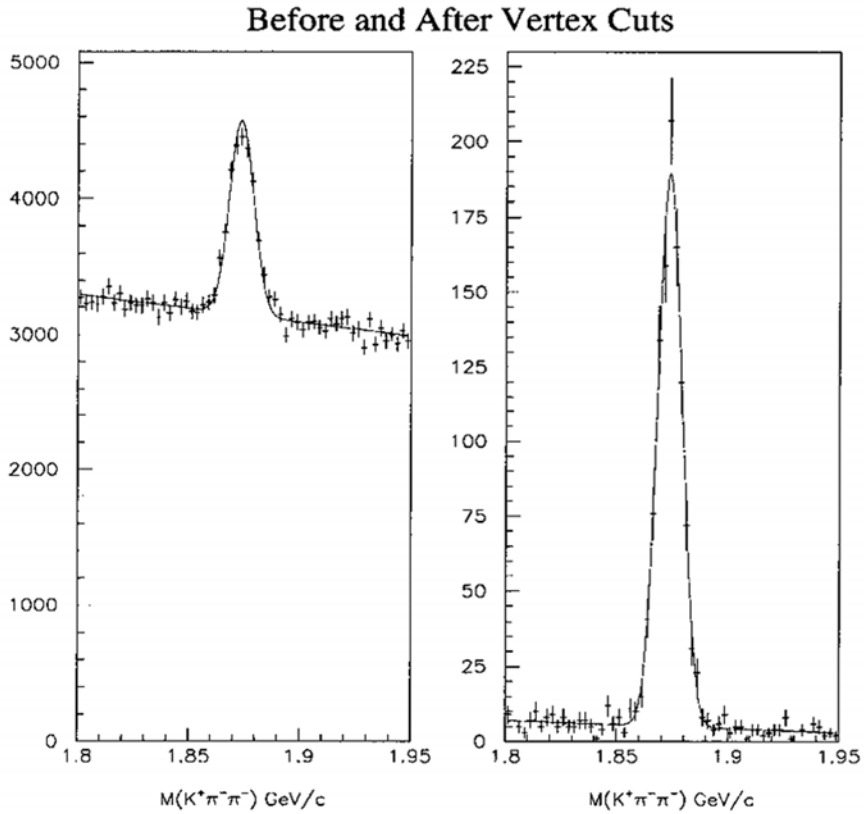

7σ vertex cut from beam spot.

Wojciech.Dulinski@ires.in2p3.fr

Extreme complexity of future HE Physics events

Requirements:

- high granularity

- reliability

Silicon detectors are the only choice!

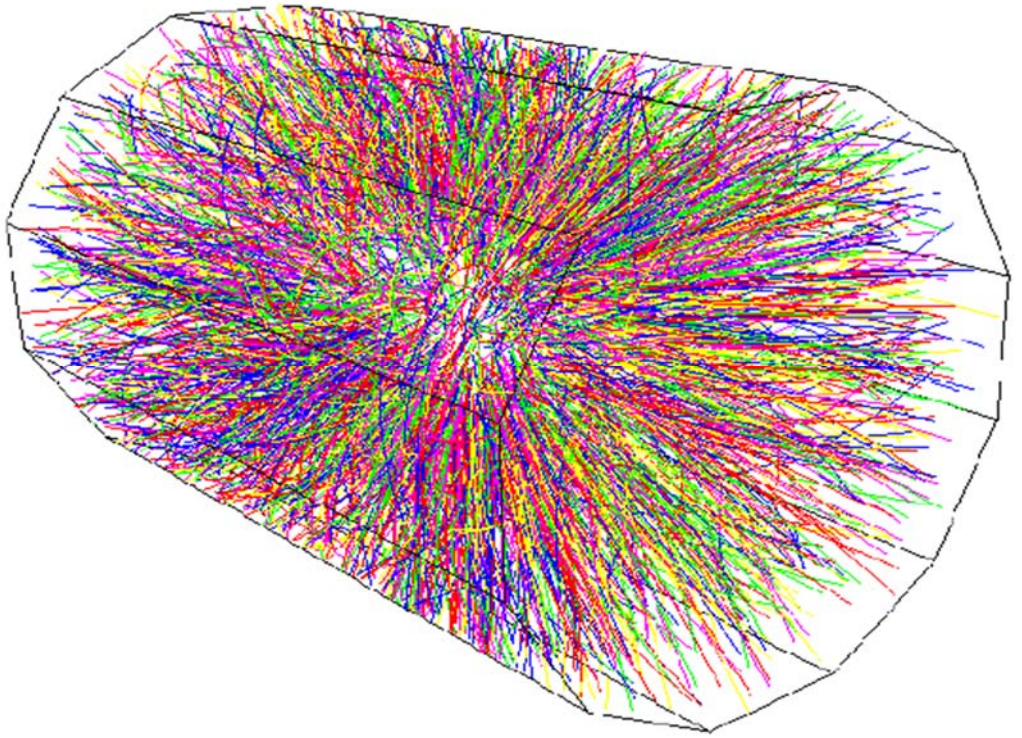

Geant-simulated Au - Au event (STAR)

Wojciech.Dulinski@ires.in2p3.fr

Physics motivation in astrophysics: space experiments

In space experiments, reliability and large system integration plays an essential role. Excellent performance (energy and spatial resolution, quantum efficiency) of new generation of silicon detectors allows exploration of new observation windows in astronomy and astrophysics.

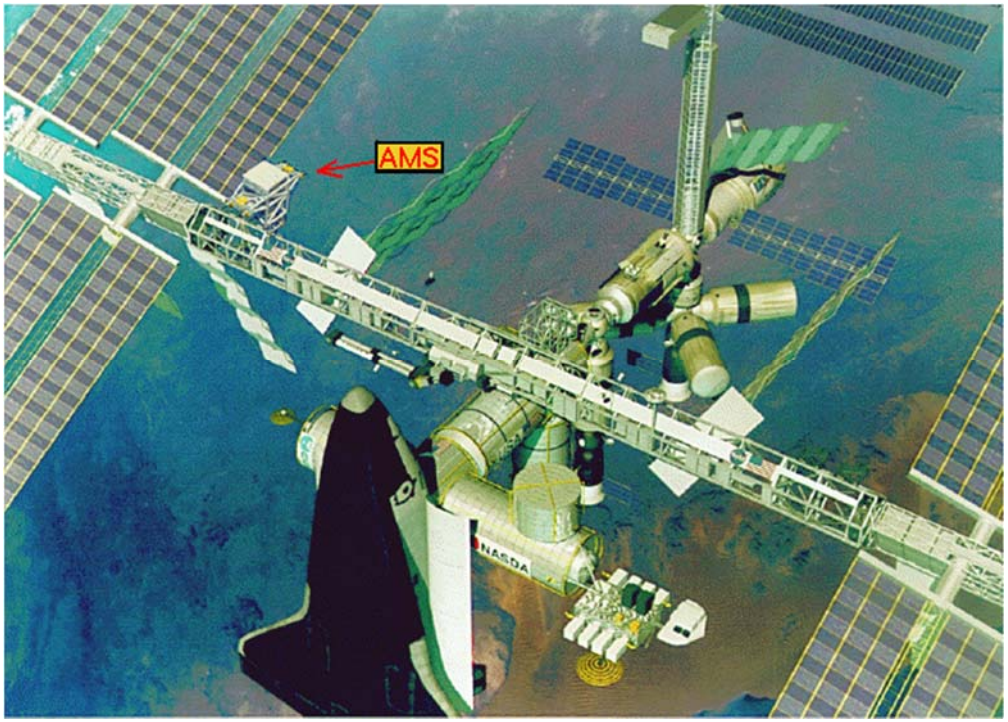

International Space Station hosting AMS experiment

HESSI – High Energy Solar Spectroscopic Imager

Wojciech.Dulinski@ires.in2p3.fr

Physics motivation in medicine: high quality&safe imaging, portable instruments

The x-ray camera images a projection of the body's density distribution and the pixel size is in the sub millimeter range.

Semiconductor x-ray imaging detectors step up the image quality and its content of information, or equivalently, they reduce the required radiation dose per image. The detectors can absorb and utilize most of the radiation without significant reduction of resolution.

The gamma camera images radioactive isotope distribution within the body. The effective pixel size is above 3 mm. The allowed radiation level and photon statistics determine the spatial resolution of the image.

Application of semiconductor detectors to gamma imaging enables design of portable systems. The detectors may somewhat improve the resolution and reduce blurring of scattered radiation. However, they need to be cost competitive with scintillator detectors in order to be widely used in gamma cameras.

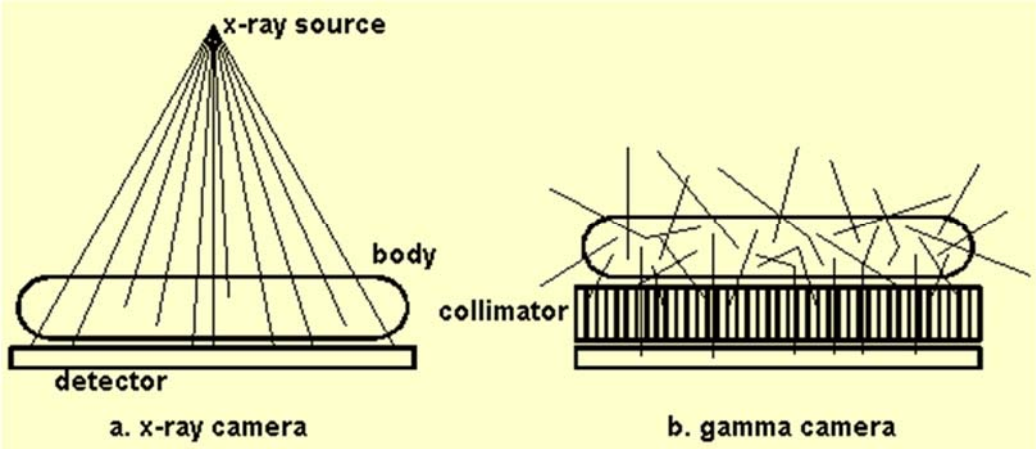

Wojciech.Dulinski@ires.in2p3.fr

The Generic Semiconductor Radiation Detector

In general, the following steps must take place in the process of Ionising Radiation detection :

- **Radiation Interaction with the detector active medium : transfer of a part of initial radiation energy to the detector (OR total absorption with total energy transfer).**
- **Charge Carriers Creation inside detector : effective use of absorbed energy.**
- **Efficient Charge Carriers Transport across detector volume using internal electric field : useful signal (electric current pulse) generation.**
- **Amplification and processing of a primary signal with the help of an (external) electronic circuits : interface with data acquisition/storage system.**

In consequence, good ionising radiation detector should optimise all above steps...

Wojciech.Dulinski@ires.in2p3.fr

Radiation

Non-ionizing

Ionizing

Directly

- energetic charged particles: electrons (betas), protons, alphas…

Indirectly

- neutrons

- photons : X and gamma rays, visible light…

Out of above list, photons (electromagnetic radiation) are of special interest for medical imaging applications.

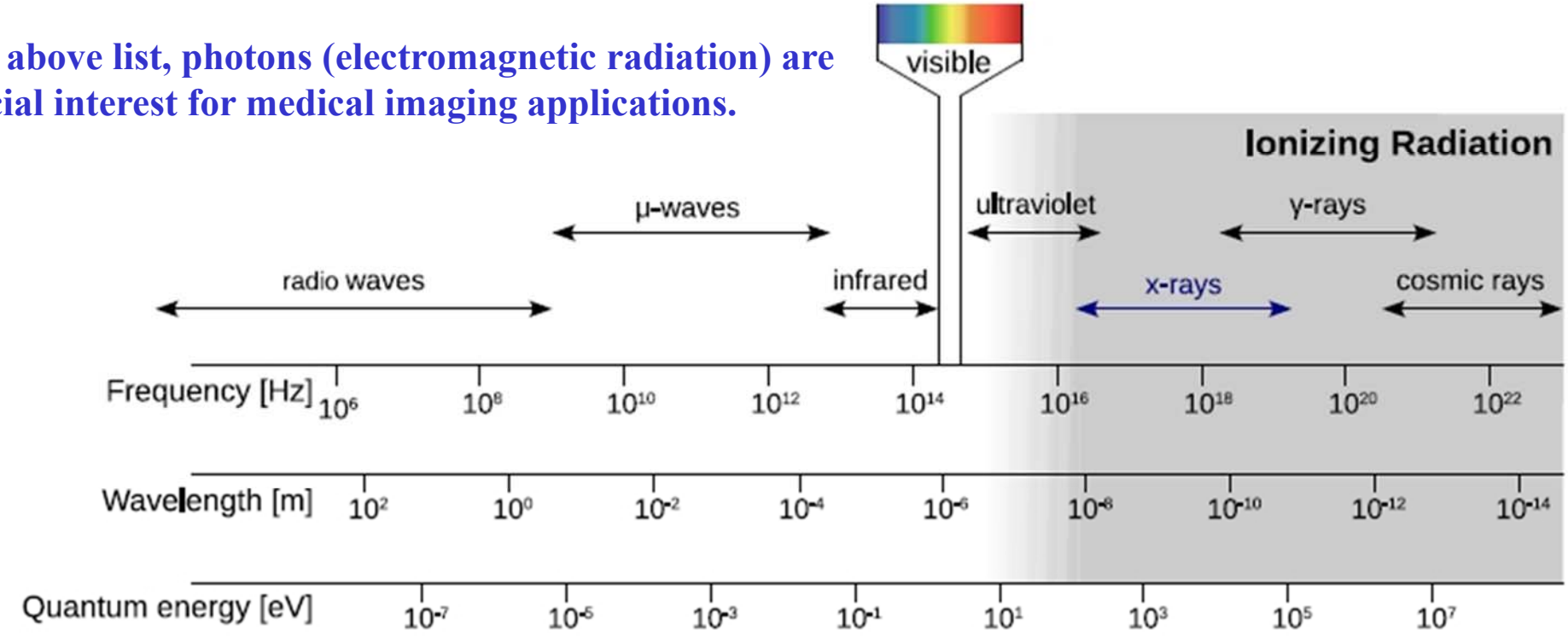

Electromagnetic Radiation Spectrum

Wojciech.Dulinski@ires.in2p3.fr

Radiation Interaction

Charged particles : inelastic collisions with the atomic electrons of the material : the Bethe-Bloch Formula. The stopping power $dE/dx \sim z^2\rho(Z/A)/\beta^2$ where z is a particle charge; ρ, Z, A are a density, atomic number and atomic weigh of absorbing material, β=v/c is the particle velocity

Neutrons : nuclear reaction with the production of charged secondary particles

Photons : Photoelectric Effect, Compton Scattering, Pair Production

In the case of photons, the most 'wanted' is a Photoelectric Effect, because in this case totality of incoming energy is transferred to detector medium in a relatively small volume (~10 μm diameter)

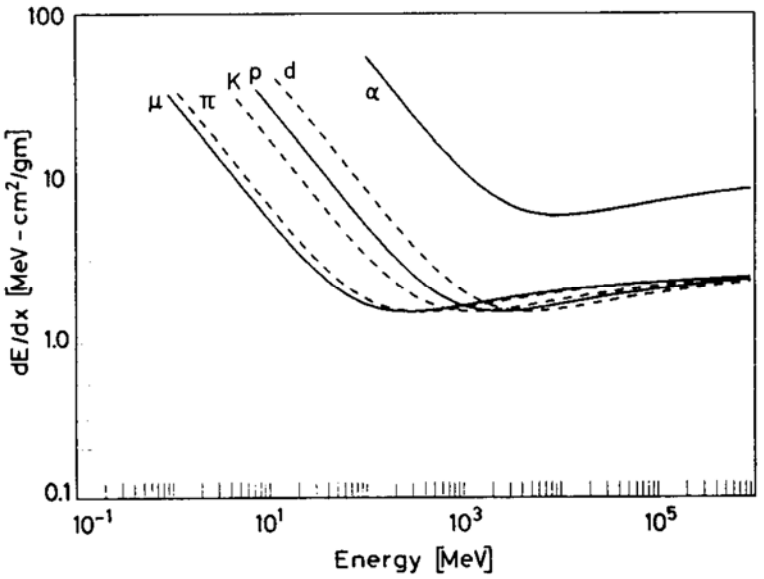

The stopping power dE/dx as function of energy for different particles

Wojciech.Dulinski@ires.in2p3.fr

The Interaction of Photons

The probability of gamma or x-ray photon interaction with a detector material of atomic number Z is proportional to Z^n ($4<n<5$) for photoelectric interaction, Z for Compton scattering and Z^2 for pair production.

$$I(x) = I_0 e^{-\mu x}$$

Where :

I : photon flux

x : absorber thickness

μ : linear attenuation coefficient

$l = 1/\mu$: absorption length

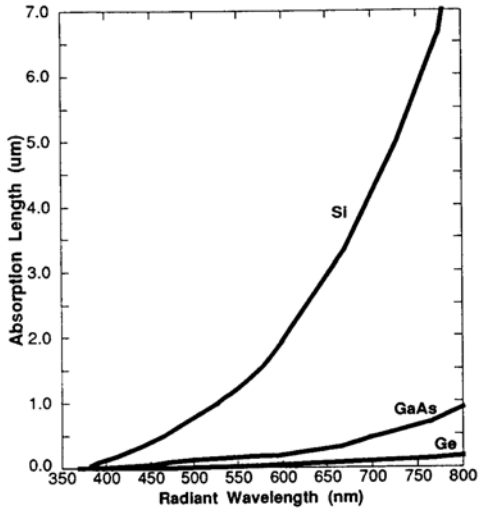

Absorption length in Si, GaAs and Ge for visible light range.

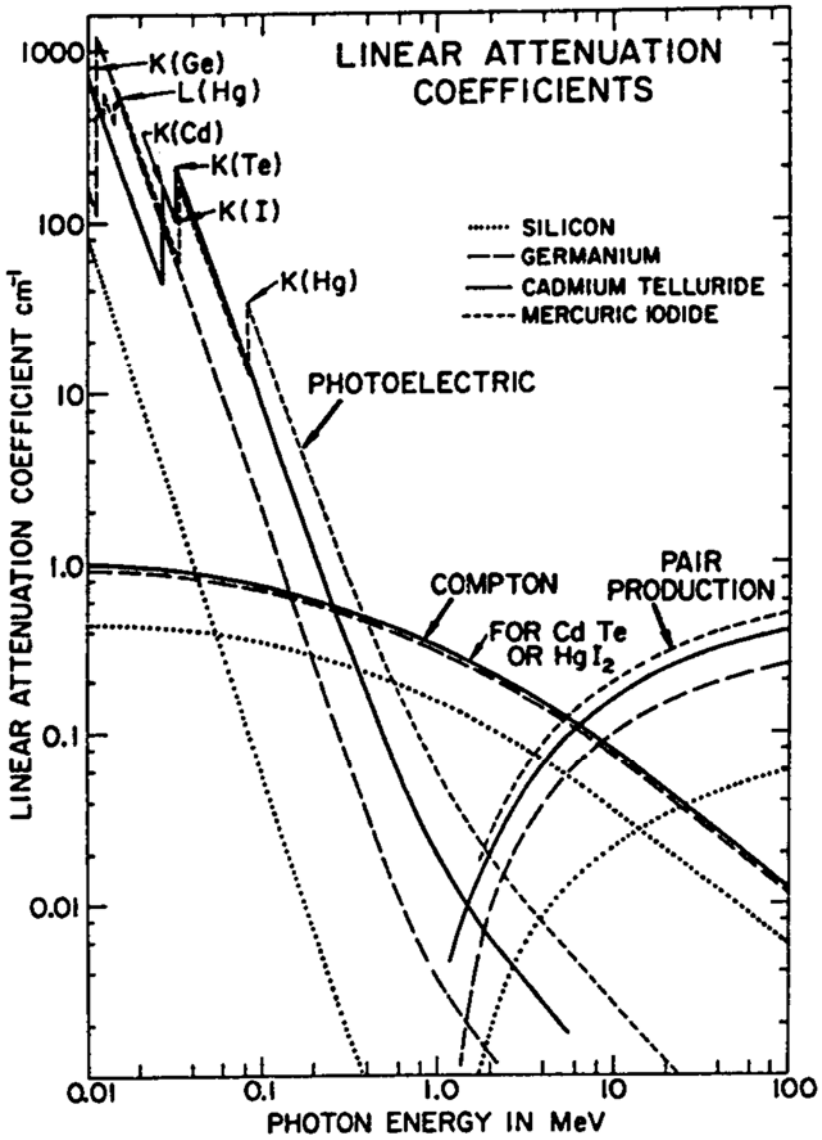

Linear attenuation coefficient in silicon, germanium, cadmium telluride and mercuric iodide

Wojciech.Dulinski@ires.in2p3.fr

The Interaction of (slow) Neutrons

Neutrons are detected through nuclear reactions which result in energetic particles as protons, alpha particles, recoil nucleus, fission fragments. The most popular reaction for the conversion of slow neutrons into directly detectable particle is the $^{10}B(n,\alpha)$ reaction:

$$B + n \dashrightarrow Li + \alpha + 2.792\ MeV$$

$$B + n \dashrightarrow Li^* + \alpha + 2.310\ MeV\ (E_{Li}=0.84\ MeV,\ E_{\alpha}=1.47\ MeV)$$

Another method is to use neutron capture reaction (by gadolinium, vanadium, rhodium...), leading to a beta-active isotope.

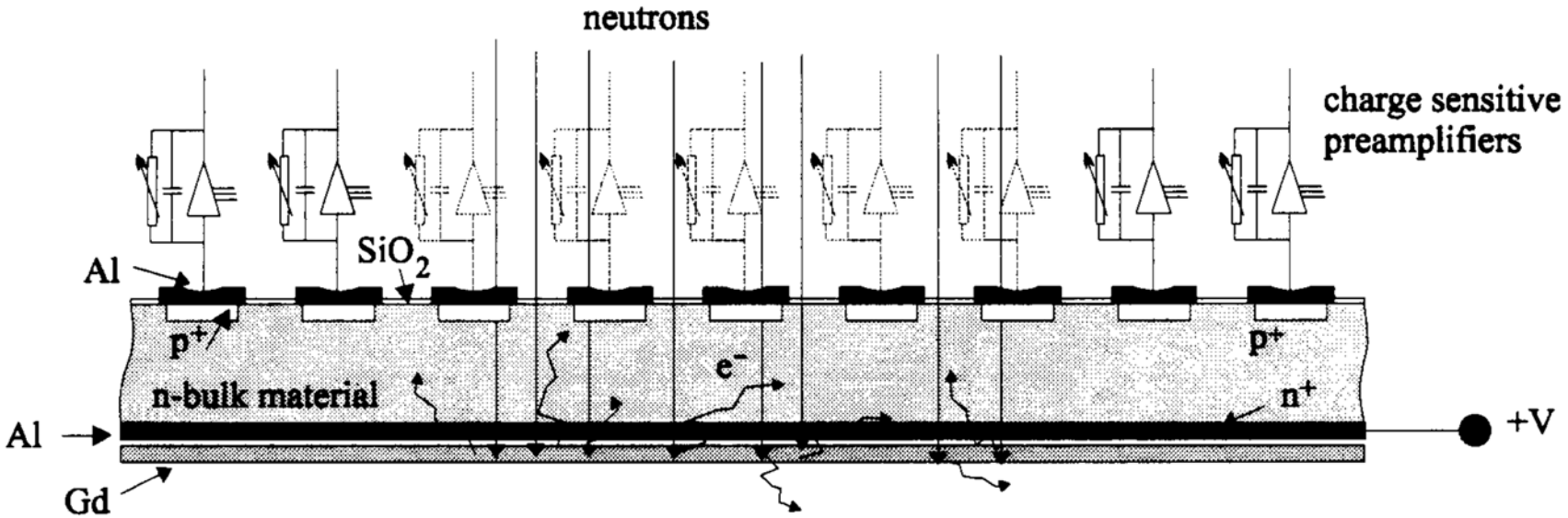

Wojciech.Dulinski@ires.in2p3.fr

Charge Carriers Creation

The number of charge carriers created inside detector active volume after absorption of energy E depends on the material parameter w, which is an average energy needed for creation of one pair of charge carriers.

$$N = E/w$$

The intrinsic energy resolution:

$$R = 2.35\frac{\Delta N}{N} = 2.35\sqrt{\frac{Fw}{E}}$$

where F is the Fano Factor (on the order of 0.12 in silicon)

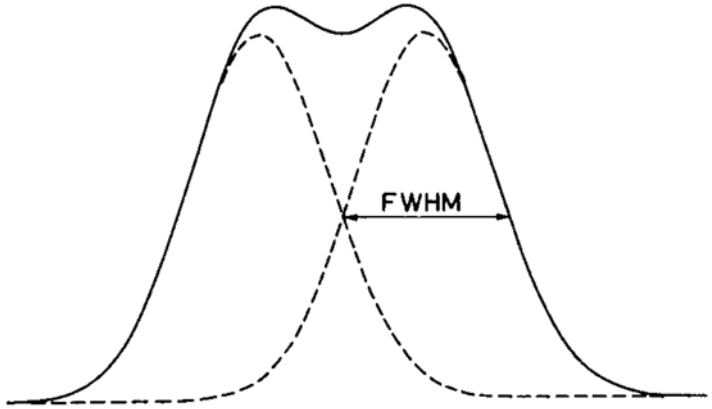

Definition of energy resolution

Wojciech.Dulinski@ires.in2p3.fr

Charge Carriers Transport

Free charge carriers in semiconductor are mobile. Drift is movement of carriers due to an electric field :

$$\vec{V_d} = \vec{E}\mu$$

where μ is mobility. Mobility depends on temperature, impurity concentration and (for higher E values) on E.

Diffusion is random thermal motion : the RMS radius of charge distribution increases as the square root of a drift time :

$$\sigma = \sqrt{2Dt}$$

where $D = kT\mu/q_e$.

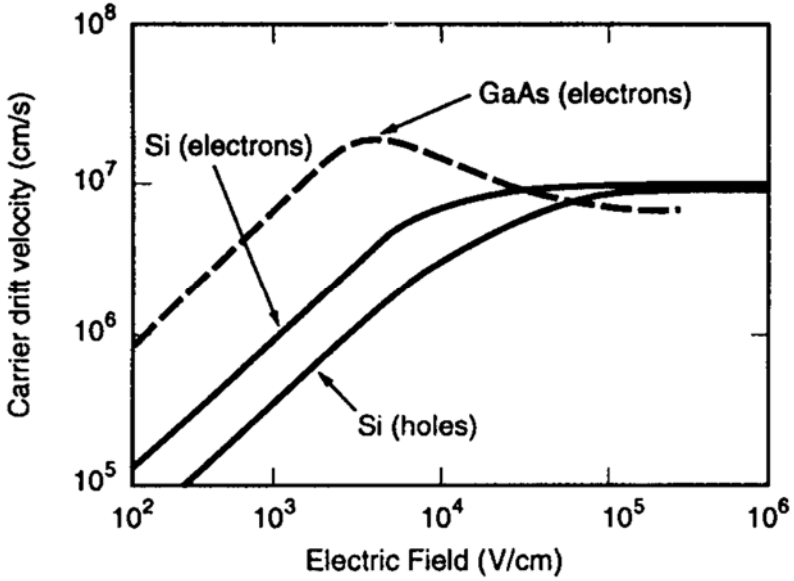

Carrier drift velocity as a function of electric field

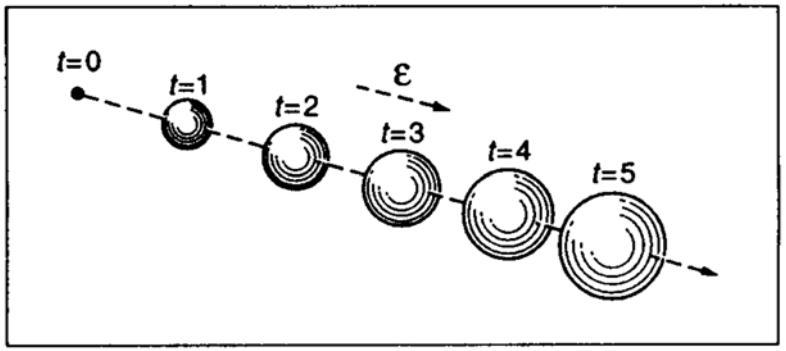

Combined drift and diffusion of initially compact charge cluster

Wojciech.Dulinski@ires.in2p3.fr

The Generic Semiconductor Radiation Detector

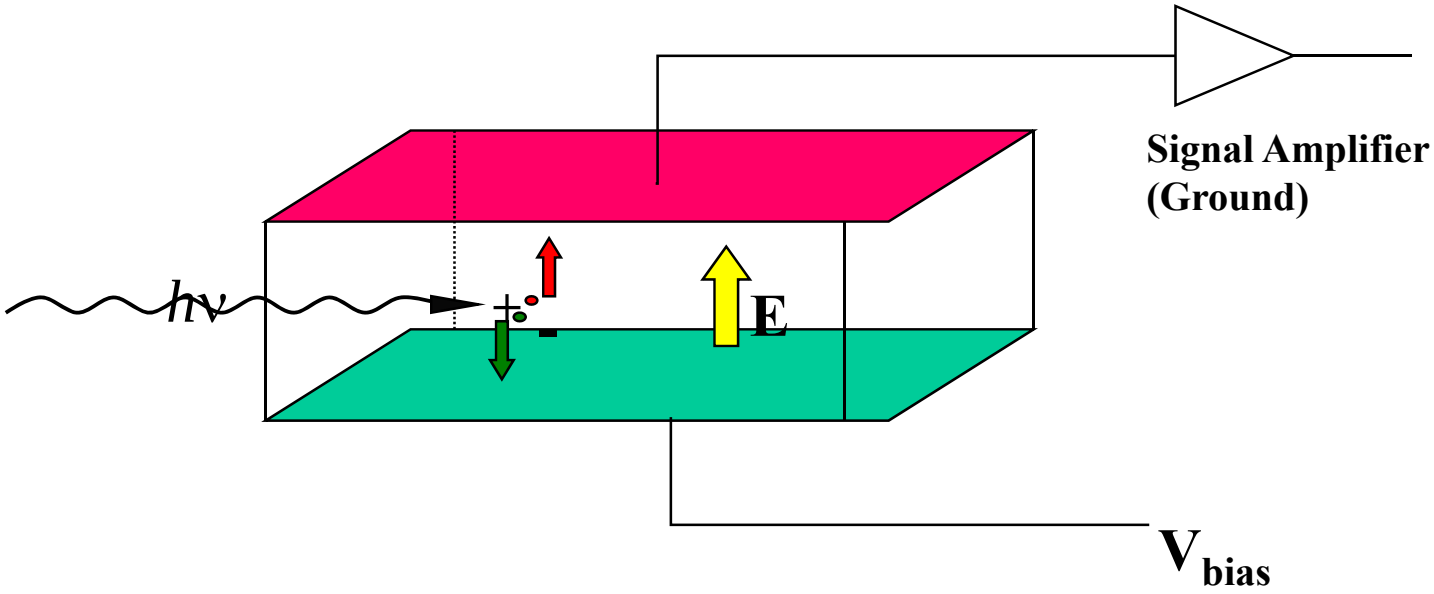

Shape of a Radiation-Generated Cloud

- Visible and UV light: single e-h pair
- X-Rays: "point" interaction, $N_{e-h} = E_X/3.6$ eV
- α particle: short, dense track (Bragg curve)
- β radiation: low density (close to MIP), scattered path
- High-energy particles: uniform low density track (MIP)
- Non-relativistic charged particle: $dE/dX \sim z^2/E$

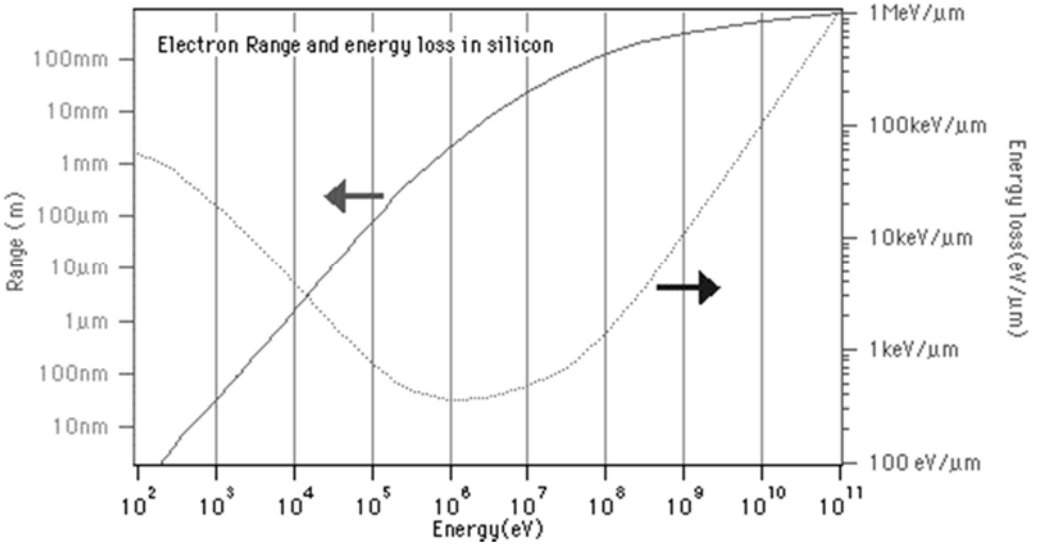

Wojciech.Dulinski@ires.in2p3.fr

Derivation of a pulse shape from an ion chamber (1)

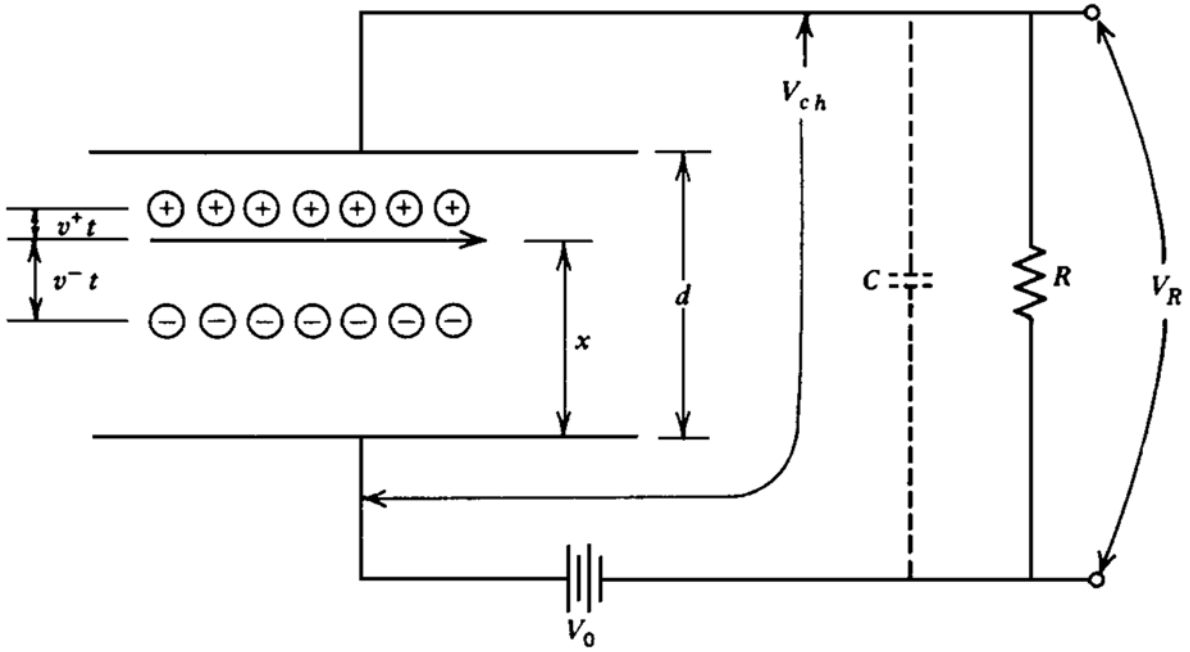

Original stored energy	=	Energy absorbed by ions	+	Energy absorbed by electrons	+	Remaining stored energy

$$(1/2)\,CV_0^2 = n_0eEv^+t + n_0eEv^-t + (1/2)\,CV_{ch}^2 \quad (E \text{ is an electric field})$$

$$(1/2)\,C(V_0^2 - V_{ch}^2) = n_0eE(v^+ + v^-)t$$

$$(1/2)\,C(V_0 + V_{ch})(V_0 - V_{ch}) = n_0e(V_{ch}/d)(v^+ + v^-)t$$

Approximations: $(V_0 - V_{ch}) = V_R$, $(V_0 + V_{ch}) = 2V_0$, $(V_{ch}/d) = (V_0/d)$

Wojciech.Dulinski@ires.in2p3.fr

Derivation of a pulse shape from an ion chamber (2)

$$(1/2)\, C(2V_0)V_R = n_0 e(V_0/d)(v^+ + v^-)t$$

$$V_R = (n_0 e/dC)(v^+ + v^-)t$$

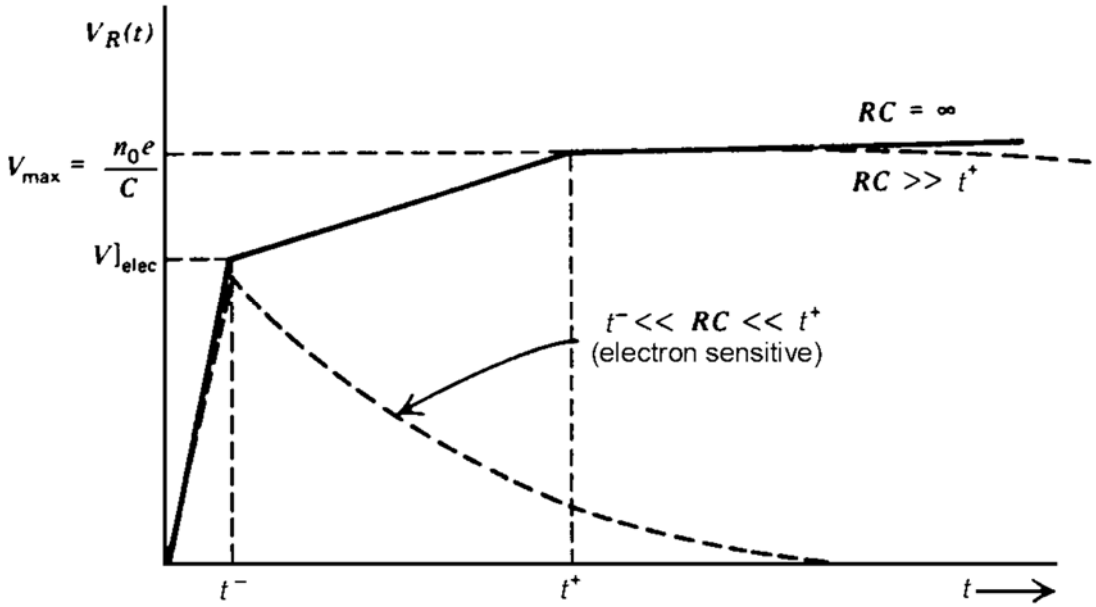

After a time of $t^- = x/v^-$, the electrons reach the anode ==> $V_R = (n_0 e/dC)(v^+ t + x)$

After a time of $t^+ = (d - x)/v^+$, the ions reach the anode ==> $V_R = (n_0 e/dC)[(d - x) + x)]$

Or : $V_R = n_0 e/C = Q/C$

General case of a current induced in segmented detector : Ramo's Theorem (see later)

Wojciech.Dulinski@ires.in2p3.fr

Choice of detector material

Many parameters should be taken into account :

- type of ionising radiation to be detected, in particular energy range in the case of photons

- type of work to be done : spectroscopy, imaging, both …

- in the case of imaging : simple counting or also energy measurements

- total area/volume/segmentation (number of channels)

- system aspects : room or cryogenic temperature

- radiation damage

- availability and price of the material

Wojciech.Dulinski@ires.in2p3.fr

Choice of detector material

Material	Z	E_g[eV]	w [eV]	μ_e[cm^2/Vs]	μ_h[cm^2/Vs]	τ_e[s]	τ_h[s]	ε	ρ[g/cm^3]
C (diamond)	6	5.4	13.2	1800	1200	10^{-8}	$<10^{-8}$	5.5	3.51
Si	12	1.12	3.61	1350	480	$>10^{-3}$	$2\ 10^{-3}$	11.7	2.33
Ge	32	0.67	2.98	3900	1900	$>10^{-3}$	10^{-3}	16	5.33
GaAs	32	1.42	4.70	8500	450	10^{-8}	10^{-7}	12.8	5.32
CdTe	50	1.56	4.43	1050	100	$3\ 10^{-6}$	$2\ 10^{-6}$	11	6.2
CdZnTe		1.5-2.2	5	1350	120	10^{-6}	$5\ 10^{-8}$		6
HgI_2	54	2.13	4.20	100	4	10^{-6}	10^{-5}	8.8	6.4
a-Si	12	1.8	4	1	0.005	$7\ 10^{-9}$	$4\ 10^{-6}$	11.7	2.3
a-Se	34	2.3	7	0.005	0.14	10^{-6}	10^{-6}	6.6	4.3

There are many others: SiC, TlBr, InP…

Wojciech.Dulinski@ires.in2p3.fr

Choice of detector material for tracker : silicon!

Bethe-Bloch equation applied for silicon and for minimum-ionising particles (γ~3.5) gives:

dE/dx = 39 keV/100μm

-an energy deposition of ~3.6 eV will produce an e-h pair in silicon

-minimum-ionising particle will produce ~10 000 e-h pairs traversing 100 μm of silicon

- because of Landau fluctuation : E_{peak} ~7300 e-h pairs per 100 μm of silicon

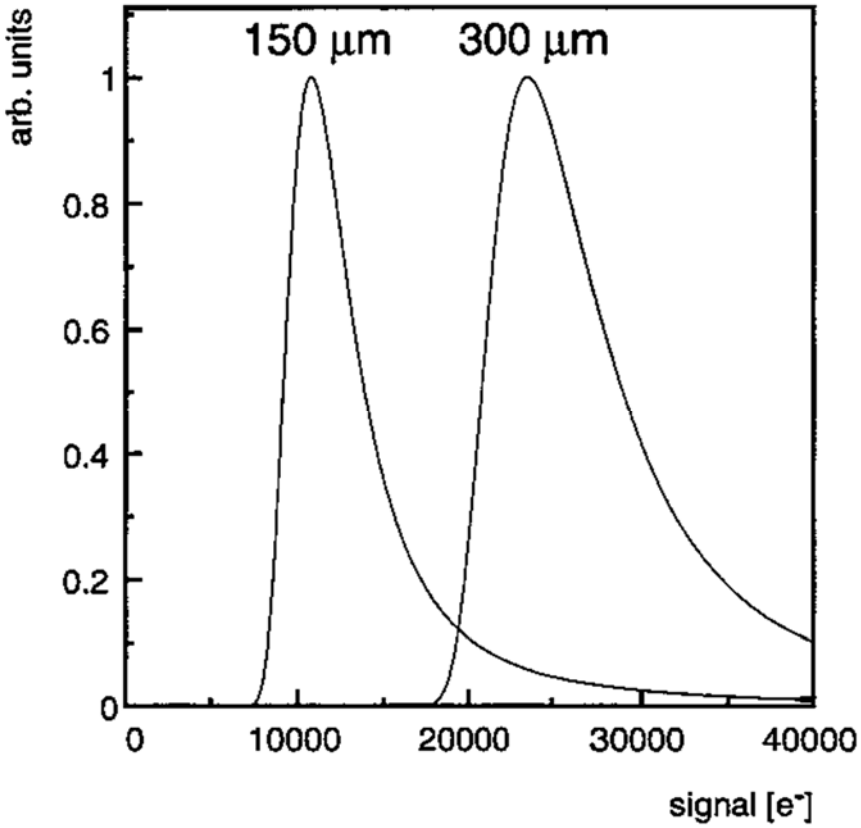

Landau distribution (calculated) for a 300μm and a 150μm thick silicon detector.

Wojciech.Dulinski@ires.in2p3.fr

Physics and Properties of Semiconductors: crystal structure

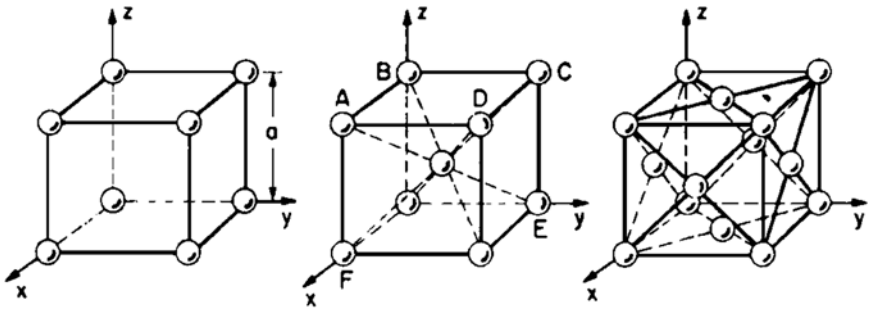

Three cubic-crystal unit cells. (a) Simple cubic. (b) Body-centered cubic. (c) Face-centered cubic

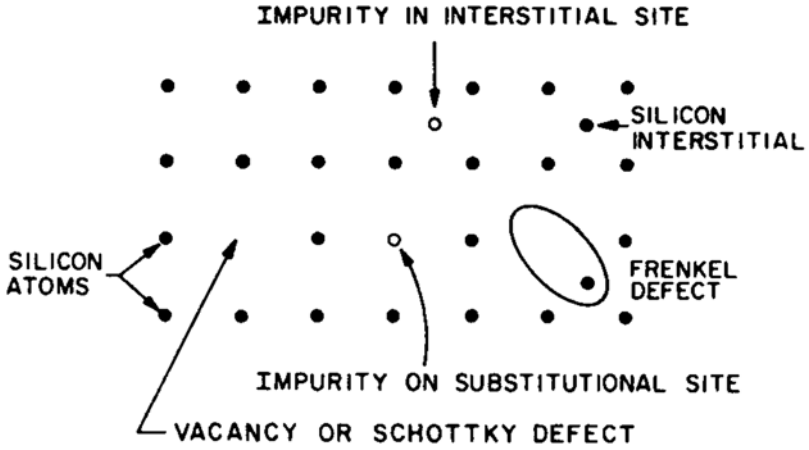

The location and types of point defects in a simple lattice

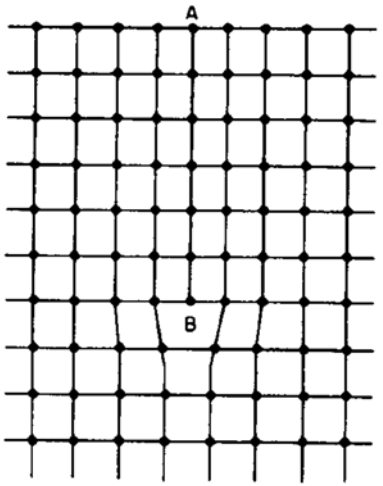

An edge dislocation in a cubic lattice created by an extra plane of atoms

Wojciech.Dulinski@ires.in2p3.fr

Physics and Properties of Semiconductors: valence bonds

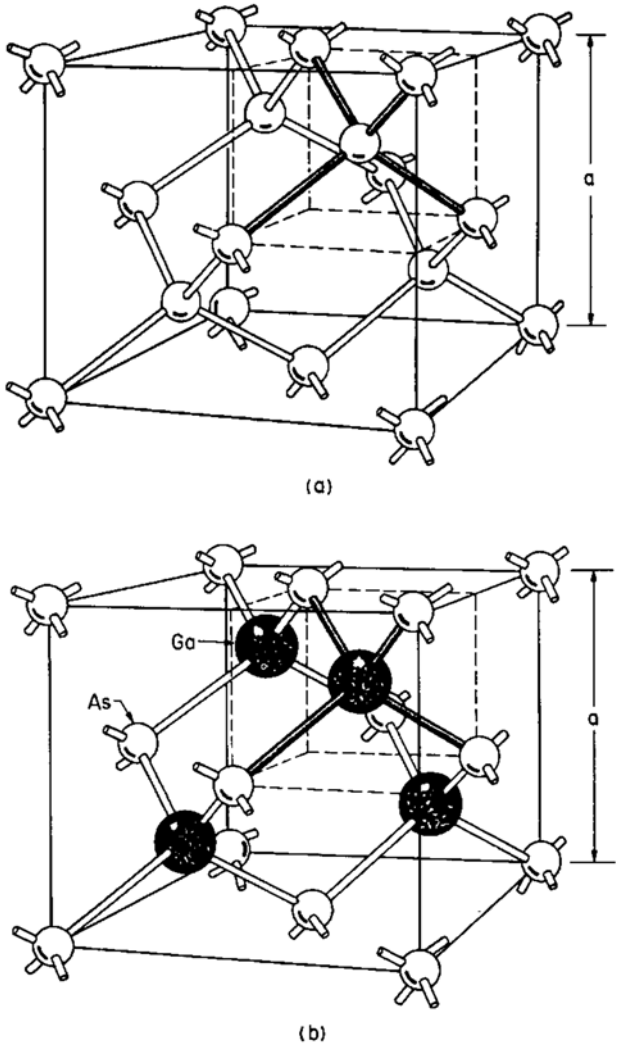

a). Diamond lattice (germanium, silicon)

b). Zincblende lattice (GaAs) (a is the lattice constant)

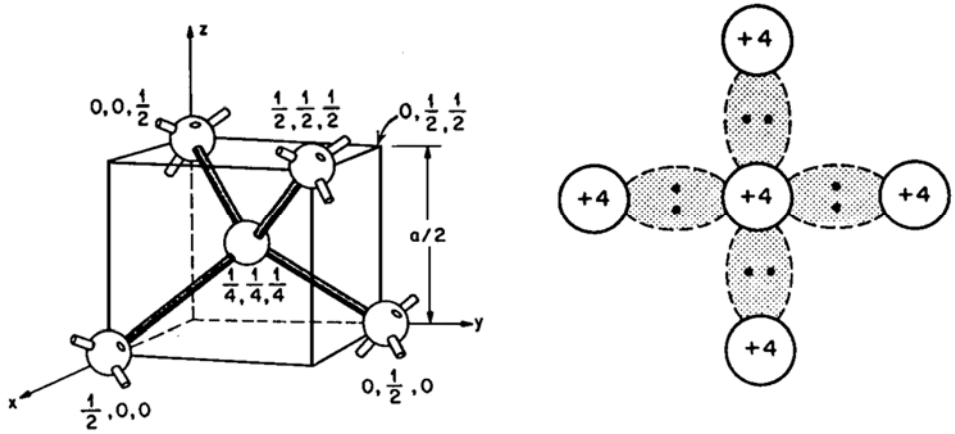

(a) A tetrahedron bond. (b) Schematic two-dimensional representation of a tetrahedron bond.

Wojciech.Dulinski@ires.in2p3.fr

Physics and Properties of Semiconductors: energy bands

Semiconductors are crystalline materials whose outer shell atomic levels exhibit en energy band structure : a valence band, a “forbidden” energy gap and conduction band.

Electrons in the valence band are tightly bound and remain associated to their respective lattice atoms.

Electrons in the conduction band are detached from their parent atoms and are free to move across the crystal.

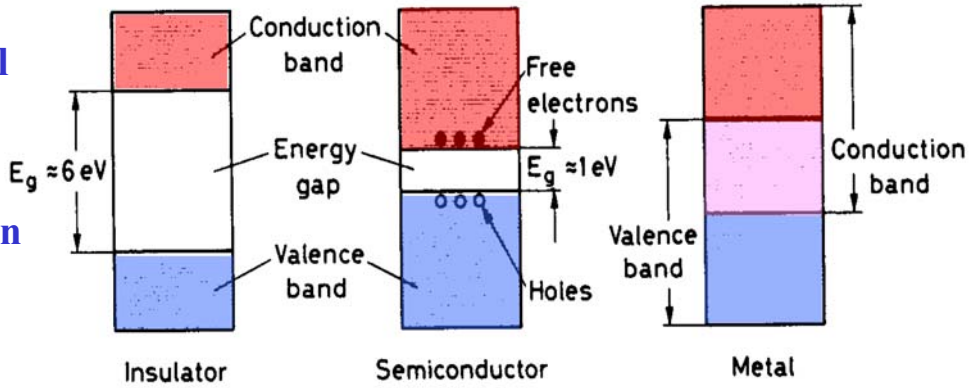

Energy band structure of conductors, insulators and semiconductors

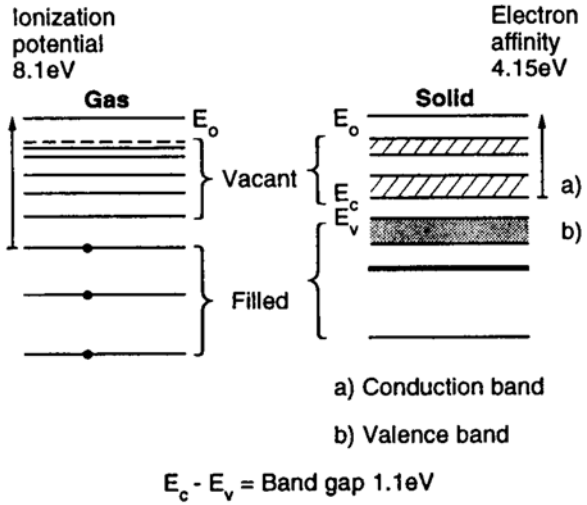

Allowed energy levels in gaseous silicon which become energy bands in the solid material]

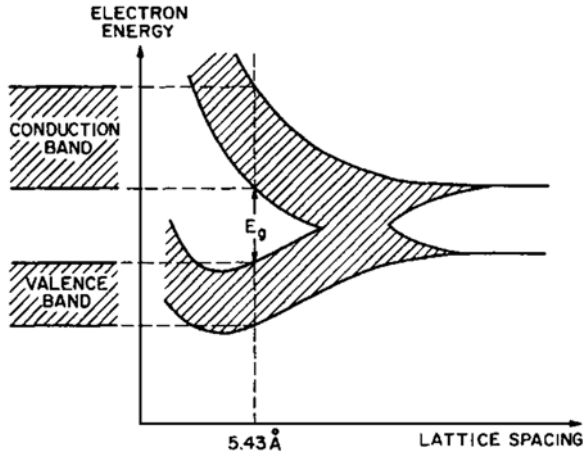

Formation of energy bands as a diamond lattice crystal is formed by bringing together isolated silicon atoms

Wojciech.Dulinski@ires.in2p3.fr

Charge Carriers in Semiconductor : Intrinsic Material

Probability of occupation by en electron of a given state is given by Fermi-Dirac statistics :

$$f(E) = 1/(1+\exp(E-E_f)/kT)$$

Fermi level E_f is the energy at which the probability is one-half. For energy levels which are at least a few kT units above or below the Fermi level (kT=0.026 eV at room temperature) :

$$f(E) = \exp(-(E-E_f)/kT) \text{ ; for } E>E_f$$

$$f(E) = 1 - \exp(-(E_f-E)/kT) \text{ ; for } E<E_f$$

The charge carriers concentration :

$$n = N_C \exp(-(E-E_f)/kT) \text{ (electrons)}$$

$$p = N_V \exp(-(E_f-E)/kT) \text{ (holes)}$$

where N_C and N_E (both $\sim T^{3/2}$) are effective density of states

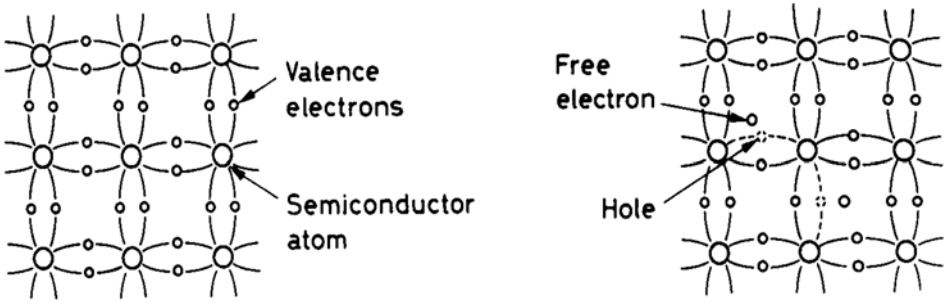

Covalent bonding of silicon : at 0 K, all electrons participate in bonding (left), at higher temperature some bonds are broken by thermal energy leaving a hole in the valence band (right)

Wojciech.Dulinski@ires.in2p3.fr

Charge Carriers in Semiconductor : Intrinsic Material

For intrinsic semiconductors : $n=p=n_i$ and

$$E_f = E_i = (E_c+E_v)/2 + kT/2 \ln(N_v/N_c)$$

(Fermi level close to middle of the gap)

Also :

$$pn = N_v N_c \exp(-E_g/kT)$$; where $E_g = E_c-E_v$

and :

$$n_i \sim T^{3/2}\exp(-E_g/2kT)$$

For silicon in room temperature :

$n_i \sim 1.5\ 10^{10}$

Only 1 in 10^{12} atoms is ionised!

The current density :

$J = d_c v = en_i(\mu_e+\mu_h)E$; where d_c is charge density, v velocity and μ mobility

intrinsic material resistivity : $\rho = 1 / en_i(\mu_e+\mu_h)$

For silicon in room temperature :

$\rho = 230\ k\Omega\ cm$

Wojciech.Dulinski@ires.in2p3.fr

Energy representation, direct and indirect semiconductors

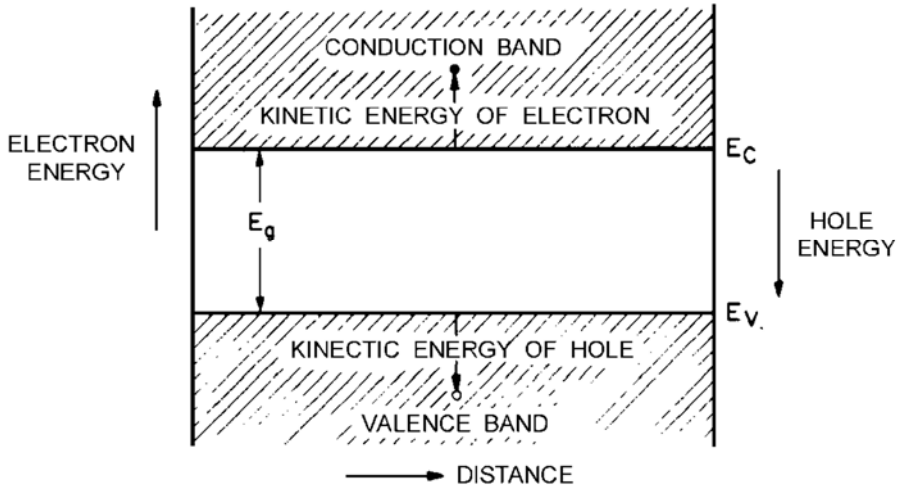

The potential energy and kinetic energy in energy band representation

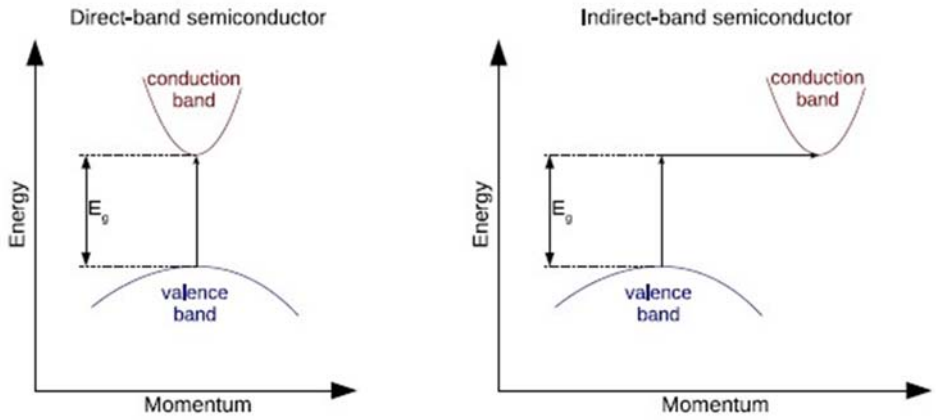

Energy band structure of Si (indirect semiconductor) and GaAs (direct semiconductor)

Wojciech.Dulinski@ires.in2p3.fr

Recombination and Trapping

An electron may recombine with a hole by dropping from the conduction band into an open level in the valence band. Direct recombination is very rare : the most important mechanism is through recombination centers resulting from impurities in crystals. A second effect which arises from impurities is trapping. In both cases the lifetime of charge carriers is degraded. In principle, this lifetime should be much longer comparing to collection time. In addition to impurities, crystal structural defects in the lattice like point effects (vacancies, interstitials) or dislocation may also give rise to similar states in the forbidden band. Unlike wanted impurities (dopants), recombination and trapping centers produce deep levels (far from conduction or valence band).

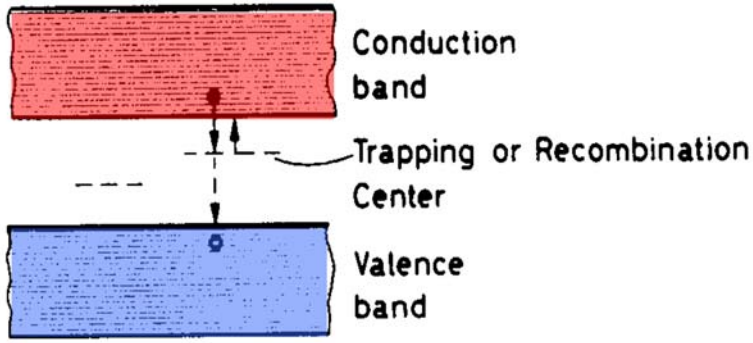

Recombination and trapping sites in the forbidden energy gap

Semiconductor detectors require relatively pure crystals. For large volume detectors, in particular, impurity concentration cannot be more than ~10^{10} per cm^3

Wojciech.Dulinski@ires.in2p3.fr

Doped Semiconductors

Doping : introduction of small amount of impurity atoms having one more (or one less) electron in their outer atomic shell. These impurities integrate themselves into crystal lattice to create so called extrinsic semiconductors. The energy levels created by an extra (missing) electron are extremely close to conduction (valence) band. Therefore, at normal temperature, all this levels are excited (filled) creating a free electron (hole).

Low off mass action when in thermal equilibrium :
$np = n_i^2 = AT^3 \exp(-E_g/kT)$

Also : $N_D + p = N_A + n$; where N_D and N_A are donor and acceptor concentration

In n-type material where $N_A=0$ and $n>>p$:

$n = N_D$ **and** $p = n_i^2 / N_D$ **(also** $\rho = 1 / e N_D \mu_e$ **)**

where **n** and **p** is majority and minority carrier concentration

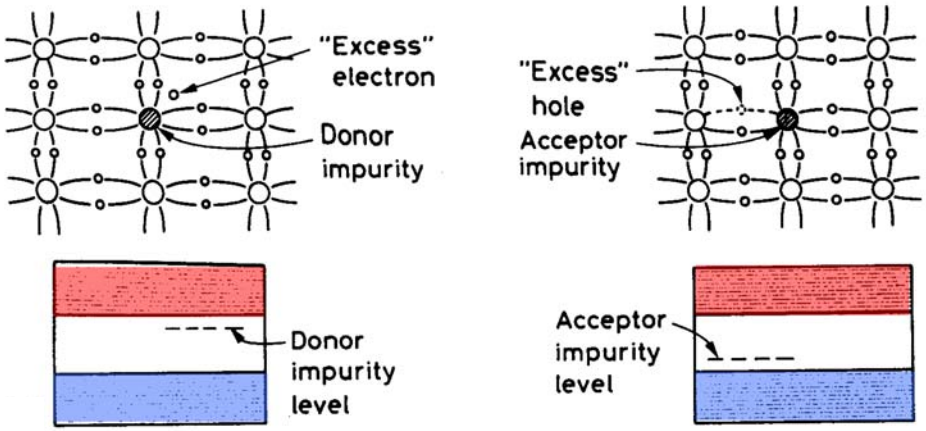

Donor impurities (to form n-type semiconductor) add excess electrons. Acceptor impurities (to form p-type semiconductor) add excess of holes

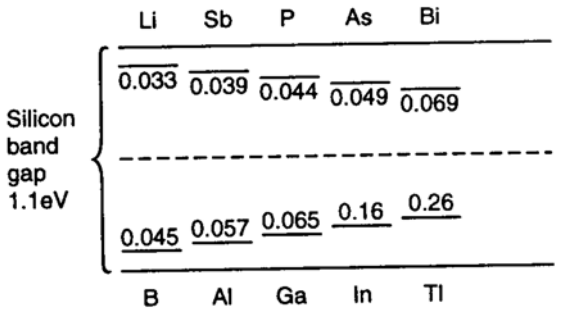

Energy levels within the band gap corresponding to various n- and p-type dopants

Wojciech.Dulinski@ires.in2p3.fr

The p-n Junction

Two crystals of opposite type are brought together : a depletion layer is formed on either side of junction.

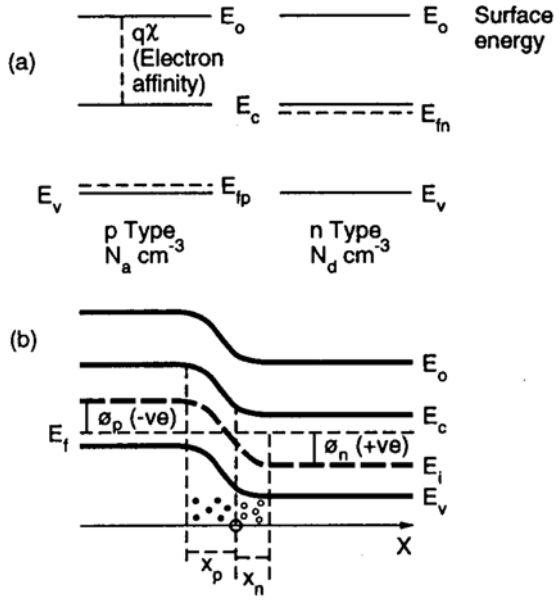

(a) Energy levels in two electrically isolated silicon samples (of p- and n-type). (b) When in contact, the Fermi level is constant throughout the material. The band edges bend in accordance with the space charge generated

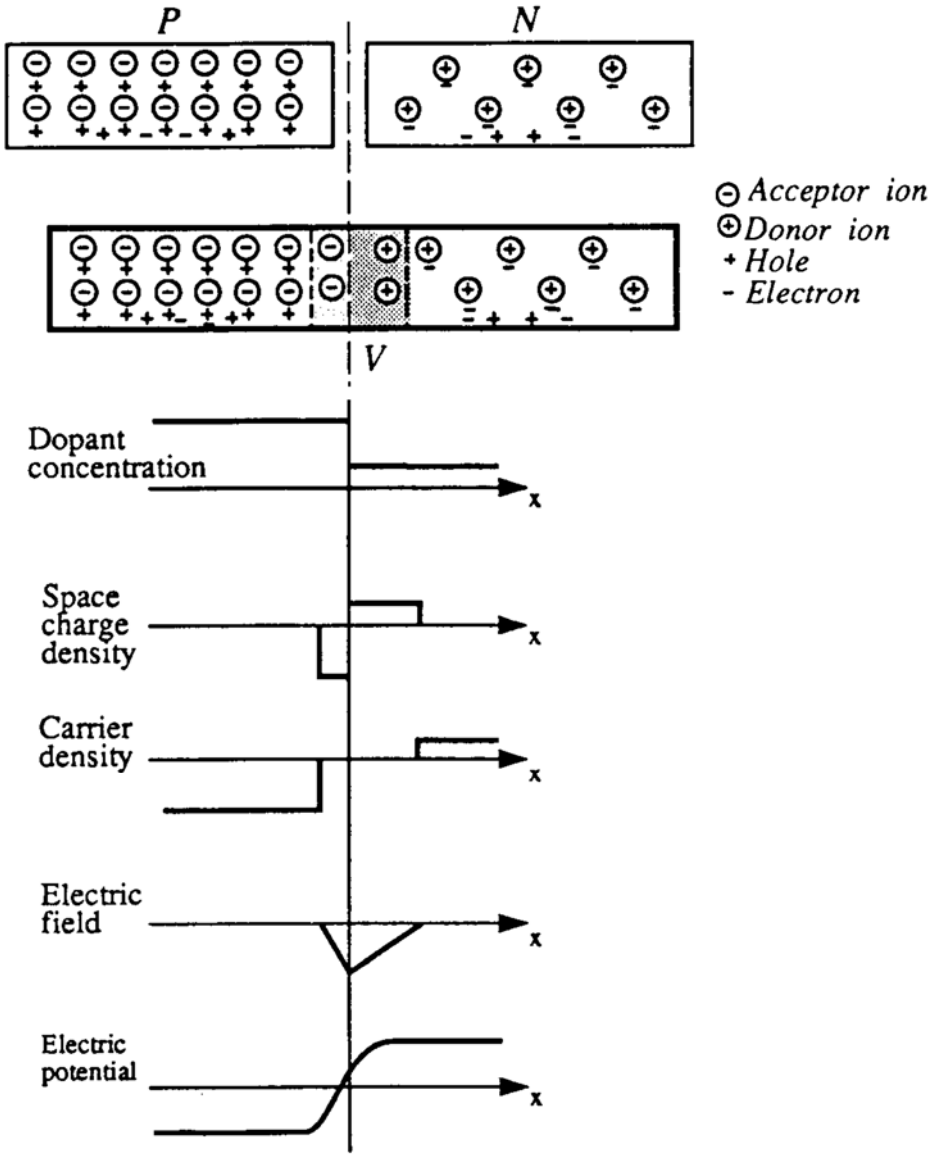

Wojciech.Dulinski@ires.in2p3.fr

Reversed Bias Junction

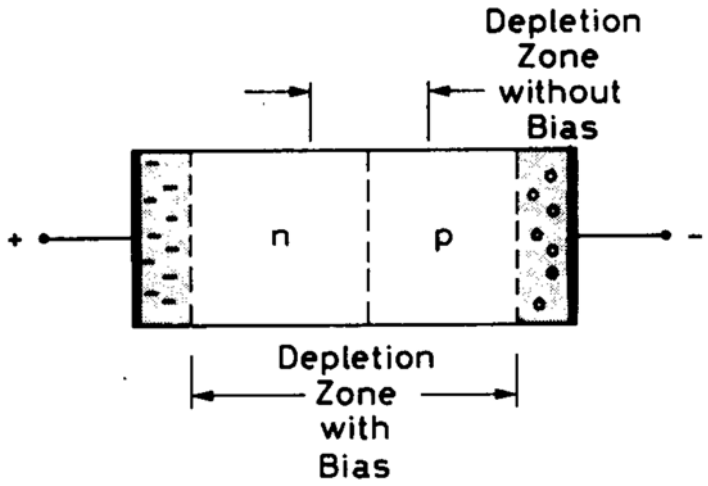

If one side of a p-n junction is more heavily doped than the other, which is usually the case, than the depletion zone will extend farther into lighter-doped side. For example, if $N_A >> N_D$, then the depletion zone is almost entirely on the n-side of the junction. The total width of depletion zone in that case is :

$$d \cong \sqrt{\frac{2\varepsilon(V_0 + V_{bias})}{eN_D}} \cong \sqrt{2\varepsilon\rho_n\mu_e V_{bias}}$$

Also Junction Capacity $\sim(\rho_n V_{bias})^{-1/2}$

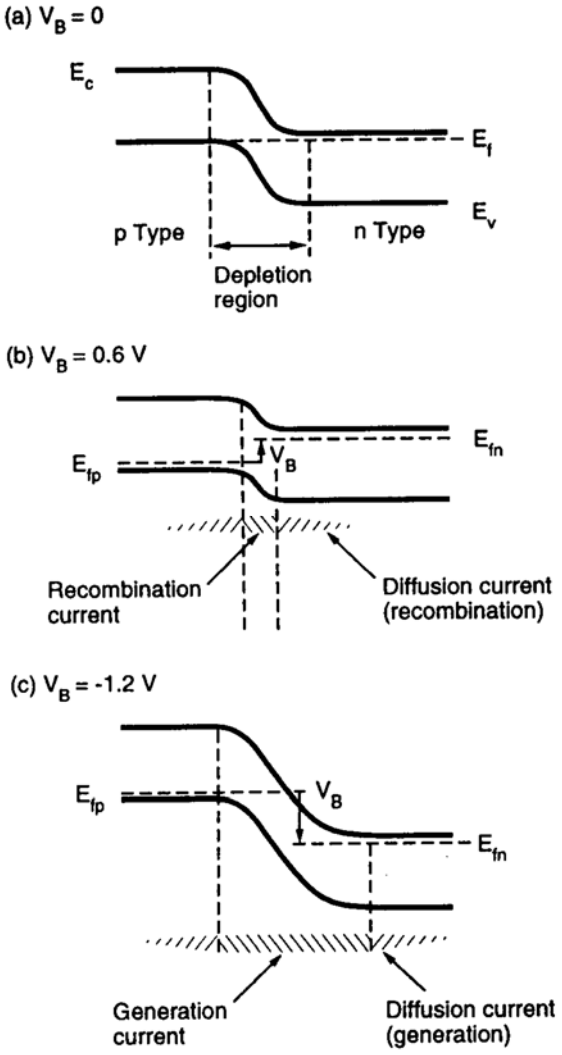

Effect of an applied voltage across the semiconductor junction

Wojciech.Dulinski@ires.in2p3.fr

Germanium Gamma-Ray Detectors

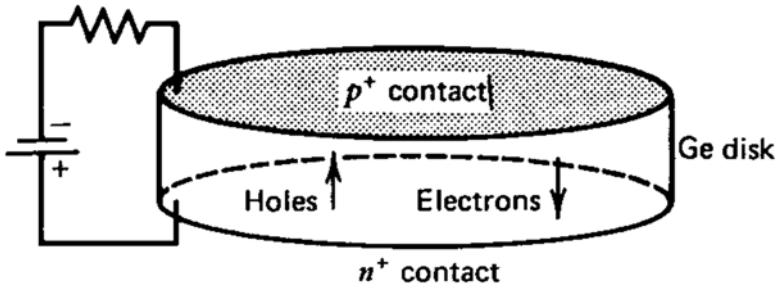

Configuration of a planar HPGe detector. The Ge semiconductor may be ν type (p+ contact is rectifying), π type (n+ contact is rectifying), or lithium drifted.

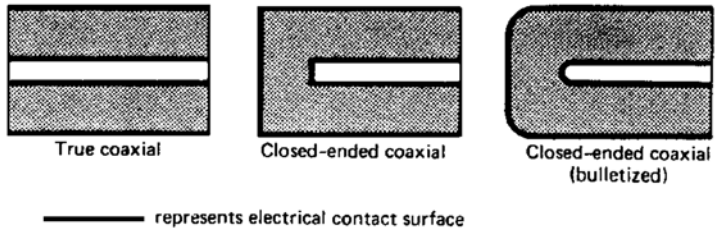

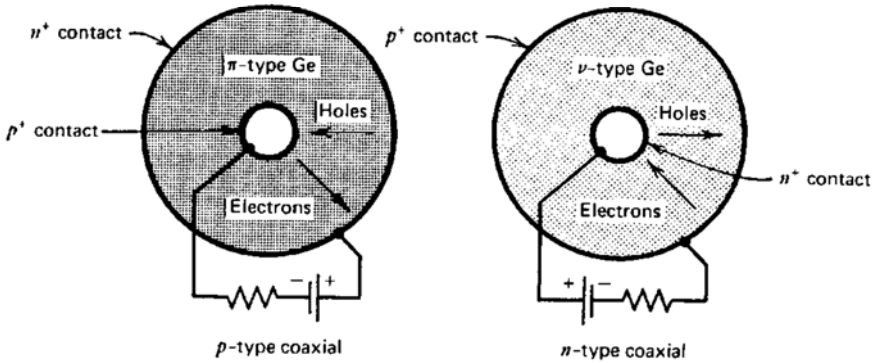

The three common shapes of a large-volume coaxial detectors..

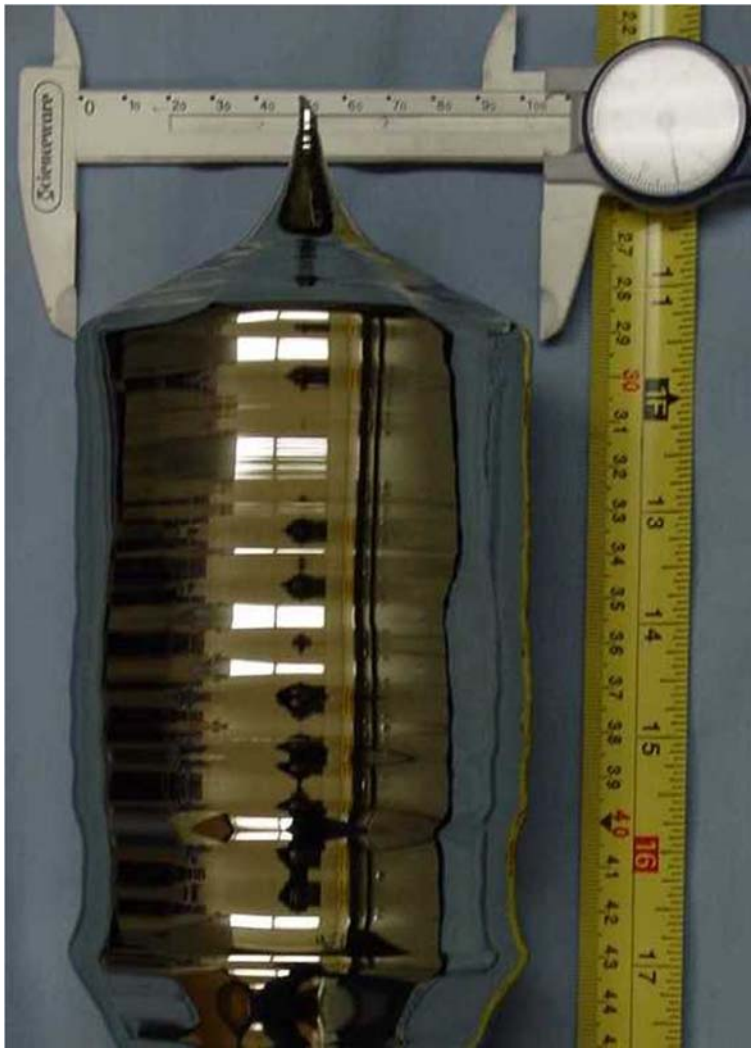

HP-Ge crystal diameter ~10 cm (2000)

Wojciech.Dulinski@ires.in2p3.fr

HPGe detector within its vacuum capsule and liquid nitrogen cooling system

Impurity concentration: $10^9 < N_d\ [cm^{-3}] < 5\ 10^9$

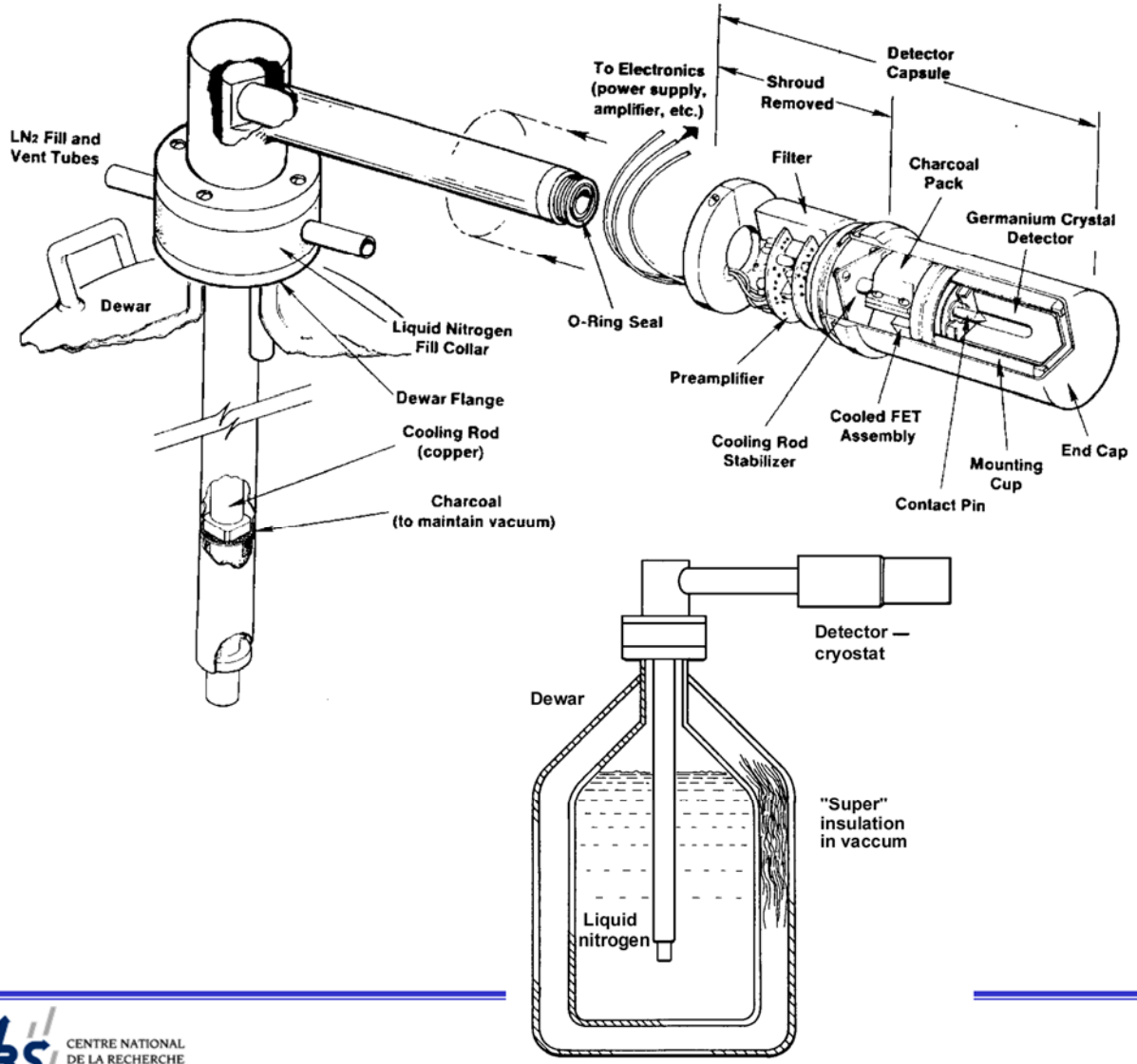

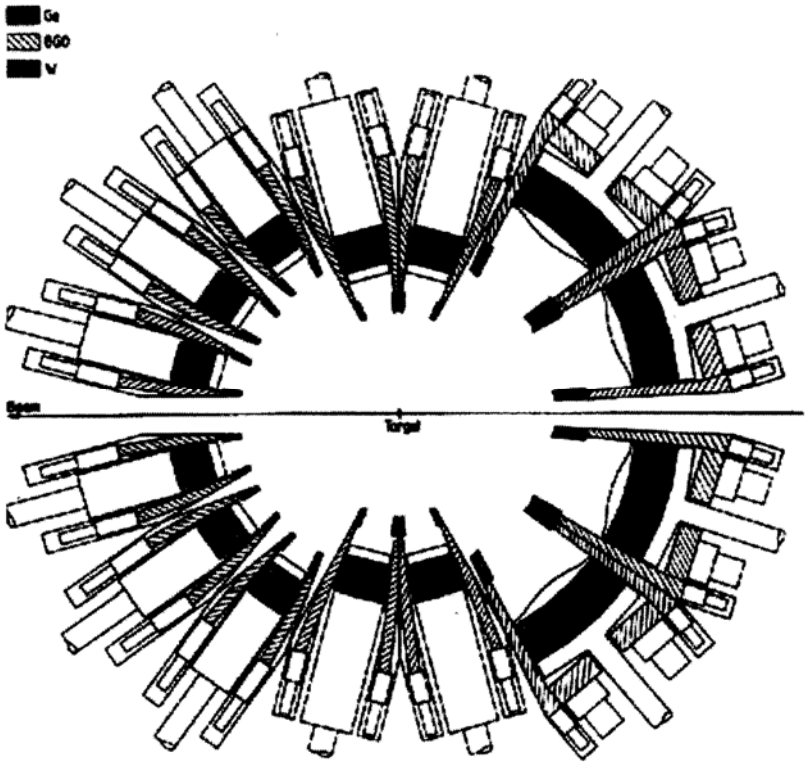

γ-detector array EUROBALL (239 Ge detectors): solution for complicated multi-photon spectroscopy

Wojciech.Dulinski@ires.in2p3.fr

Gamma-ray spectroscopy with germanium detectors

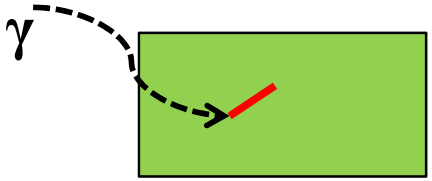

Single photoelectric

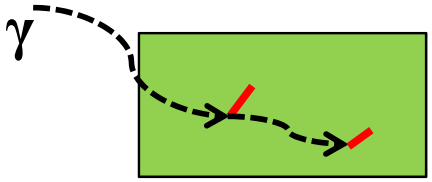

Compton + photoelectric

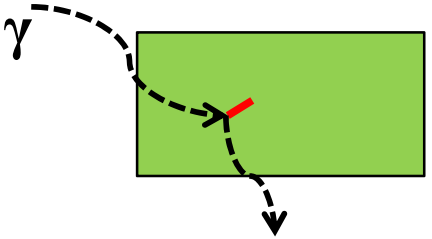

Compton + escape

Possible gamma-ray absorption ways

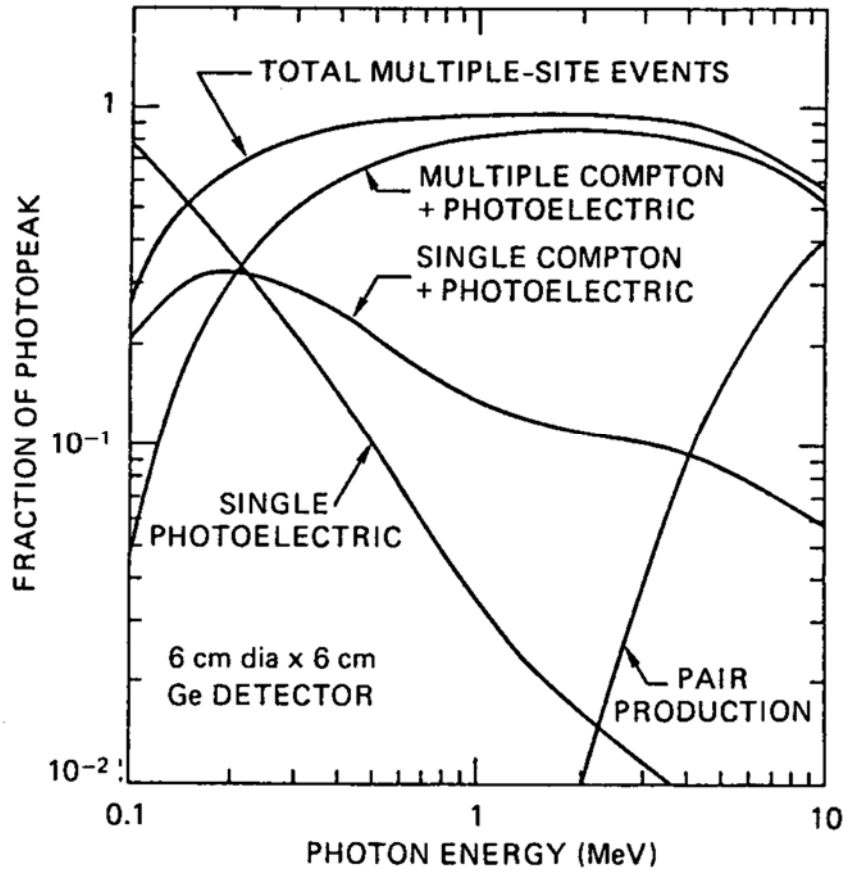

Predicted fraction of the full-energy peak contributed by different energy loss mechanisms in a 6cm x 6cm coaxial HPGe detector.

Wojciech.Dulinski@ires.in2p3.fr

Detector factors of merit for gamma-ray spectroscopy

- energy resolution ($\Delta E/E$, FWHM, σ_E)
- peak/Compton ratio

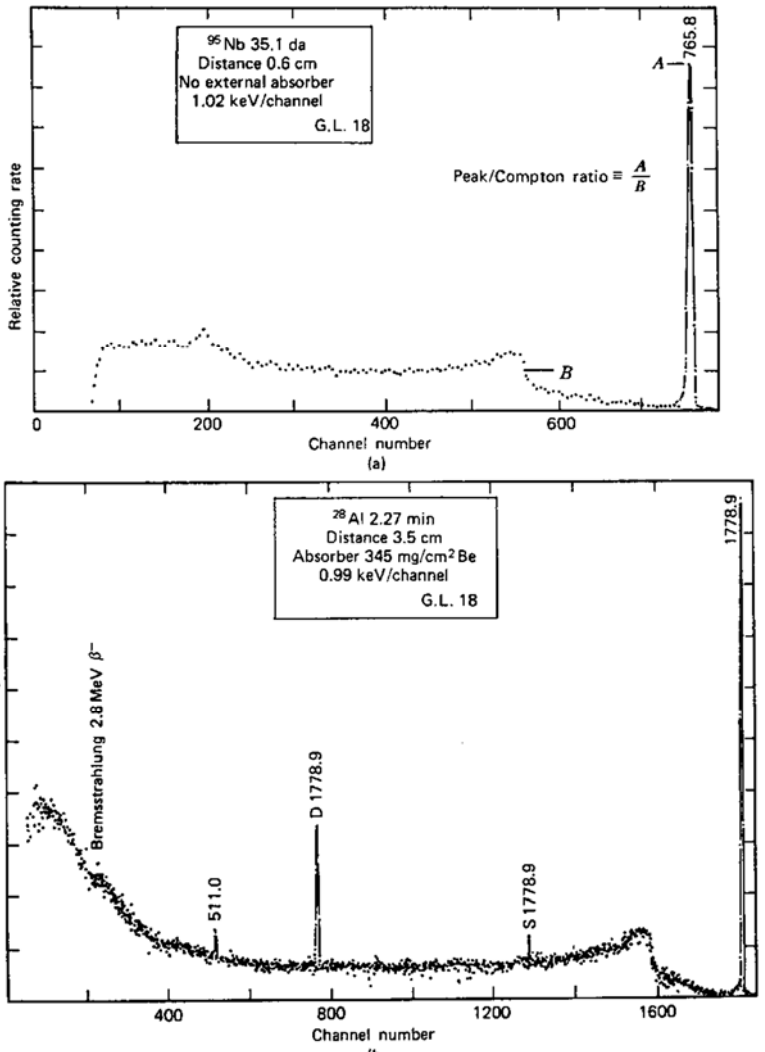

Measured pulse height spectra for monoenergetic gamma rays from a 18 cm^3 Ge(Li) detector. The full-energy peak, Compton continuum, single and double escape peak as well as a 511 keV peak from annihilation photons in surrounding materials are visible.

Wojciech.Dulinski@ires.in2p3.fr

Compton rejection by anticoincidence

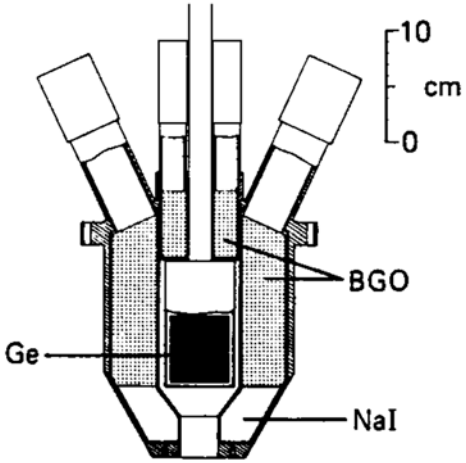

An example of a germanium detector surrounded by a Compton suppression system made up of NaI(Tl) and BGO scintillators.

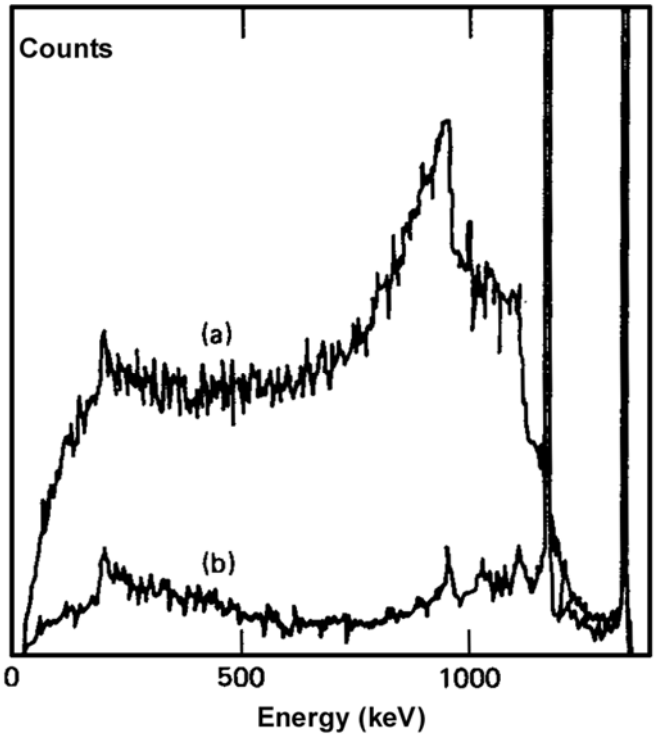

Pulse height spectra from a ^{60}Co gamma-source using the system shown at the left. (a) Normal spectrum. (b) Spectrum recorded in anticoincidence with the scintillation detectors, showing the suppression of the Compton continuum.

Wojciech.Dulinski@ires.in2p3.fr

Semiconductor Position Sensitive Detectors: Single Sided Microstrip Detector

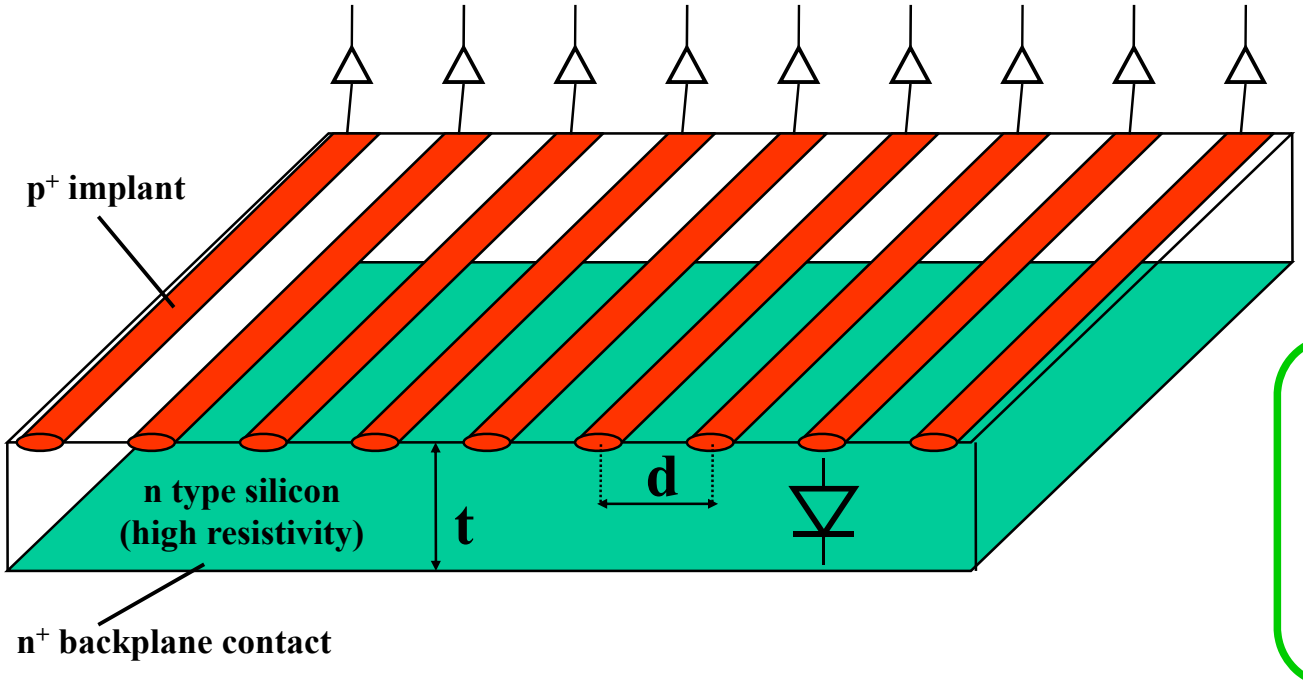

To be measured:

-hit position

- signal amplitude

Single sided microstrip detector

Typical parameters : t~300μm, d~50 μm, size ~10x10 cm

Spatial Resolution is the Factor of Merit : $\sigma \approx d/\sqrt{12}$

σ = 1.3 μm has been demonstrated

$\sigma \sim d/2\ (S/N)^{-1}$

If analog readout

Wojciech.Dulinski@ires.in2p3.fr

Semiconductor Position Sensitive Detectors: Double Sided Microstrip Detector

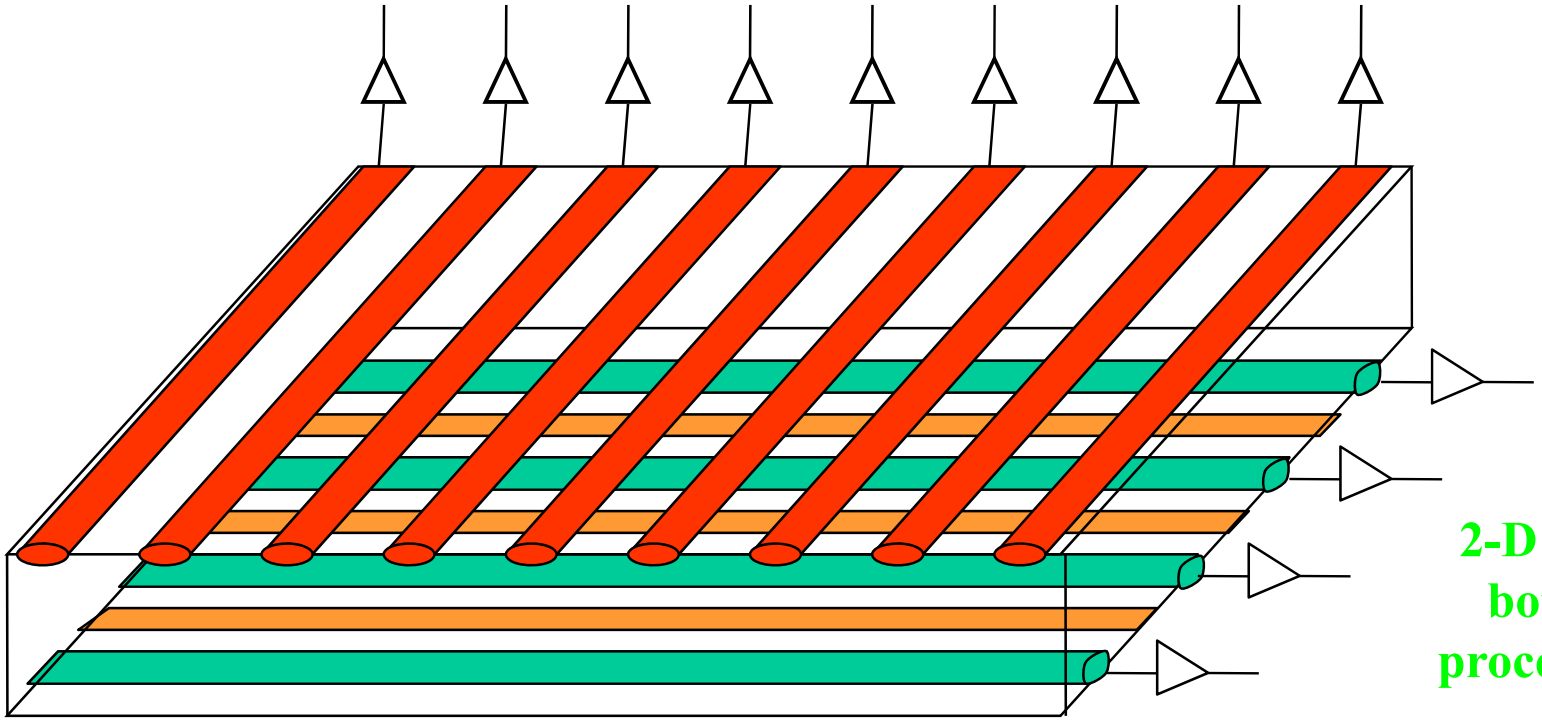

2-D Information, but both sides must be processed and read out

Problem of n-strips isolation!

Problem with multihits!

Wojciech.Dulinski@ires.in2p3.fr

Hit resolution

The position resolution will depend on how many strips the charge is deposited on

One Strip Clusters

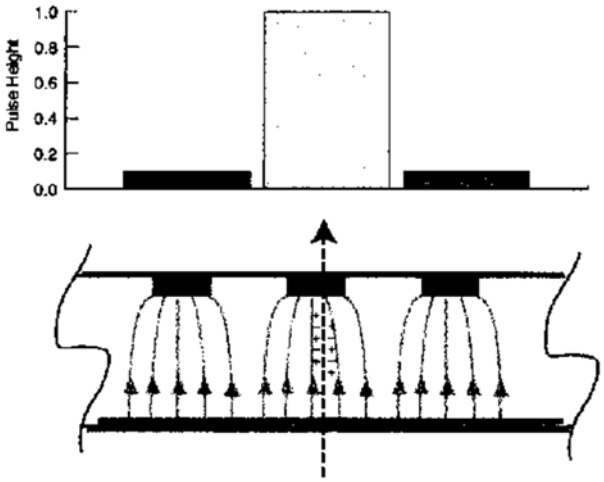

Two Strip Clusters

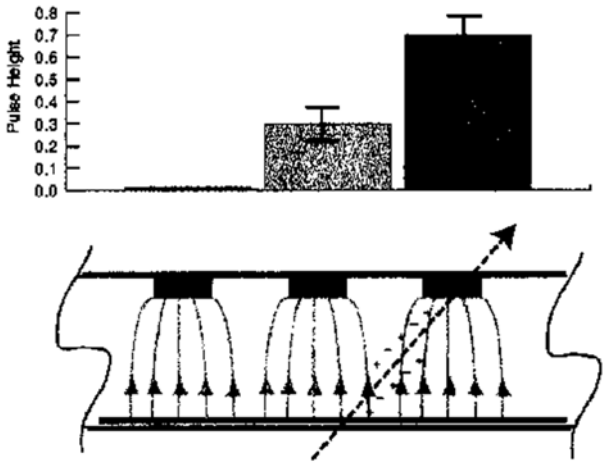

Floating Strips

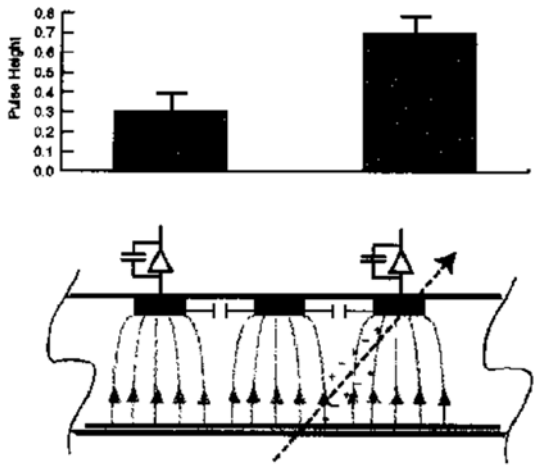

For 1 strip clusters the resolution is simply:

$$\sigma_{hit} = \frac{\Delta}{\sqrt{12}}$$

Where Δ is the strip pitch

For 2 strip clusters the centroid calculation gives the resolution of :

$$\sigma_{hit} \propto \frac{\Delta}{2}\frac{Noise}{Signal}$$

Because of capacitive coupling between strips, we don't need to readout every strip to maintain good position resolution, BUT, because of stray capacitance to the back plane, some charge from the floating strip can be lost, causing problems.

Wojciech.Dulinski@ires.in2p3.fr

Hit spatial resolution : signal processing (interpolation)

"η" algorithm
(two strip clusters)

$$\eta = \frac{Q_l}{Q_l + Q_r}$$

Hit position: $$x_0 = \frac{1}{N_{tot}} \int_0^{\eta_0} \frac{dN}{d\eta} d\eta$$

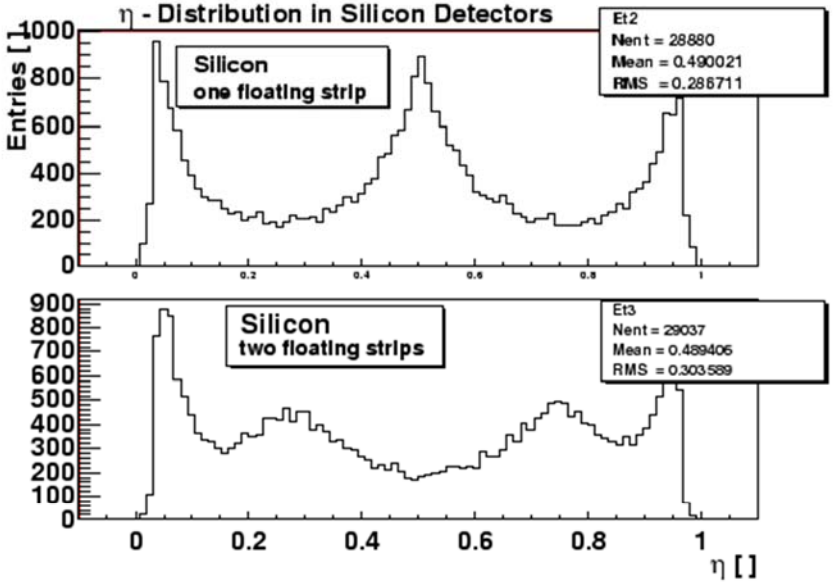

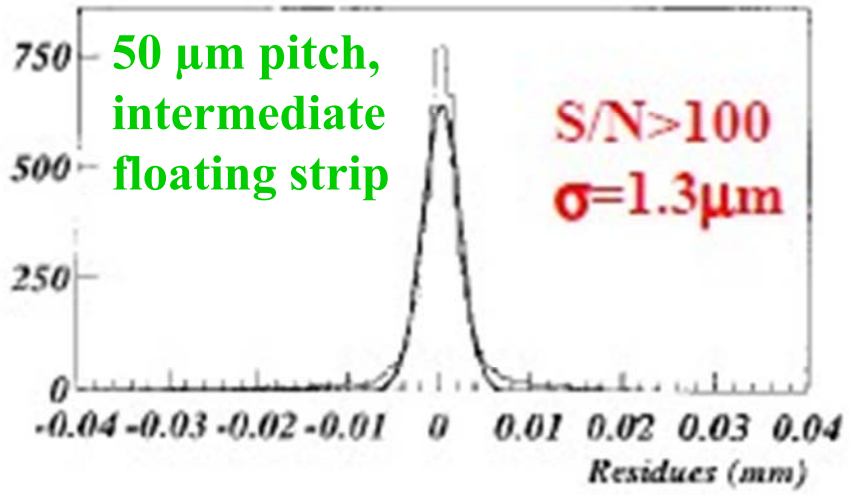

Single plane resolution

Wojciech.Dulinski@ires.in2p3.fr

Track reconstruction with strip detectors - problem of ambiguities

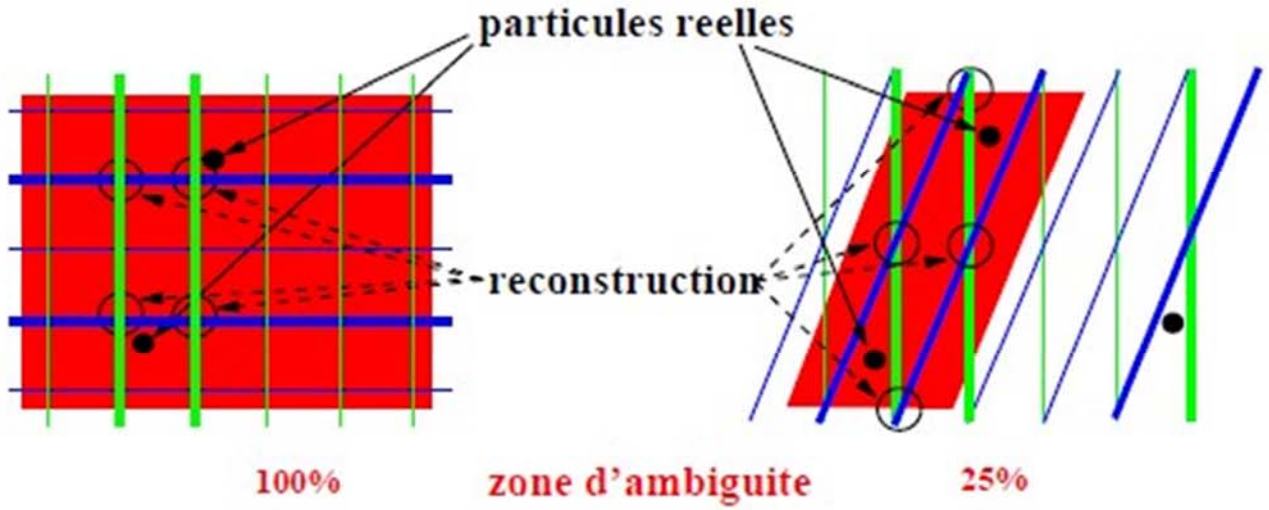

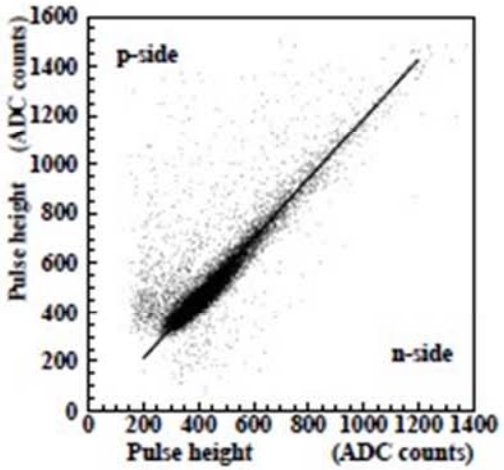

Example of ALICE detector (4.2x7.6 cm) : 15 tracks/detector. Even with stereo angle of 2° (pretty poor resolution in one direction) there is still 26% remaining ambiguous tracks

Some of ambiguities can be resolved by charge matching (double-sided detectors)

The only radical solution : pixels!

Wojciech.Dulinski@ires.in2p3.fr

Semiconductor Position Sensitive Detectors: Hybrid Pixel Detector

A pixel detector is a single sided detector segmented in both directions.

The readout chip is mounted directly on top of the pixels, each pixel has it's own readout amplifier. Metal micro balls (Bump bonding) are used to provide electrical connection between two wafers. This is relatively complicated and expensive procedure!

To be measured:

-hit position

-hit arrival time

- signal amplitude

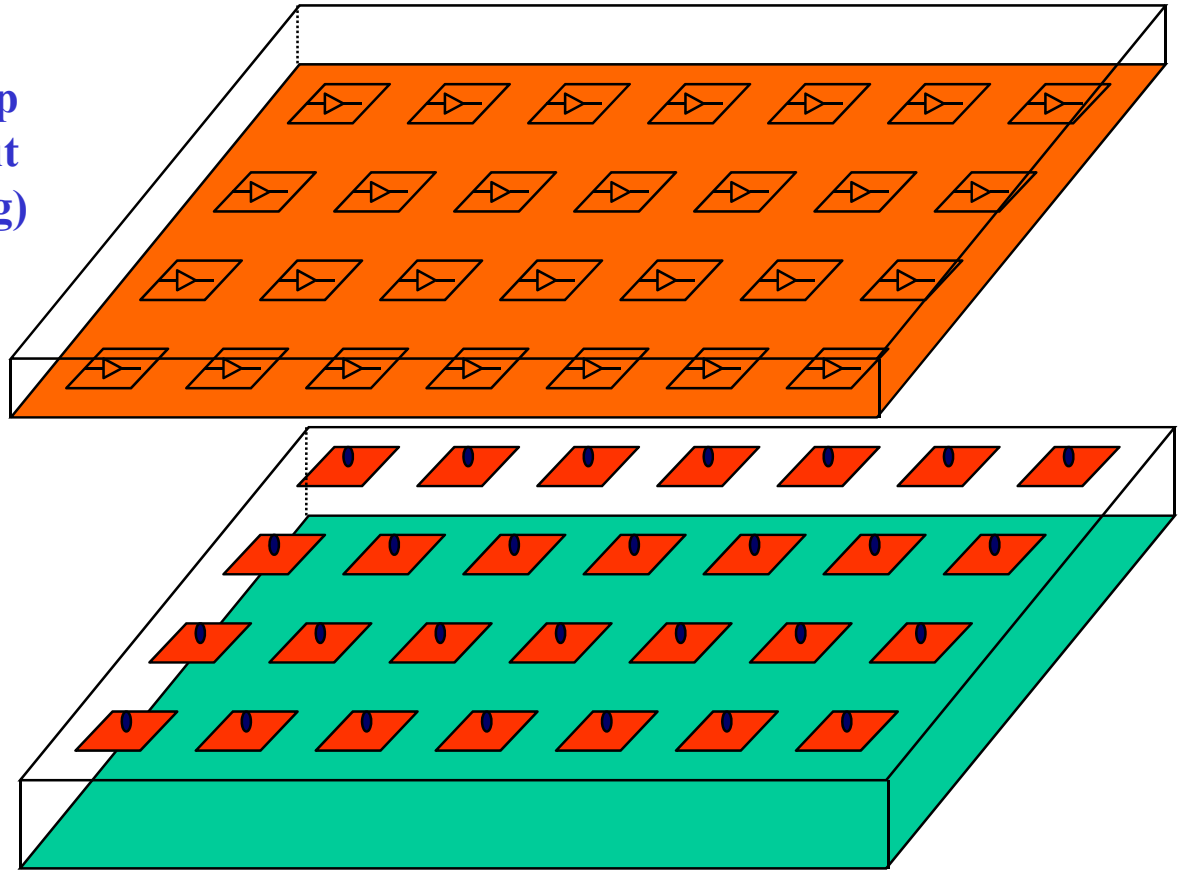

Wojciech.Dulinski@ires.in2p3.fr

Semiconductor Position Sensitive Detectors: Monolithic Pixel Detector

Both detector elements and readout electronics are integrated on the same (silicon) wafer, using slightly (?) more complicated process. High granularity, low noise, thin detectors can be fabricated this way.

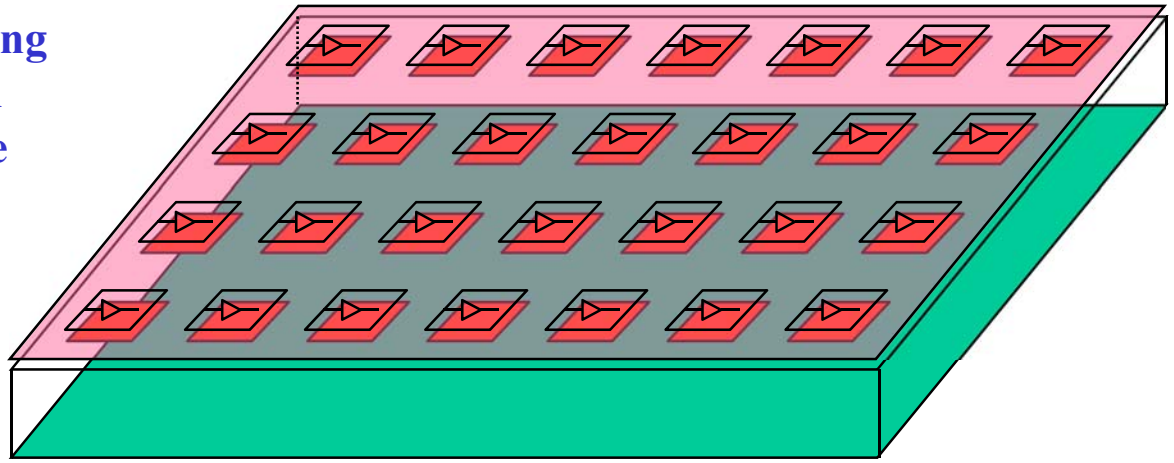

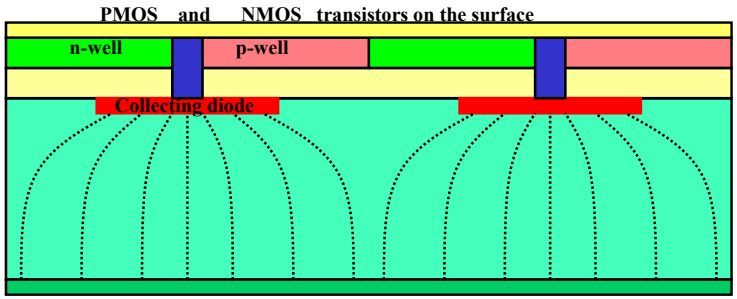

Example of possible monolithic detector implementation:
SOI CMOS + High Resistively handling wafer

Wojciech.Dulinski@ires.in2p3.fr

Past and …… present of silicon trackers!

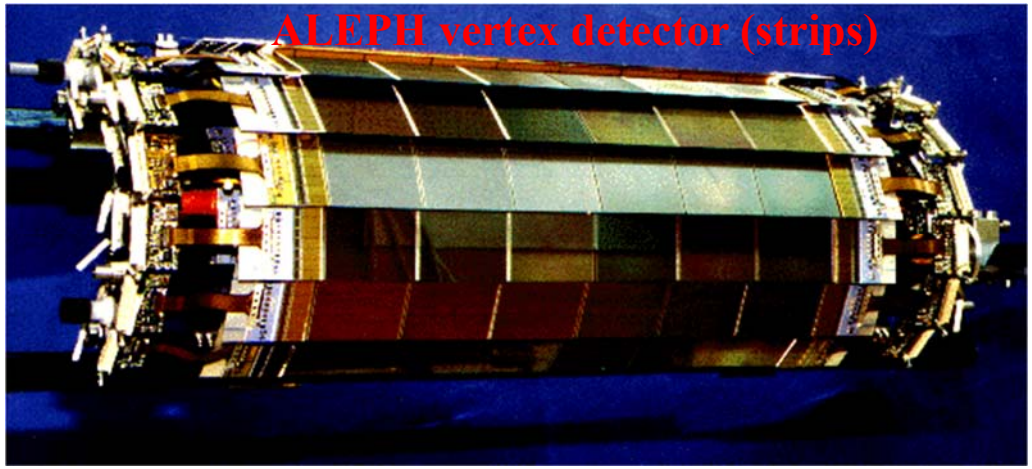

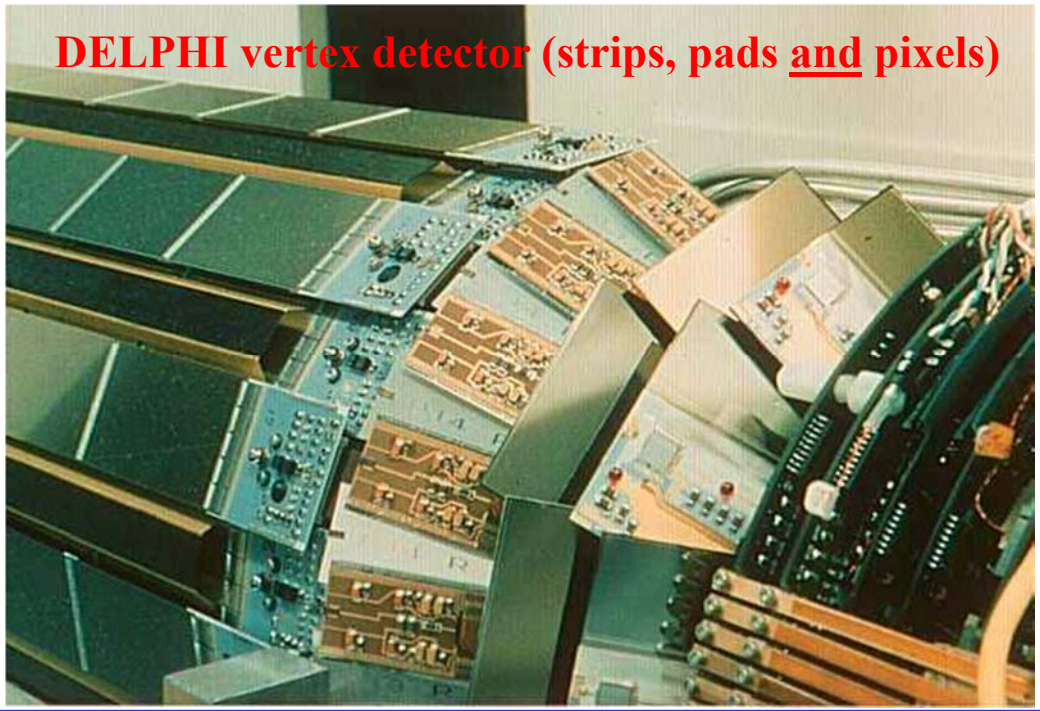

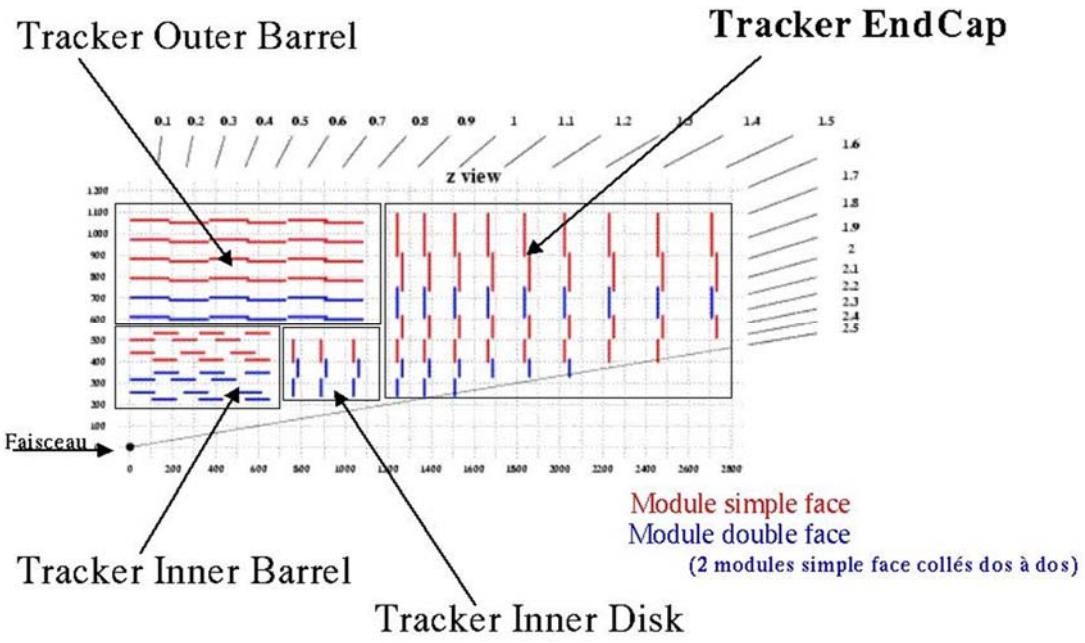

CMS tracker&vertex detector:
>200 m^2 of silicon!

Wojciech.Dulinski@ires.in2p3.fr

Alpha Magnetic Spectrometer on International Space Station (ISS)

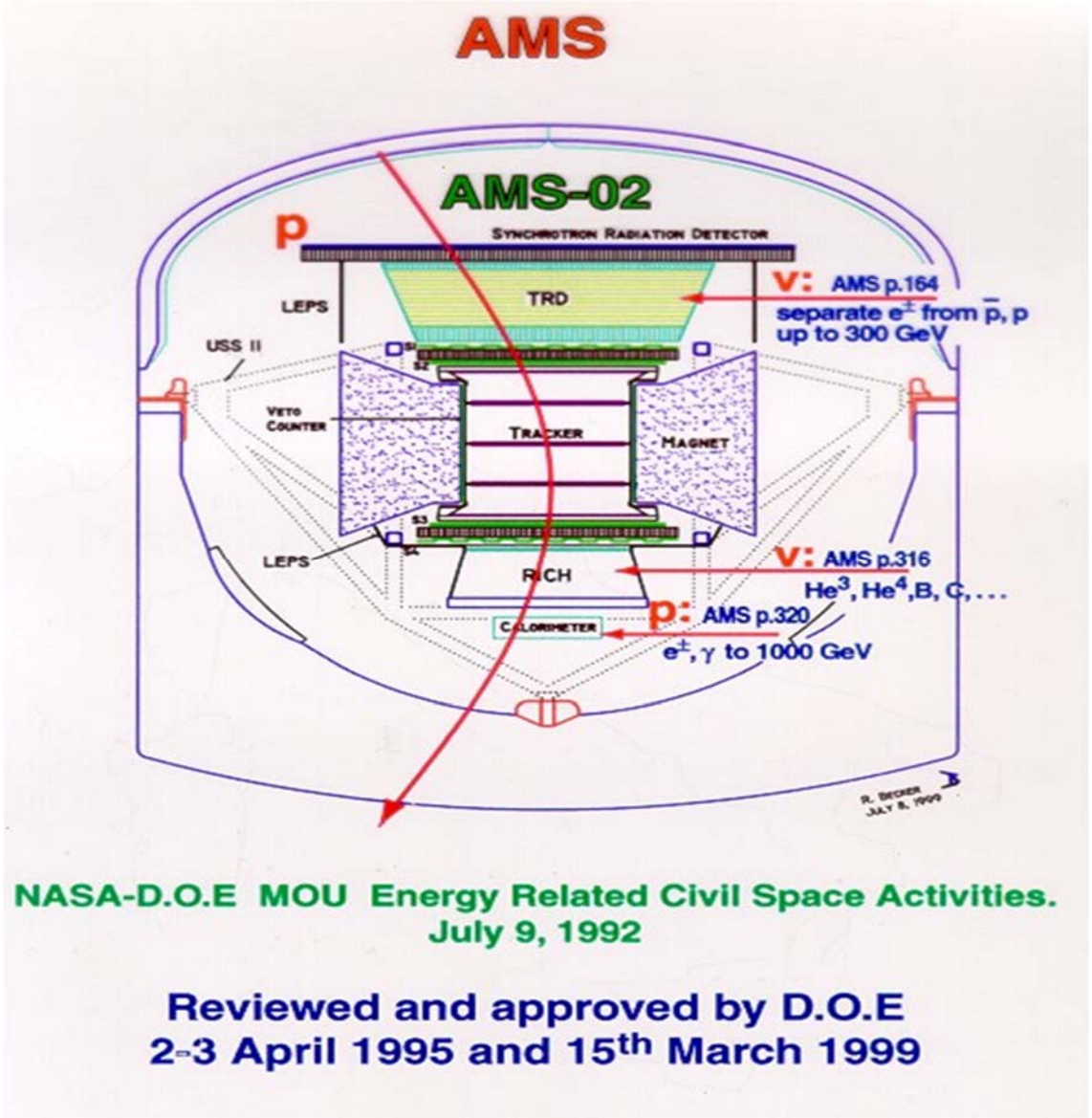

Silicon Tracker

- **Aim:**
  - **Rigidity (P/Ze) measurements**
  - **Sign of Charge**
  - **Absolute Charge (dE/dX , in addition to ToF system)**
- **Tracker detector based on 8 thin layers of double-sided silicon microstrips, with a spatial resolution better than 10 μm, ≈ 200.000 of electronics channel and ≈ 800 W of power.**
- **A complex detector, qualified for operation in space, with its ≈ 6 m² of active surface will be the largest ever built before the LHC @ CERN.**

Wojciech.Dulinski@ires.in2p3.fr

Gamma-Ray Large Area Space Telescope (GLAST → FERMI)

Pair conversion γ telescope using silicon tracker (~80m^2) in space!

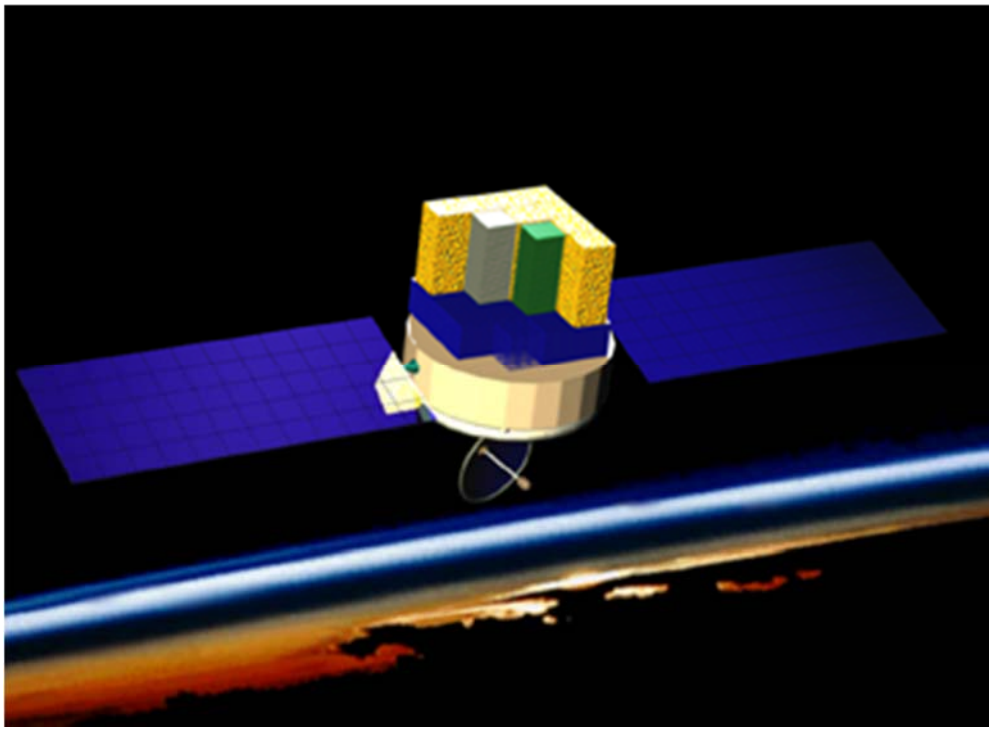

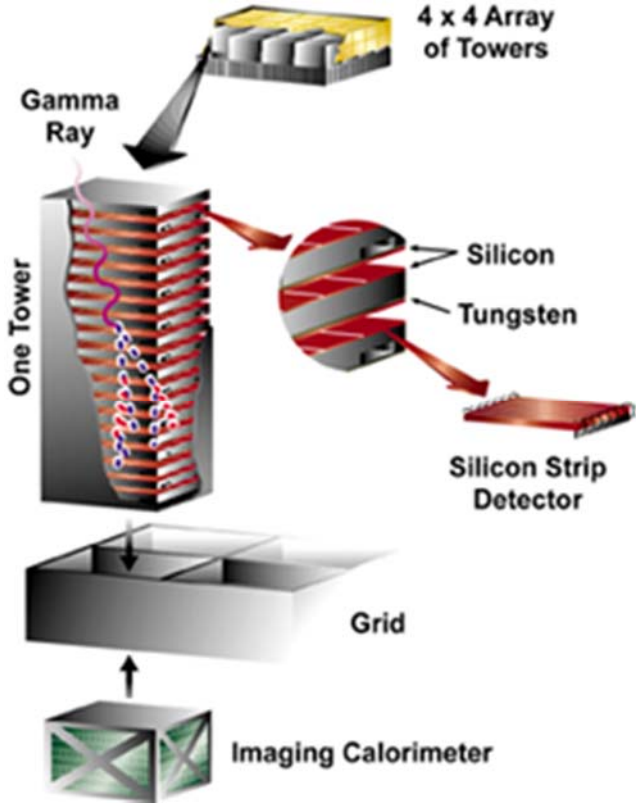

Large Area Telescope

Wojciech.Dulinski@ires.in2p3.fr

Bulk Radiation Damage in Silicon Detectors: Primary Damage

Motivation: promising new physics is related to some very rarely produced particles, high event rate is necessary in many modern experiments. It means that detectors and electronics will be harshly irradiated! Example: Vertex Detectors at ATLAS and CMS will receive >10^{15} n_{1MeVeq}/cm^2 over the lifetime!

PKA : Primary Knock on Atom

-average recoil energy for PKA produced by 1 MeV neutrons is 50 keV

Displacement threshold in Silicon

-Single lattice atom (Frenkel pair): E_d~25eV

-Defect Cluster: E_c~5keV

Neutrons (elastic scattering)

-E_n > 185 eV for single displacement

-E_n > 35 keV for cluster

Electrons

-E_e > 255 keV for single displacement

-E_e > 8 MeV for cluster

60Co-gammas

-Compton electrons with max. E~1MeV (no cluster production)

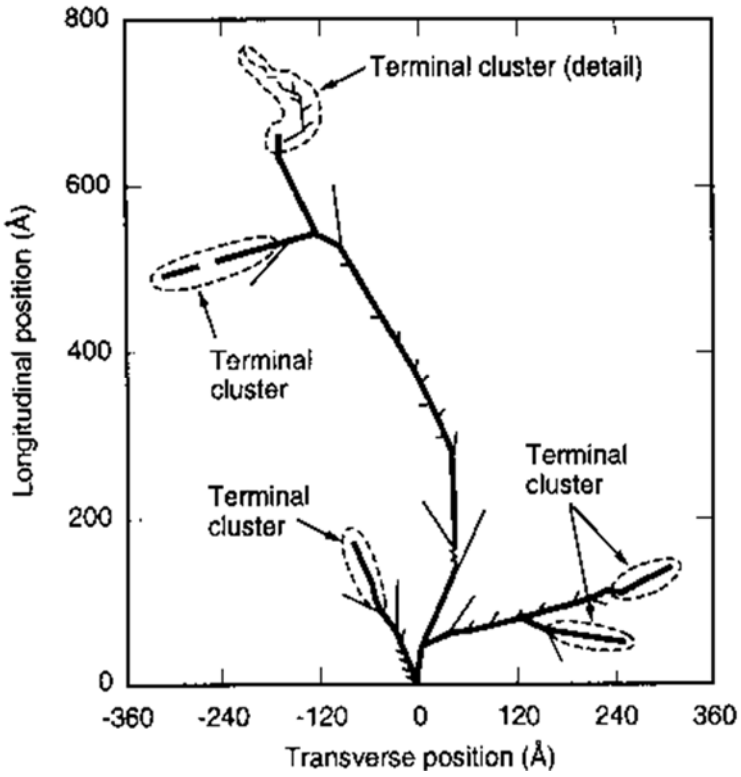

Wojciech.Dulinski@ires.in2p3.fr

Effect of damage in Silicon

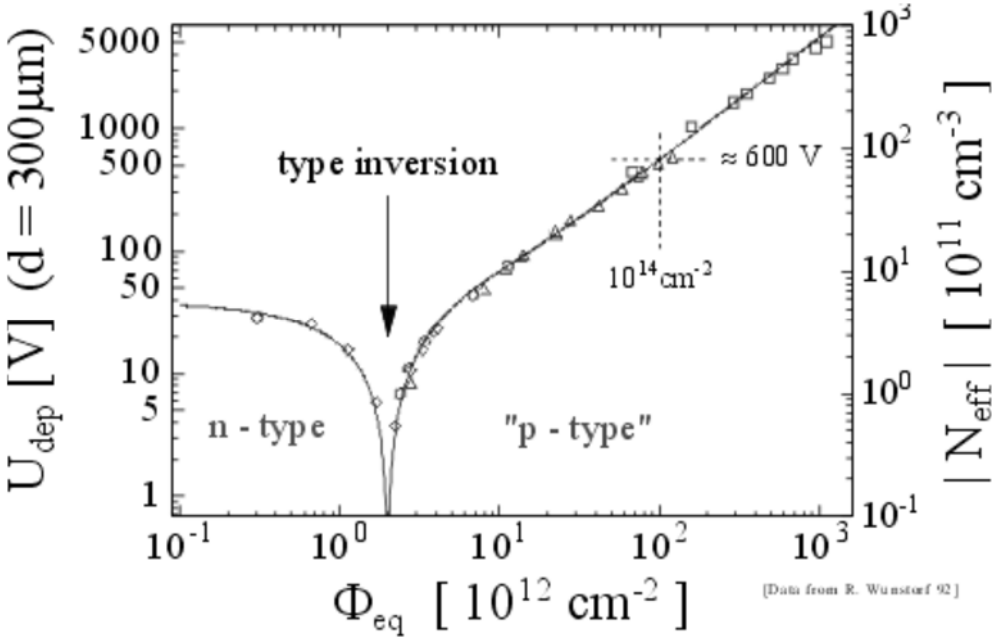

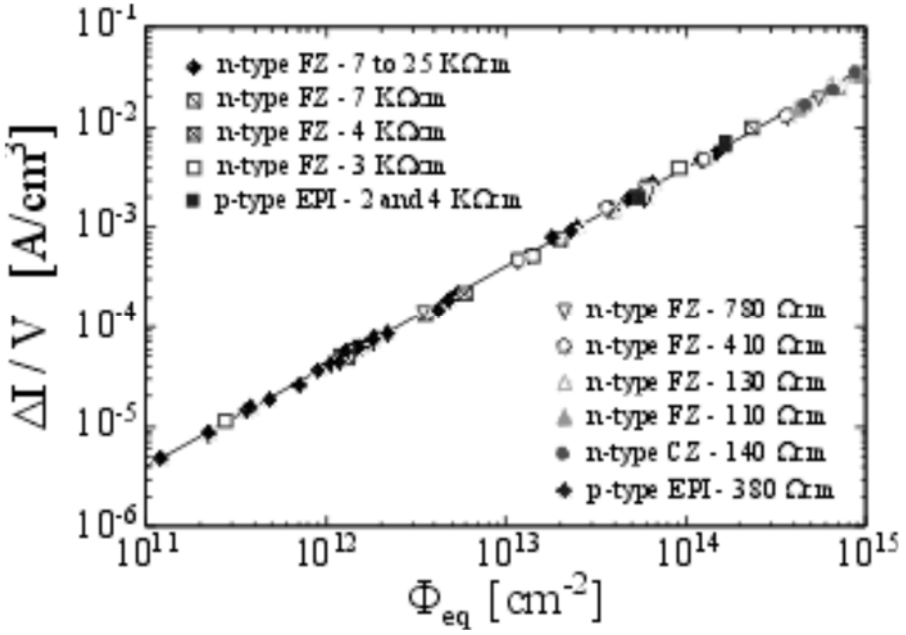

Changes in N_{eff} (effective doping concentration) and in full depletion voltage

$$N_{eff} \sim V_{dep}/d^2$$

Increase of a leakage current:

$$\Delta I = \alpha \Phi_{eq}$$

where α is a (universal) damage parameter

Wojciech.Dulinski@ires.in2p3.fr

Another solution for extreme irradiation: Silicon Radiation Sensor with Three Dimensional Electrode Arrays

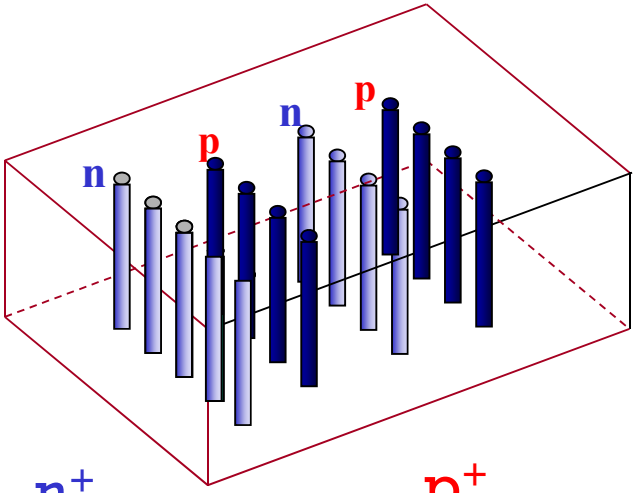

- SHORT COLLECTION PATHS 50 μm (300μm)
- LOW DEPLETION VOLTAGES <10V (60V)
- RAPID CHARGE COLLECTION 1-2n (25 ns)
- EDGELESS CAPABILITY active edges
- LARGE AREA COVERAGE active edges
- SUBSTRATE THICKNESS INDEPENDENT :
  - BIG SIGNALS
  - X-RAY DETECTION EFFICIENCY for low Z materials

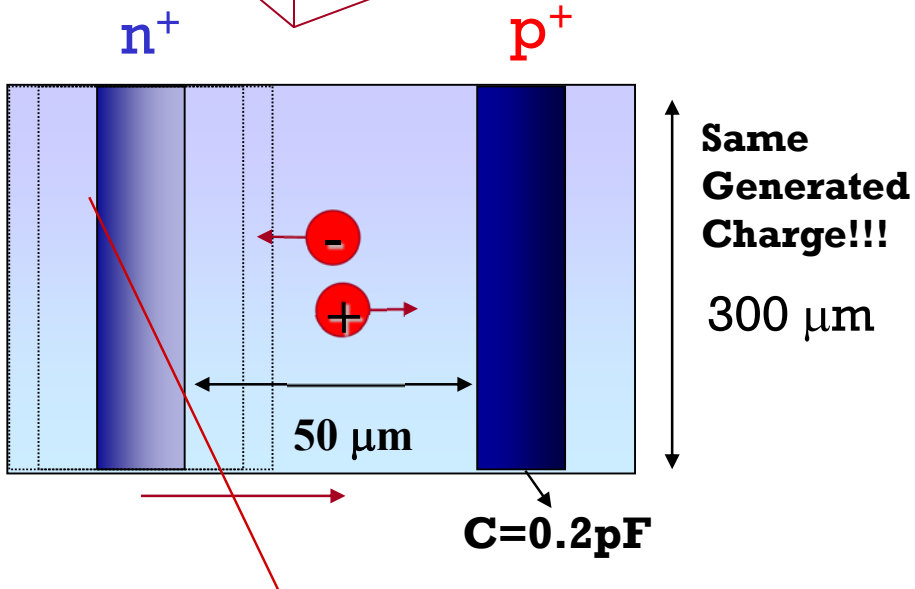

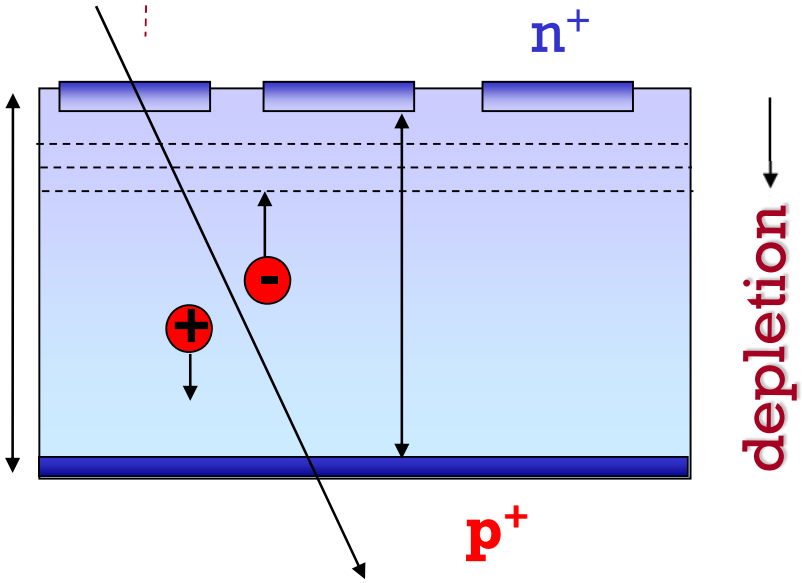

S. Parker, C. Kenney, 1995

Wojciech.Dulinski@ires.in2p3.fr

Still another solution for extreme irradiation: CVD diamond detectors

(CH_4, 1%) + H_2(99%) + energy (plasma) => CVD diamond layer
(T<1000°C, p<100 mbar)

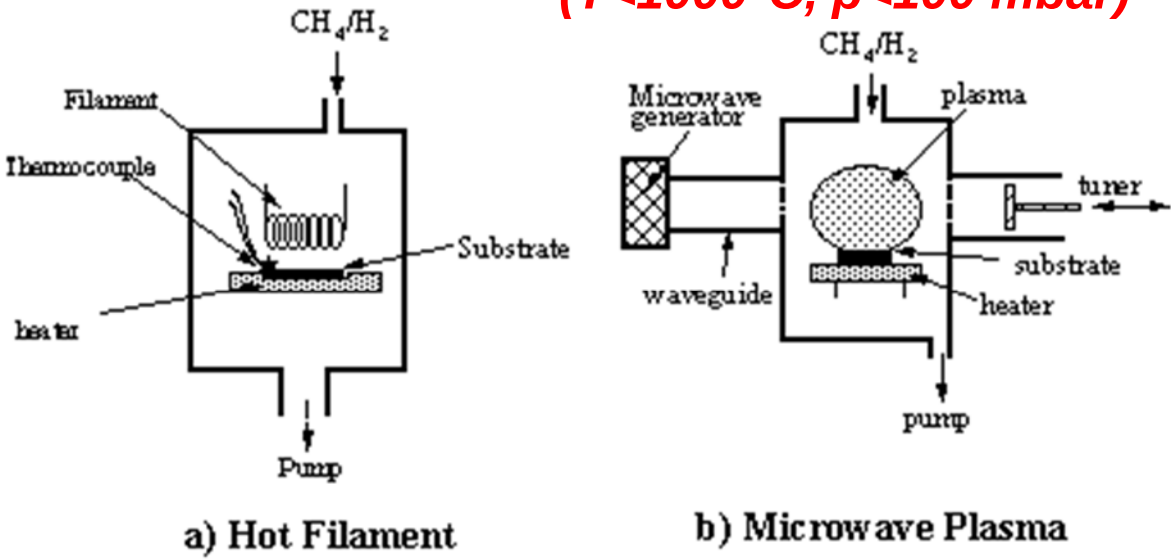

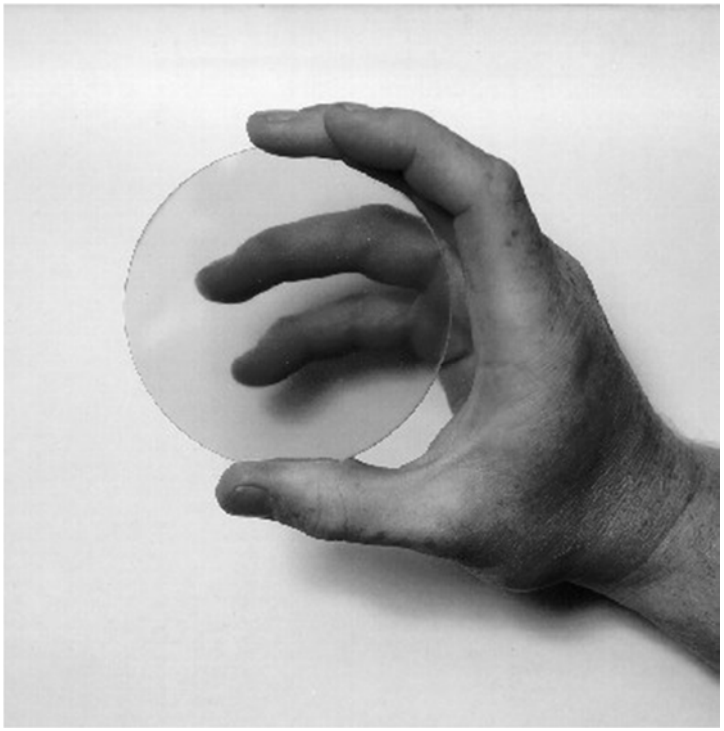

CVD diamond 4” wafer

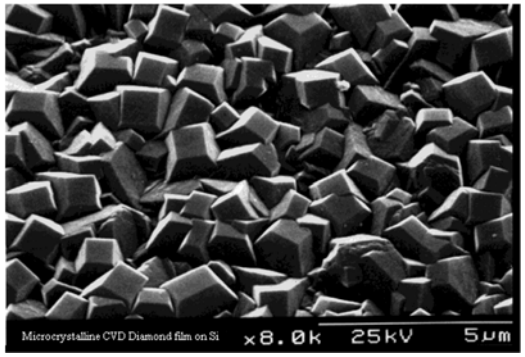

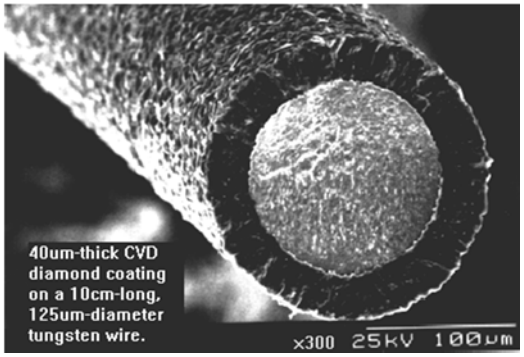

Couche du diamant : structure polycristalline

Wojciech.Dulinski@ires.in2p3.fr

Microstrip Silicon Detectors has been introduced in 1980, following introduction of the Planar Technology for detector fabrication.

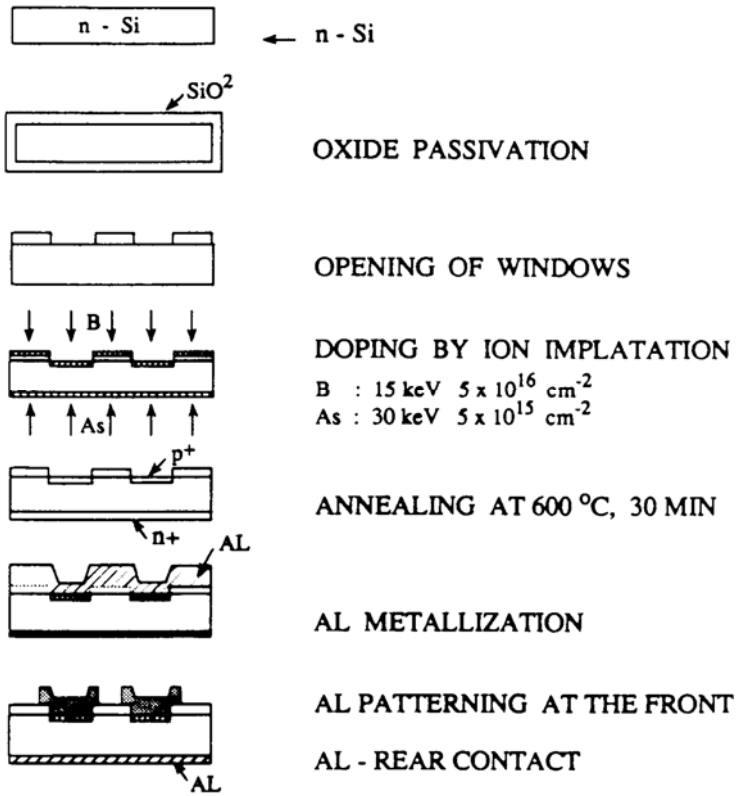

The planar process for detector fabrication. From:
Kemmer, NIM 226 **(1984)** 89

Today this technology is mature, systems having total sensor area of ~m^2 (10^5 readout channels) has been built for High Energy Physics (LEP) Experiments. Next generation of experiments will require both area and number of channels increased by factor of 100.

Wojciech.Dulinski@ires.in2p3.fr

CMOS Process: Complementary Metal-Oxide-Semiconductor (transistors)

The technology for constructing majority of today's electronics: microprocessors, memories, image sensors…

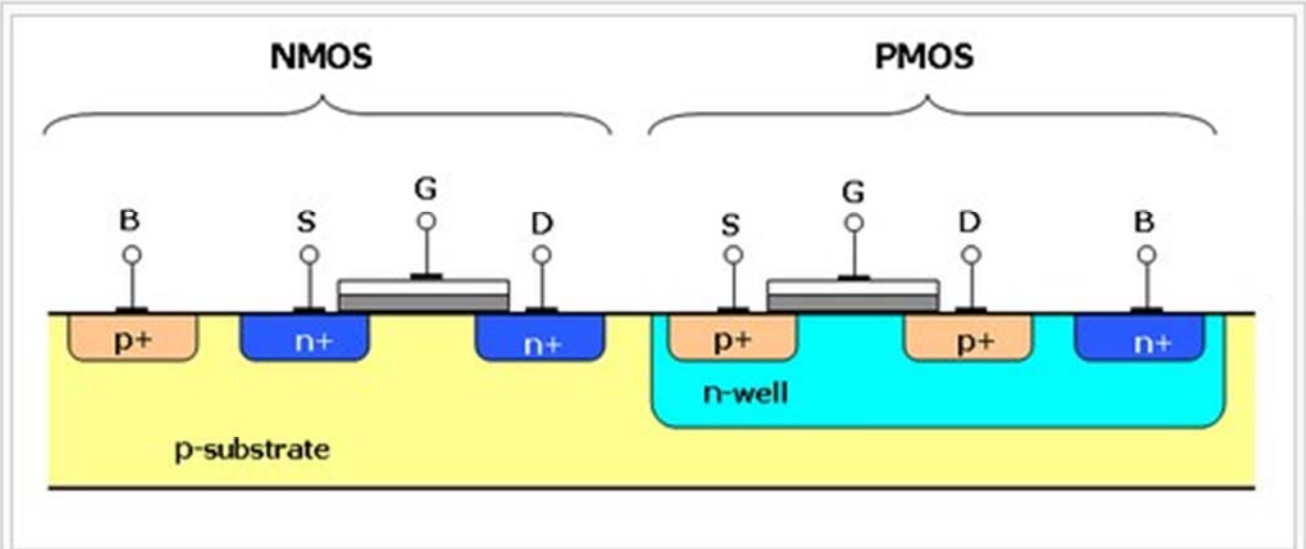

Cross section of two transistors in a CMOS gate, in an N-well CMOS process

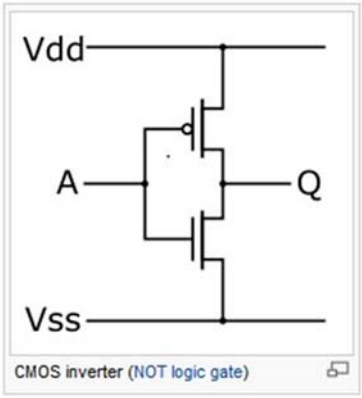

CMOS inverter (NOT logic gate)

Inverter (buffer):
2 CMOS transistors

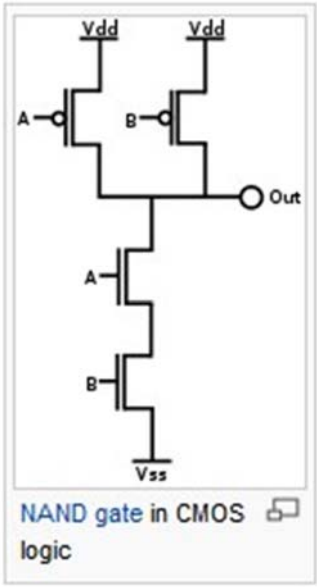

NAND gate in CMOS logic

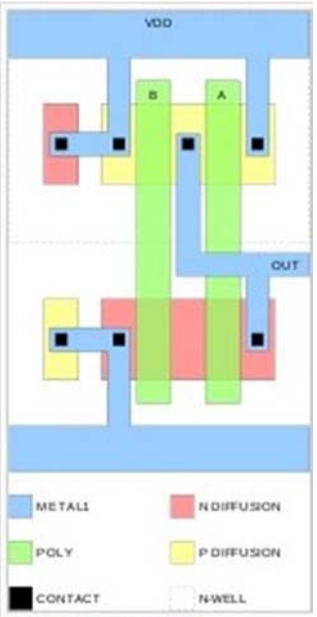

The physical layout

Logic gate (NAND):
4 CMOS transistors

Wojciech.Dulinski@ires.in2p3.fr

Current induced in segmented detector : Ramo's Theorem

$$i(t) = q\vec{v} \bullet \overrightarrow{P_k}$$

Where $\overrightarrow{P_k}$ is a pseudo-field (weighting field): $\overrightarrow{P_k} = -\vec{\nabla} V_k$

and V_k is a pseudo-potential calculated using following assumption:

1). V_k = 1 on the segment of interest
2). V_k = 0 elsewhere

$\vec{v}$ is a charge carrier velocity
(mobility and local physical electric field product)

Wojciech.Dulinski@ires.in2p3.fr

Strip detector: signal shape calculated using Ramo's Theorem

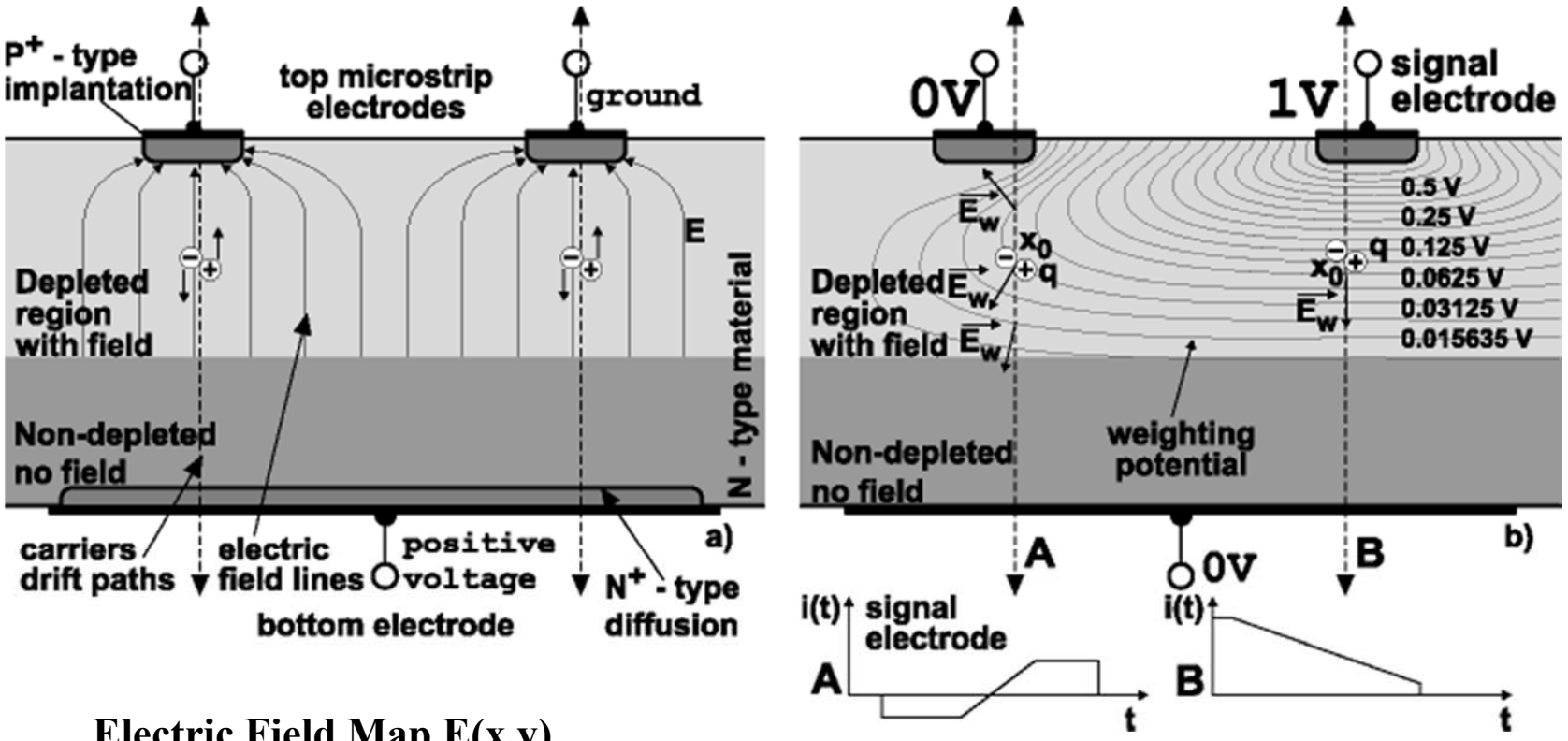

Electric Field Map E(x,y)

Drift velocity V(x,y)

Pseudo-field $P_k(x,y)$

Current I(t)

Wojciech.Dulinski@ires.in2p3.fr

Basic signal processing: integrating mode

What is used for amorphous-Silicon arrays (the detector is an amorphous silicon photodiode).

Charge preamplifier

Correlated double sampling (CDS)

Output voltage is proportional to the difference of V_2 - V_1

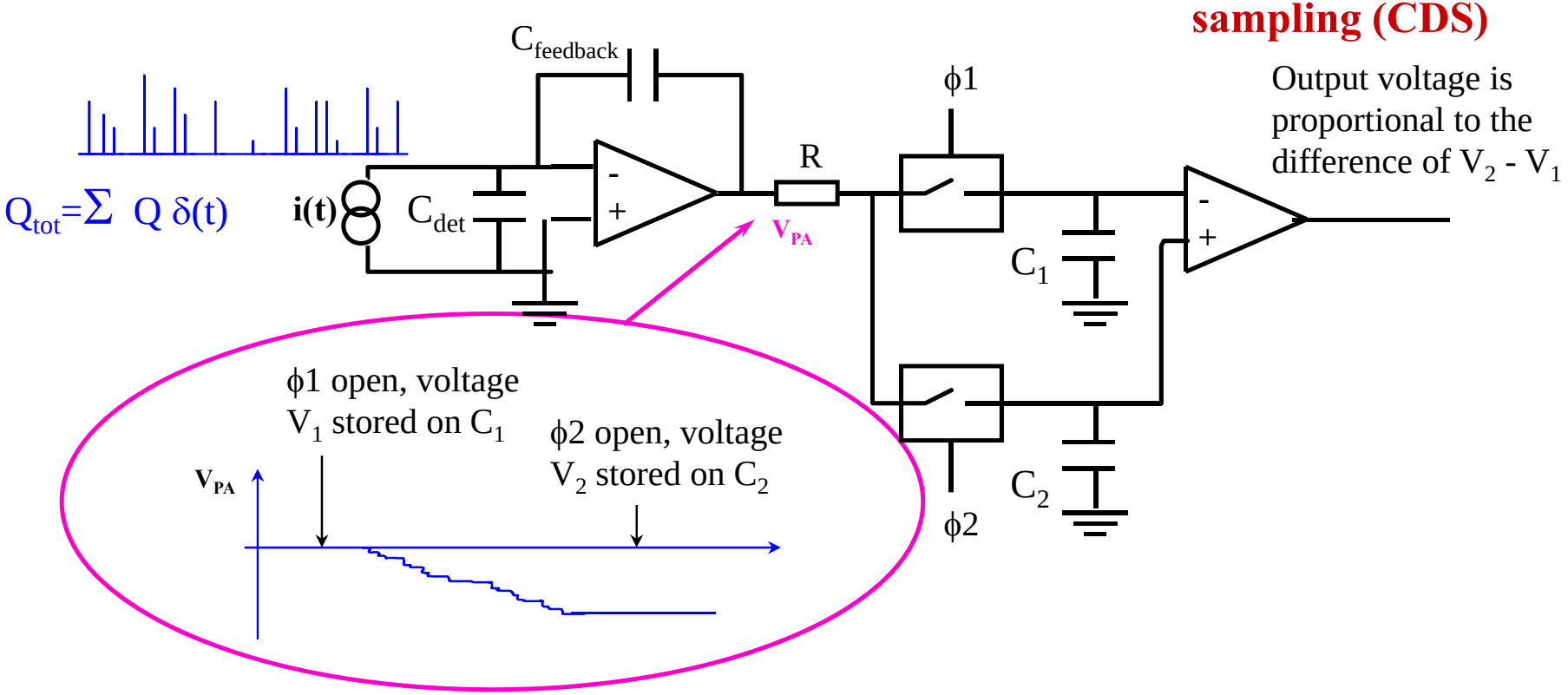

Wojciech.Dulinski@ires.in2p3.fr

Basic signal processing: single particle detection mode

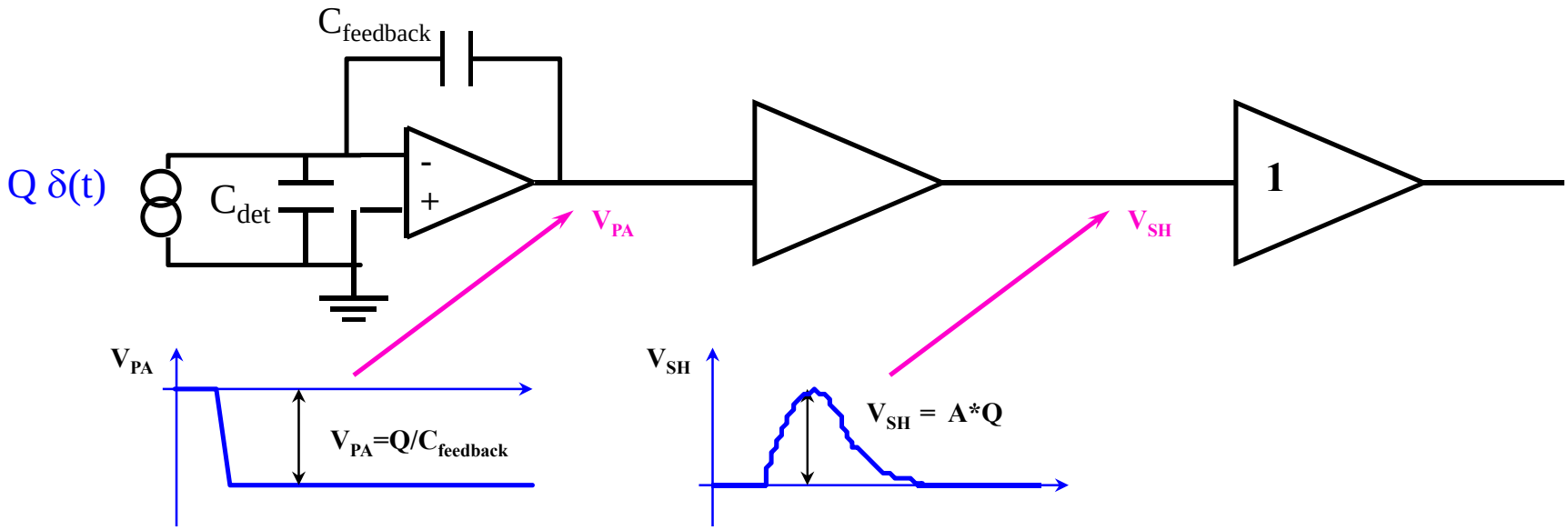

Charge preamplifier

Output signal proportional to the charge created by the radiation.
Charge proportional to the energy lost by the particle.

Shaper

The infinite step at the output of the charge preamplifier is transformed in a short pulse with amplitude proportional to Q.
It also filters the noise.

Buffer

It transforms impedances and optimises the power transfert.

Wojciech.Dulinski@ires.in2p3.fr

Semiconductor Position Sensitive Detectors: Silicon Drift Detector (SDD)

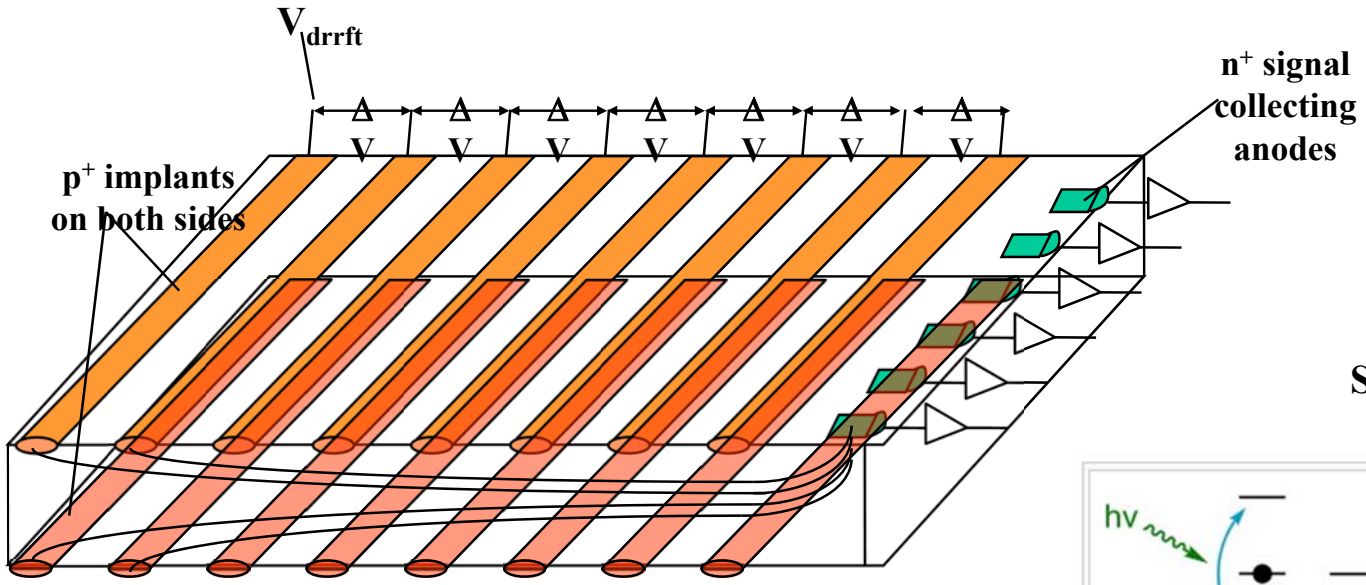

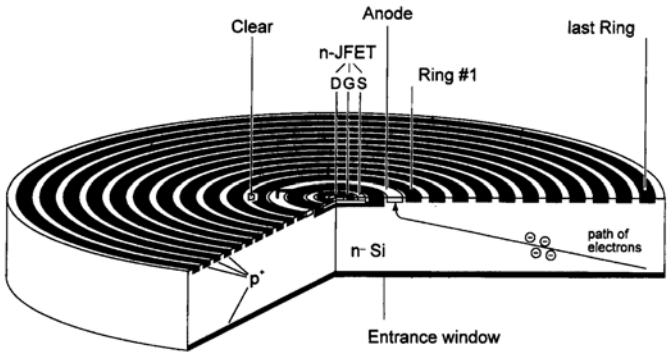

Silicon Drift Chamber used as photodetector

To be measured:
hit position, arrival time, signal amplitude

4 modes of operation: no time, external/ internal start, controlled drift

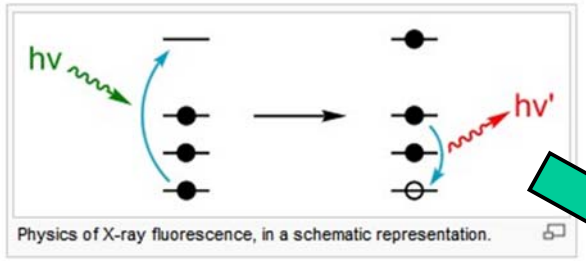

Physics of X-ray fluorescence, in a schematic representation.

Soft X-ray spectroscopy (fluorescence analysis, PIXE…)

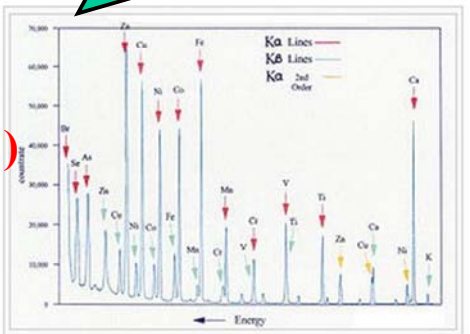

Figure 2: Typical energy dispersive XRF spectrum

Tracking in particle physics:
STAR (disaster!), ALICE (seems OK)

Excellent candidate for (space) Compton telescope???

Wojciech.Dulinski@ires.in2p3.fr

Semiconductor Position Sensitive Detectors: Charge Coupled Device (CCD)

An imaging CCD consist firstly of a square matrix of potential wells, so the charge signal generated below the silicon surface can be accumulated, building up an image. Secondly, by manipulating clock voltages in the parallel register charge can be transferred in parallel from one row to the next and into linear register in the bottom of the matrix. Then the linear register is read out, cell after cell. Thus the CCD image is converted from a 2-D charge pattern to a serial train of pulses.

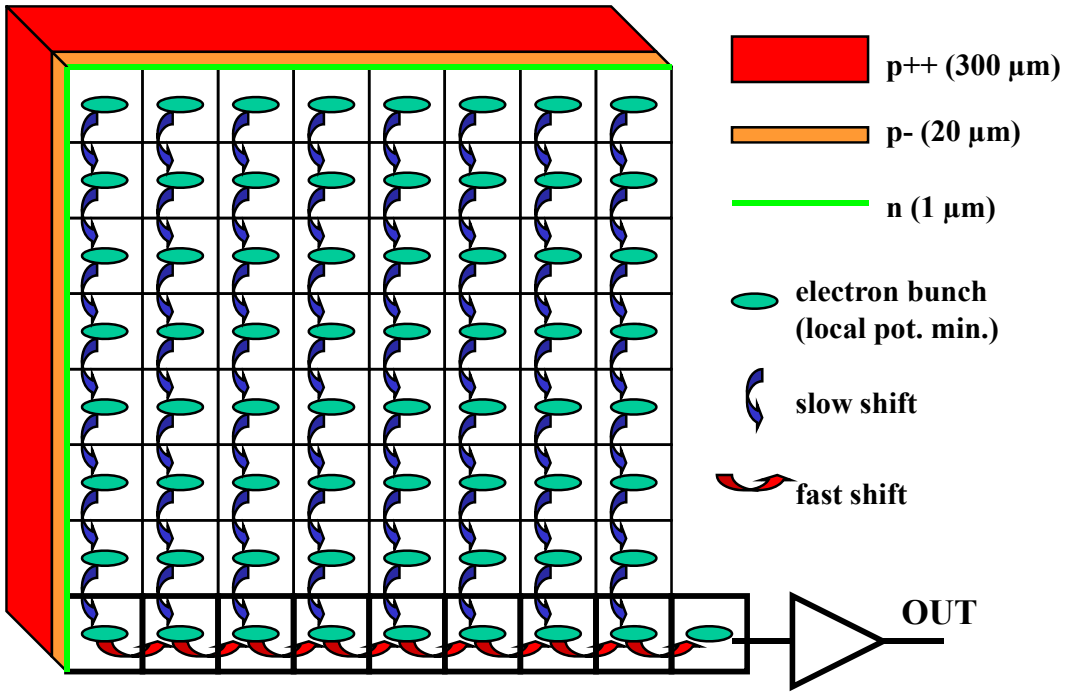

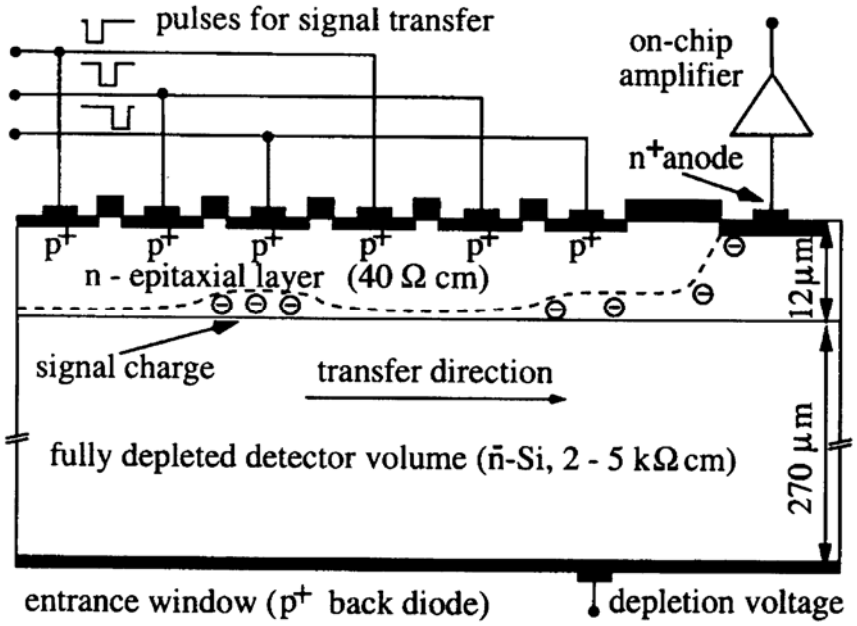

Fully depleted pn-CCD with integrated on-chip first amplification stage

Wojciech.Dulinski@ires.in2p3.fr

The EPIC/XMM camera based on pn-CCD

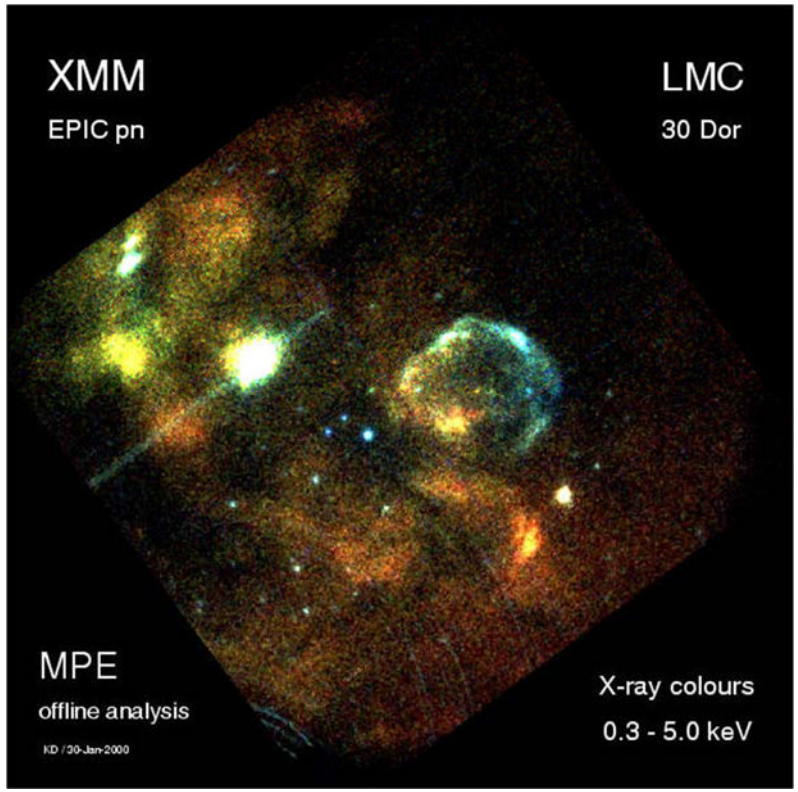

The large Magellanic Cloud in X-rays (0.3-5.0 keV). First Light Image of the pn-CCD camera.

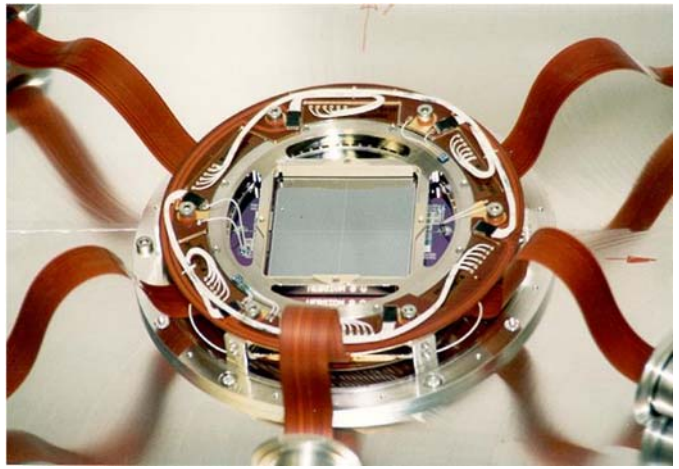

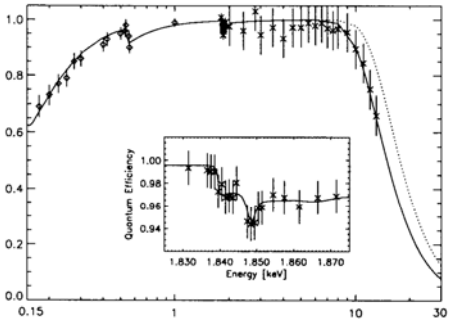

Figure 5. *Quantum efficiency of the pn-CCD. The solid line represents a 300μm thick sensitive volume, the dotted line 500μm.*

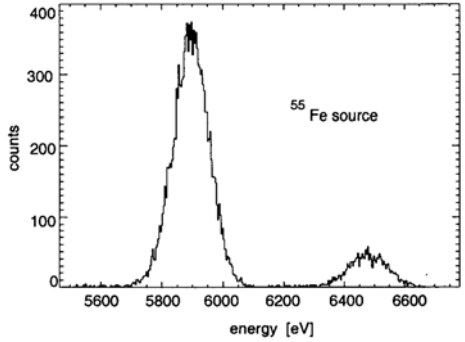

Figure 6. *Mn K_α spectrum of an ^{55}Fe source. The measured FWHM is 130 eV at -120° C .*

The 6 cm×6 cm large pn-CCD will be the heart of the EPIC/XMM camera. The picture shows the twelve chips mounted and the connections to the integrated preamplifiers. The quantum efficiency is greater than 80% over the whole XMM energy range of 200 eV to 12 keV. It is extremely radiation-resistant, has a good energy resolution, and owns an excellent time resolution.

Wojciech.Dulinski@ires.in2p3.fr

DEPFET Pixel Sensor for X-rays

- can be back illuminated, can have a fill factor of 1, can be made very large (all pros of CCD)
- does not need a charge transfer, no out-of-time events, every pixel is xy-addressable (all pros of APS)
- in addition, can have a non destructive multiple readout to reach very low noise figures

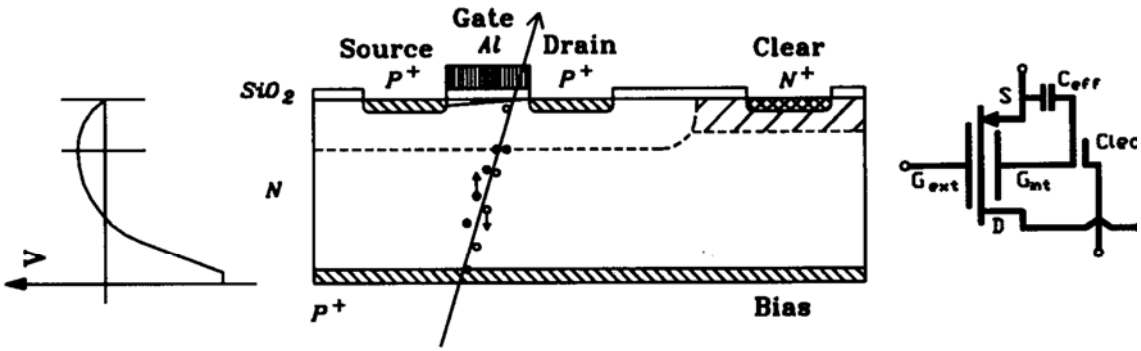

Figure 1. *The DEPFET structure and device symbol*

J.Kemmer, G.Lutz et al. NIM A 288 (1990) 92

Device concept:
combination of FET transistor with sideward depletion (drift chamber)

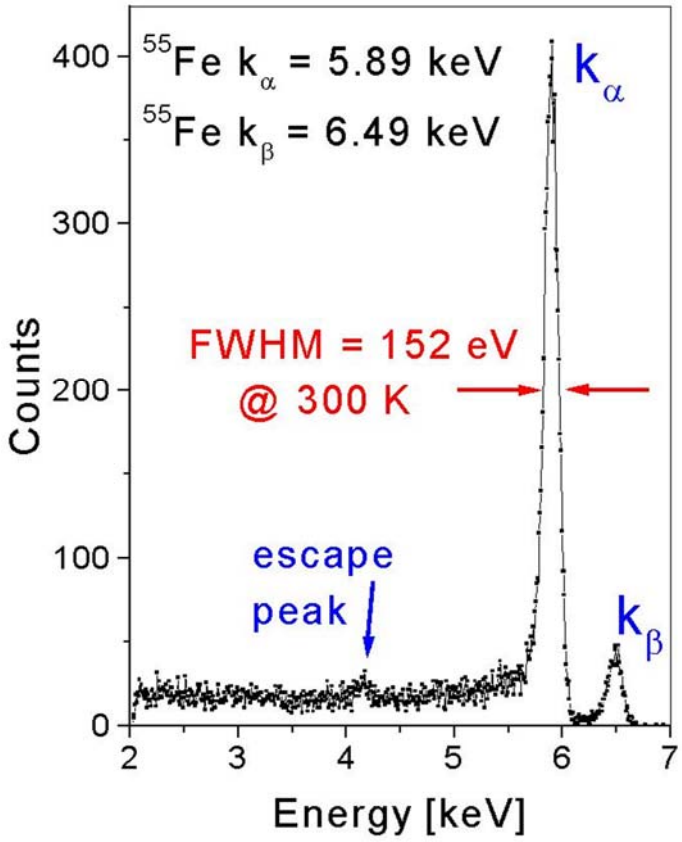

DEPFET : excellent noise figures (9 electrons rms.) at room temperature!

Wojciech.Dulinski@ires.in2p3.fr

DEPFET: non-destructive readout!

Sub-Electron noise measurements on RNDR Devices (Repetitive, Non-Destructive Readout)

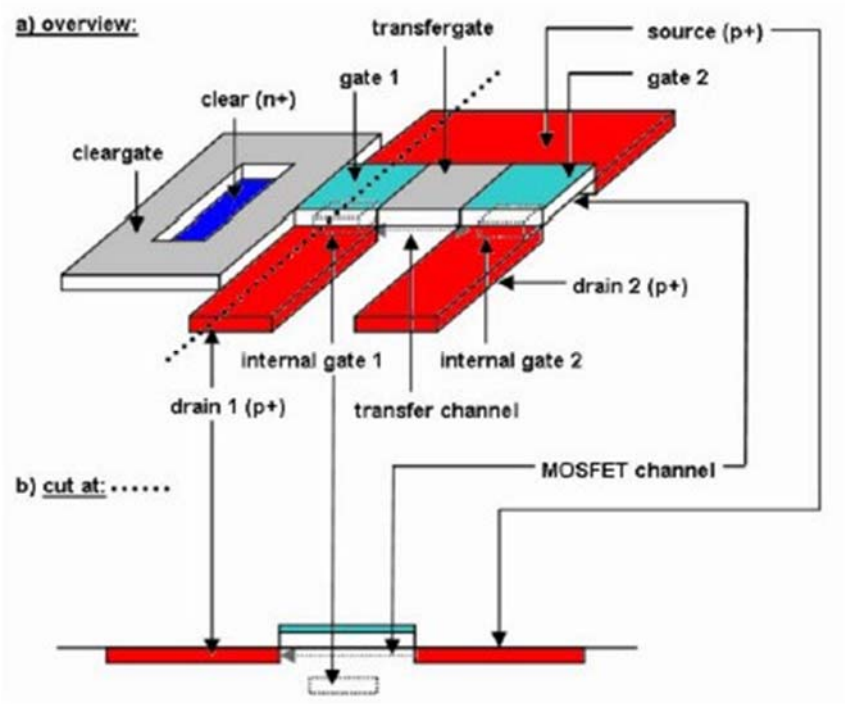

Twin-DEPFET with a CCD-like charge transfer

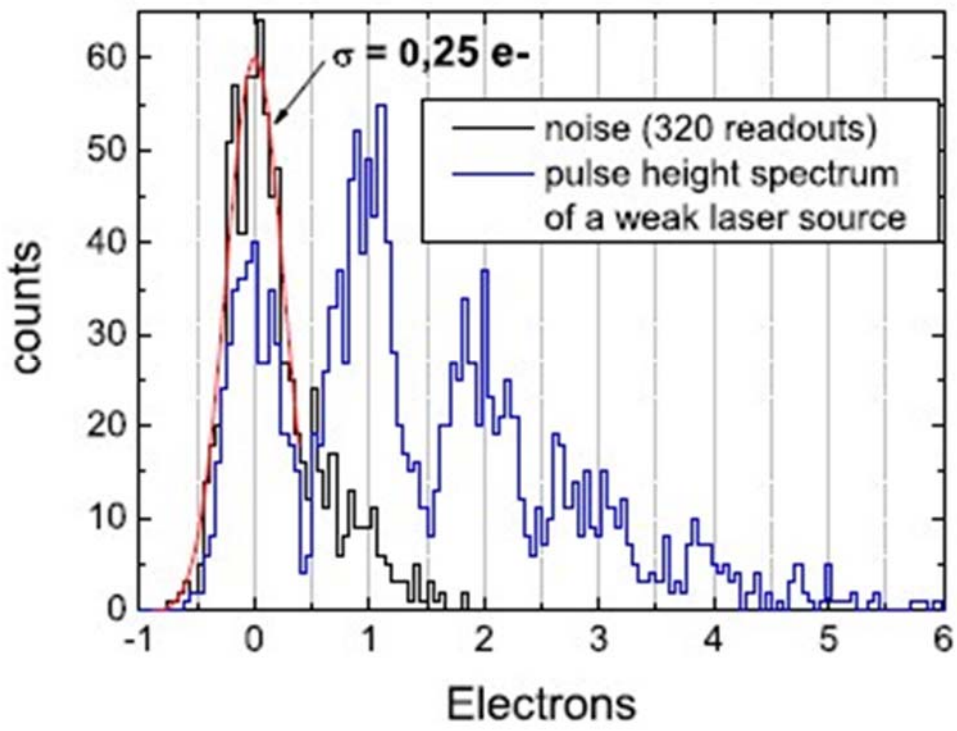

$$\sigma_{ENC} = 0.25\ e^- = 4.6\ e^- / \sqrt{360}$$

Wojciech.Dulinski@ires.in2p3.fr

Amorphous silicon array

Based on Flat Panel display technology. First theoretical studies in 1989. Pixel size down to 127 μm. Size up to about 43*43 cm^2, 14-bit data. Number of pixel up to 9 millions. Many manufacturers are close (or ready) to commercialisation for digital radiology.

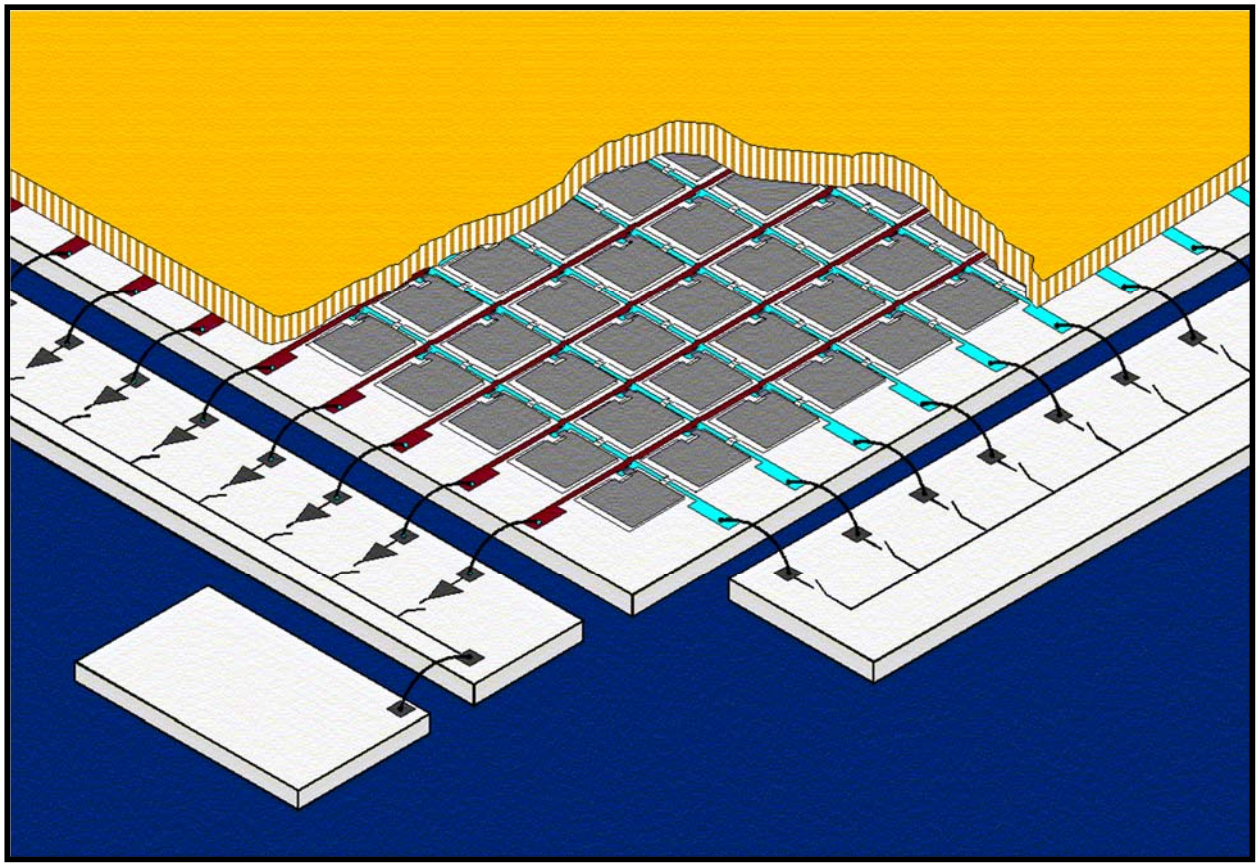

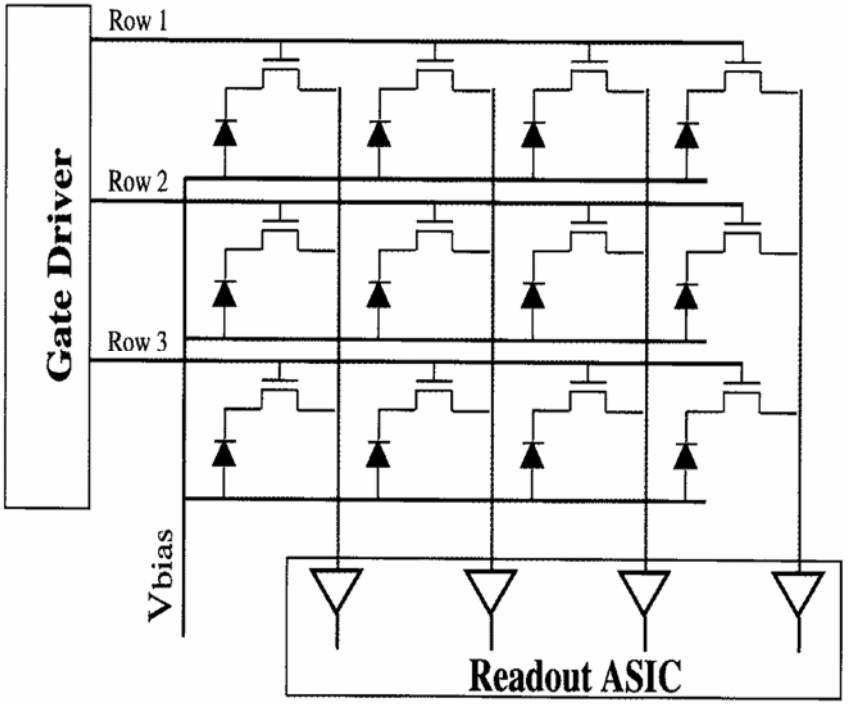

Sensor structure

Static AND dynamic detectors

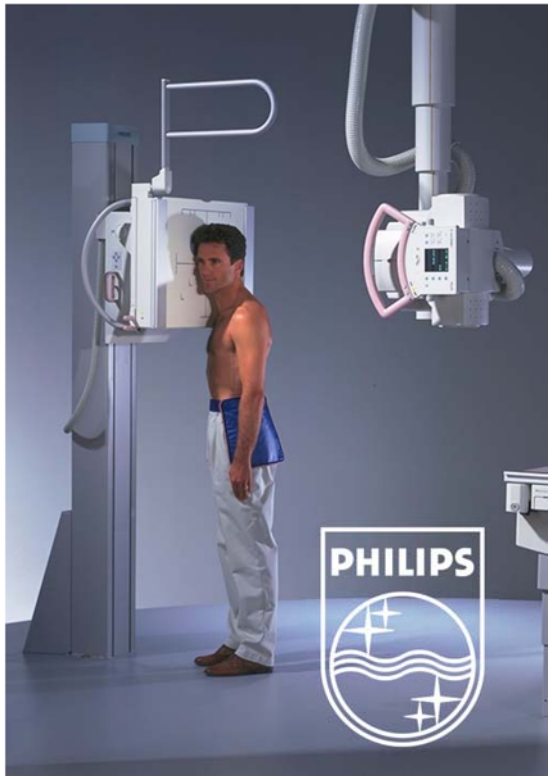

	Digital Diagnost	*Integris Allura FD*
Detection	static	static + dynamic (up to 30 frames/s)
Field of view	43 cm x 43 cm	18 cm x 18 cm
Number of pixels	3k x 3k	1k x 1k
Pixel size	143 µm x 143 µm	184 µm x 184 µm
DQE(0)	≈ 60 %	≈ 75 %

Shoulder

Heart arteries with contrast agent

Wojciech.Dulinski@ires.in2p3.fr

CdTe/CdZnTe detectors: high Z, high band-gap (room temperature) semiconductor

Detectors

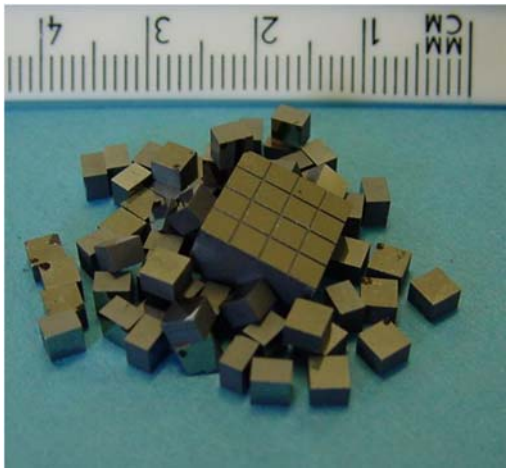

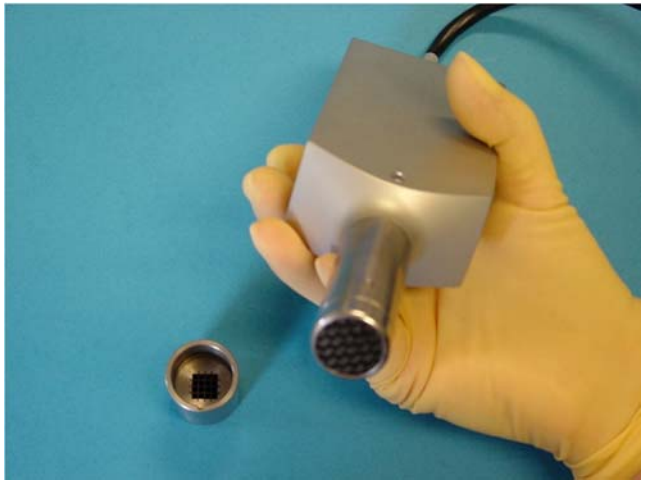

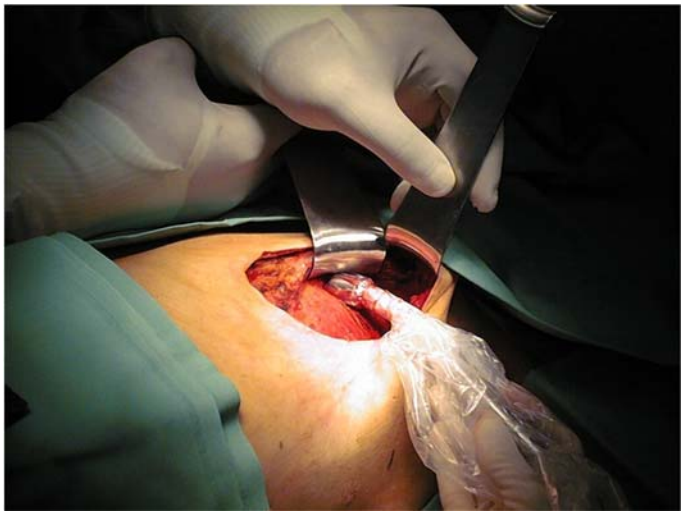

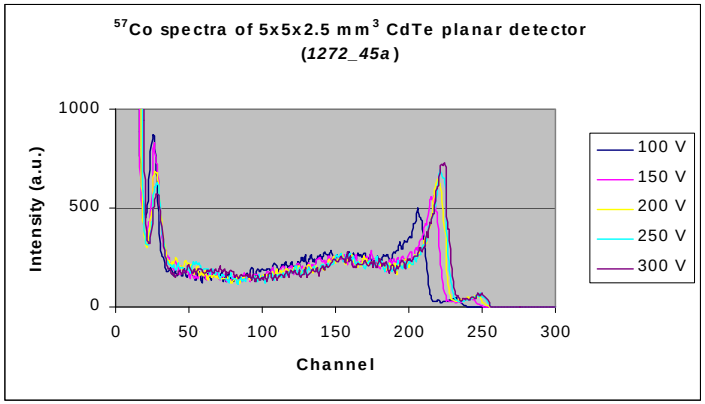

57Co spectroscopy with a small size planar detectors

CdTe 4x4 array
2.23x2.23x5mm³
(pitch 2.4 mm)

Weight = 500 g

Standard and mini-probes from:

EURORAD

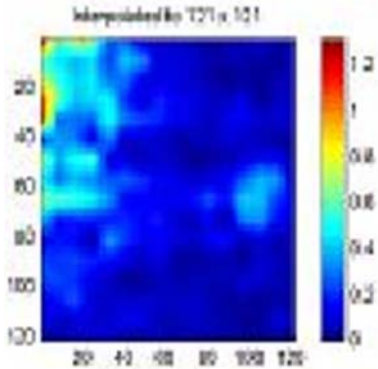

Mini-Gamma camera:
Sentinel node image

Wojciech.Dulinski@ires.in2p3.fr

Perspectives: Gamma-Ray Tracking Arrays

a way to construct a 4π Germanium shell detector

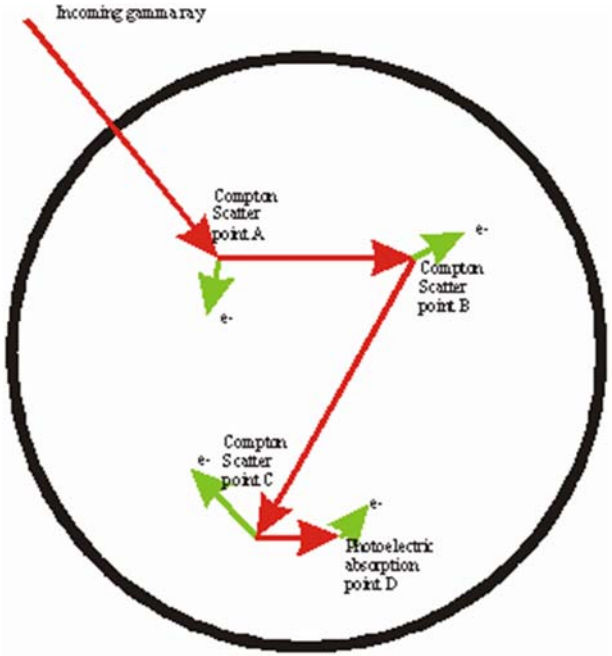

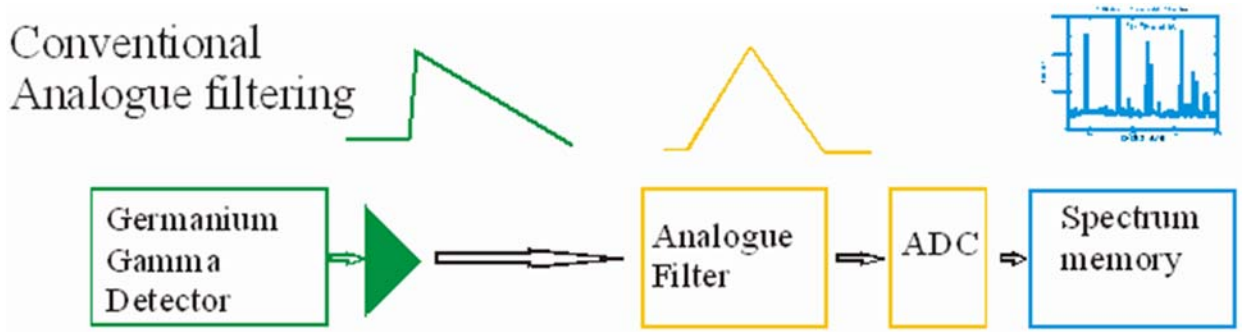

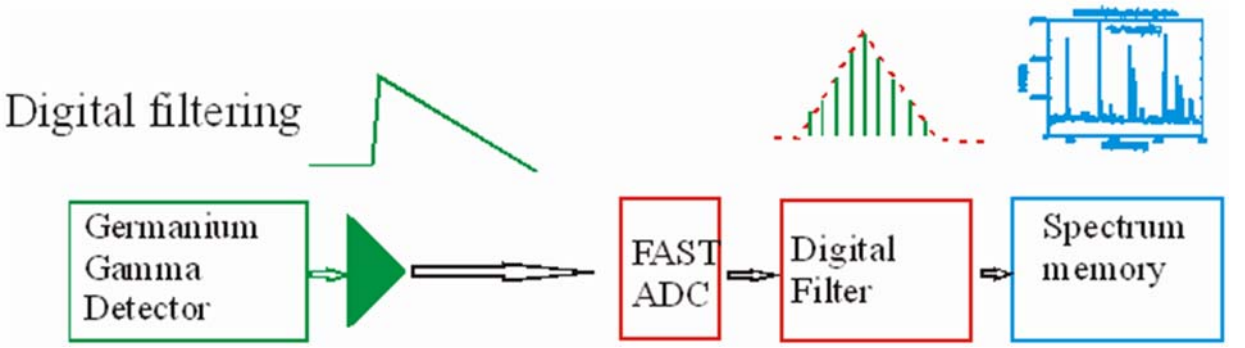

Several development items:

- segmented Ge detectors
- digital signal-processing electronics
- pulse shape analysis methods
- tracking algorithms
- simulation of tracking arrays

Wojciech.Dulinski@ires.in2p3.fr

AGATA: Advanced Gamma-Ray Tracking Array

Detectors

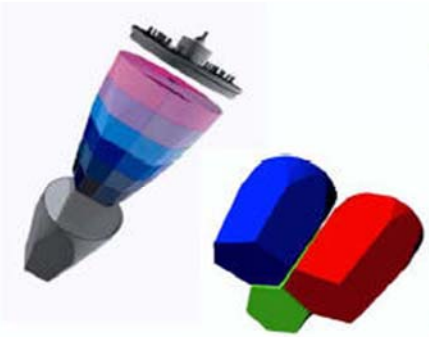

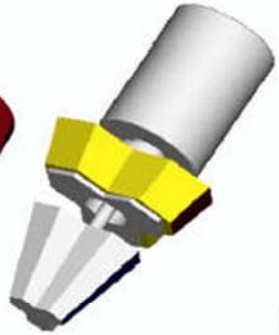

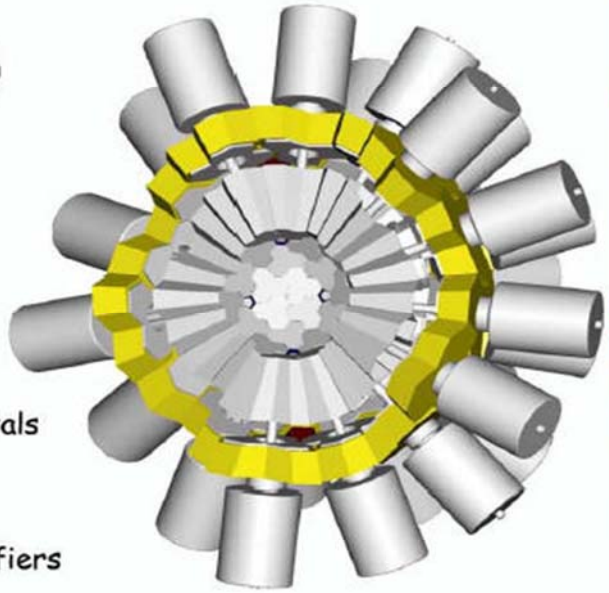

Ge crystals:
Hexaconical shape
90-100 mm long
80 mm max diameter
36 segments
Al encapsulatation:
0.6 mm spacing
0.8 mm thickness

Triple clusters:
3 encapsulated crystals
Al end-cap:
1.5 mm spacing
1.5 mm thickness
111 cold FET preamplifiers

Distance between faces of crystals:
in same cluster ~3 mm
in adjacent clusters ~9 mm

Total weight of the 60 clusters of the AGATA-180 configuration ~2.5 tons
Mounted on a self-supporting structure

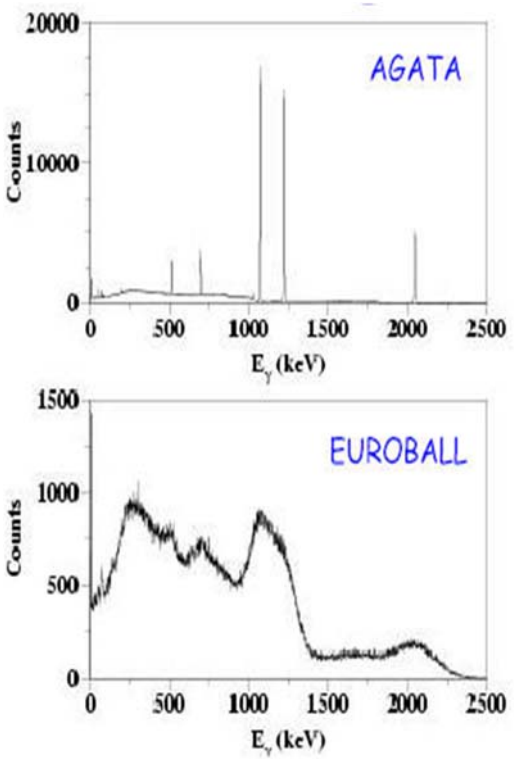

Simulated g-ray spectra comparing the response of AGATA (top) with that of a conventional Ge-array (bottom) assuming a fragmentation reaction at 100 MeV/A.

Wojciech.Dulinski@ires.in2p3.fr

Monolithic Active Pixel Sensor: use of thin epitaxial layer (10 – 20 µm) for MIP tracking. Industrial CMOS process for fabrication!

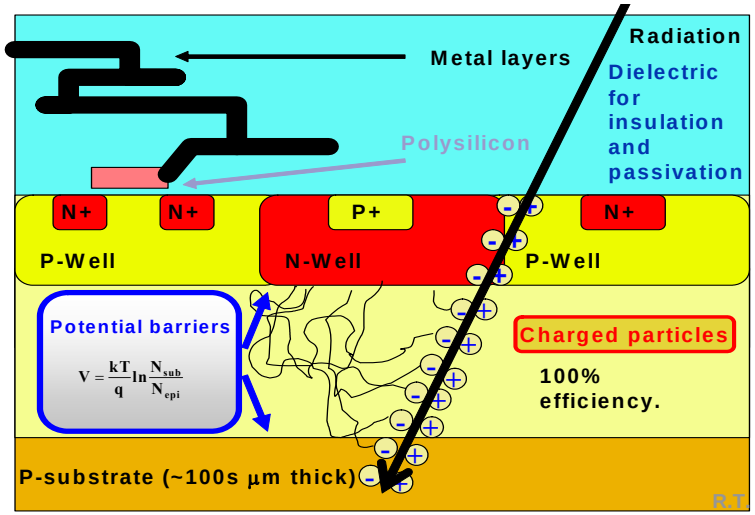

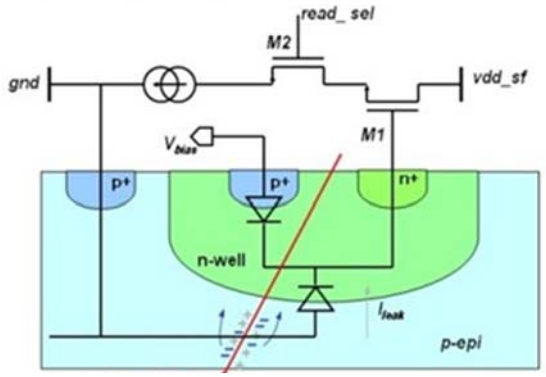

In-pixel electronics (SF, the simplest example)

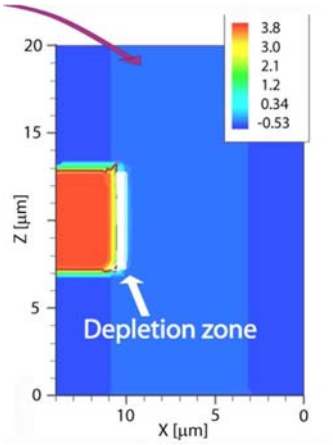

past *present*

Industrial availability of high resistivity substrate (epi) in a standard process

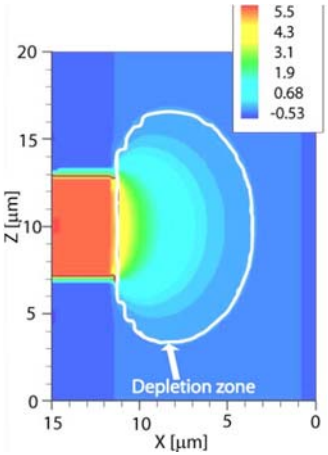

Fast and more efficient charge collection
→ should be radiation tolerant

Wojciech.Dulinski@ires.in2p3.fr

Present status of MAPS: just one example of mature design

Binary sparsified readout sensor for EUDET beam telescope:
> 2 cm^2 active area, 0.7 Mpixel tracker

- Medium speed readout (100 µm integration →10 kFrame/s)
- Spatial resolution < 4 µm for a pitch of 18.4 µm
- Efficiency for MIP > 99.5 %
- Fake hit rate < 10^{-6}
- Radiation hardness > 10^{13} n/cm^2 (high resistivity epi substrate)
- Easy to use, "off-shell" product: used already in several application

-Recent newcomer : Ultimate sensor for STAR Microvertex upgrade (~4 cm^2)

- **Radiation hardness: >10^{14} n/cm^2 attainable!**

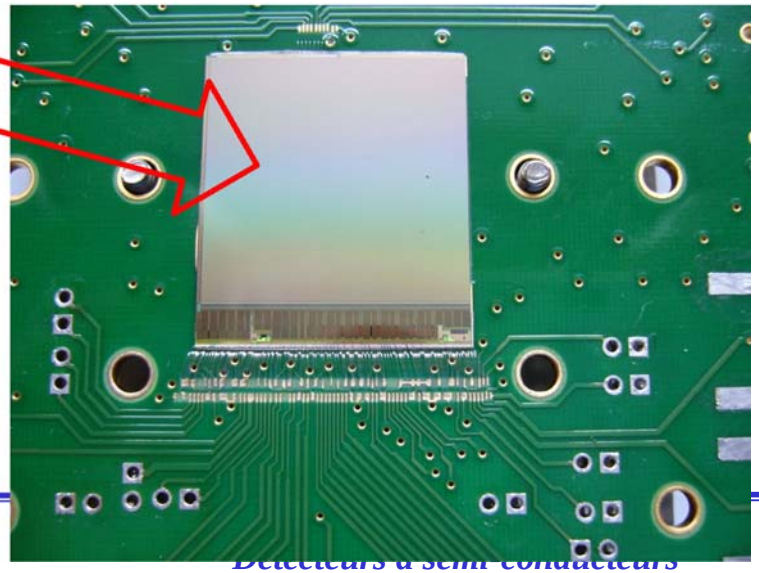

Wojciech.Dulinski@ires.in2p3.fr

One of the main feature of MAPS

Can be very thin (~25 µm of silicon in total) and still fully efficient!

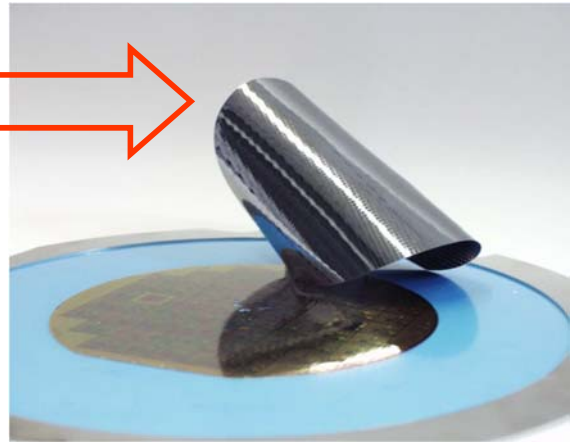

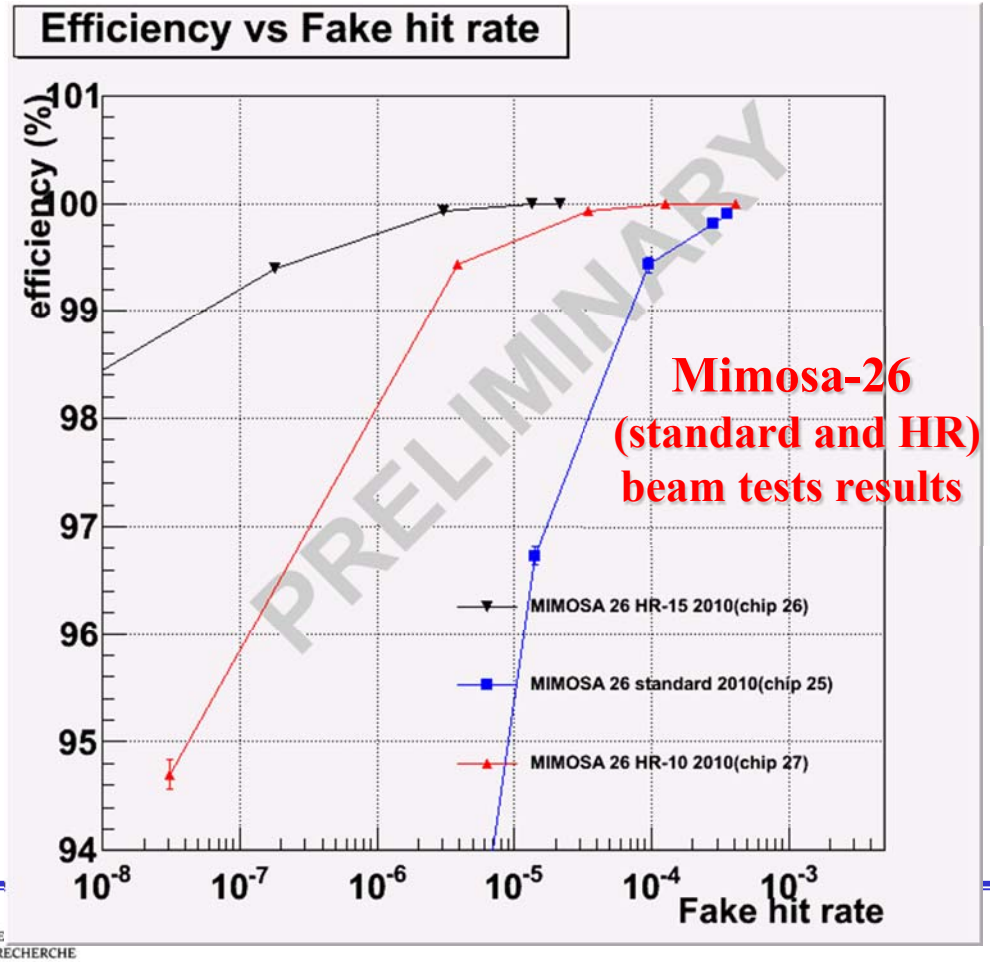

Mimosa-26 (standard and HR) beam tests results

Record spatial resolution

(Mimosa18, 10 µm pitch)

$\sigma_{x,y} \leq 0.95$ µm

Wojciech.Dulinski@ires.in2p3.fr

Applications of CMOS sensors in physics experiments

Generic beam telescope → internationale tests infrastructure

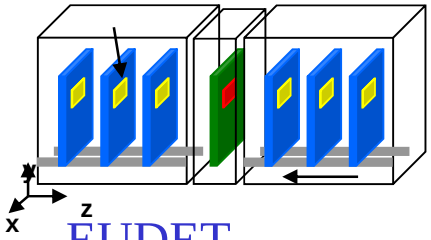

EUDET
(EU FP6)

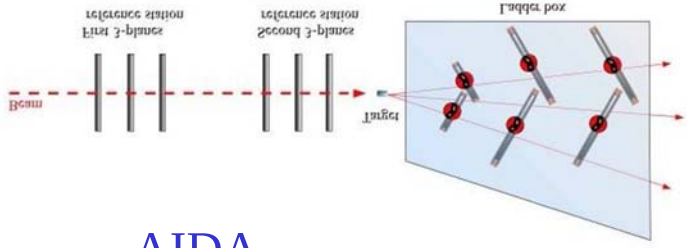

AIDA
(EU FP7)

Vertex detectors → subatomic physics experiments

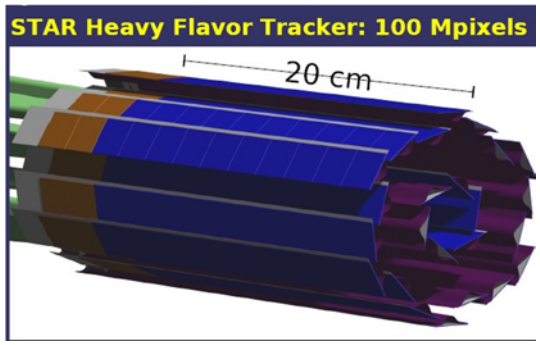

STAR
(RHIC, Brookhaven)

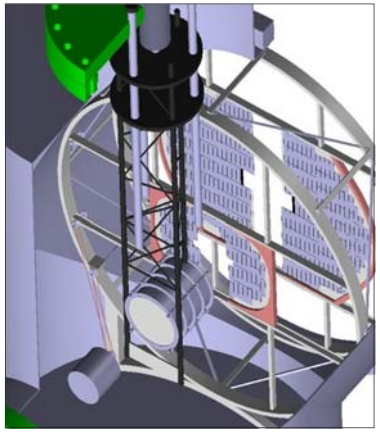

CBM
(SIS, Darmstadt)

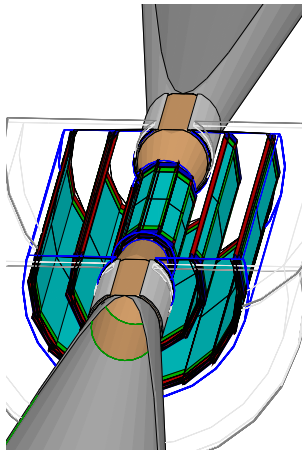

ILC
(?)

In discussion: vertex detector for ALICE and SuperB, electromagnetic calorimeter (FoCal) for ALICE/LHC → 50 m² of CMOS sensors (~5 M€)

Wojciech.Dulinski@ires.in2p3.fr

Some other applications…

Silicon Ultra Fast Cameras in Medical Application

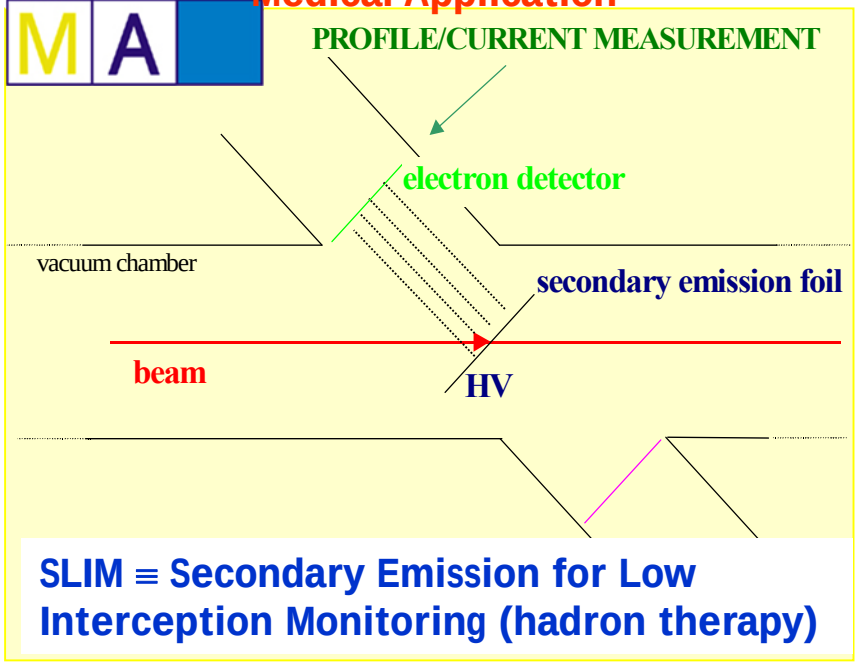

SLIM ≡ Secondary Emission for Low Interception Monitoring (hadron therapy)

eb-cmos for fluorescence microscopy

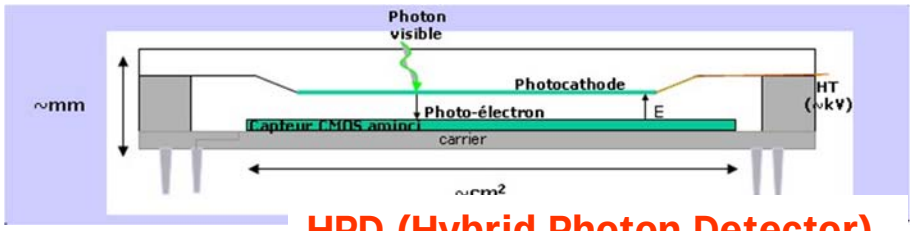

HPD (Hybrid Photon Detector)

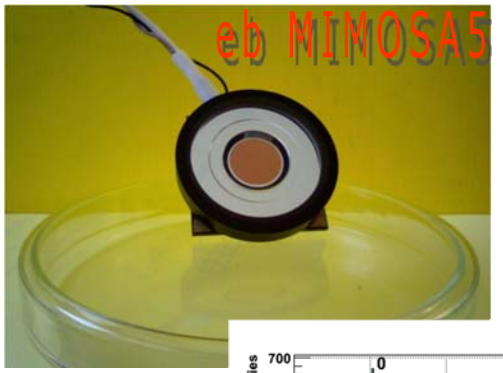

aile de drosophile avec EBMIMOSA

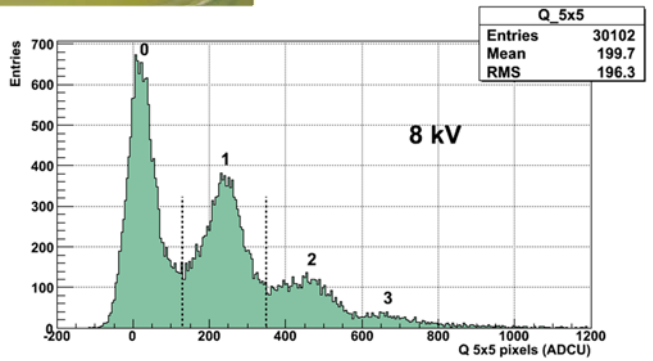

Single photo-electron spectrum

Antiproton beam profile measured with back-illuminated MimoTERA sensor

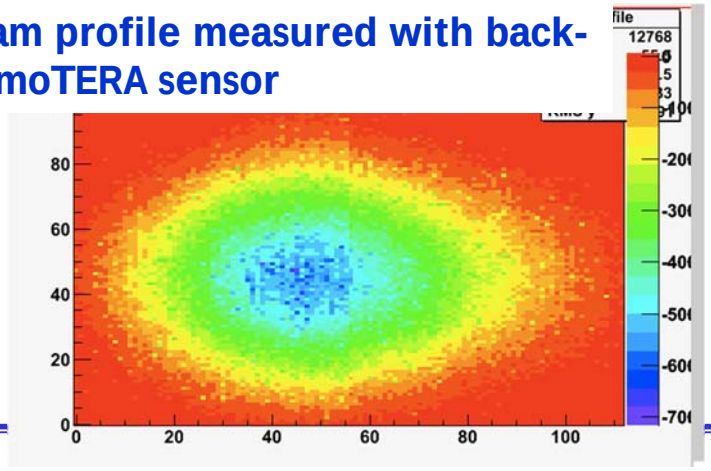

Wojciech.Dulinski@ires.in2p3.fr

Avalanche diodes for low light level, 3D-imaging

(credit to Iouri.Musienko@cern.ch for some slides)

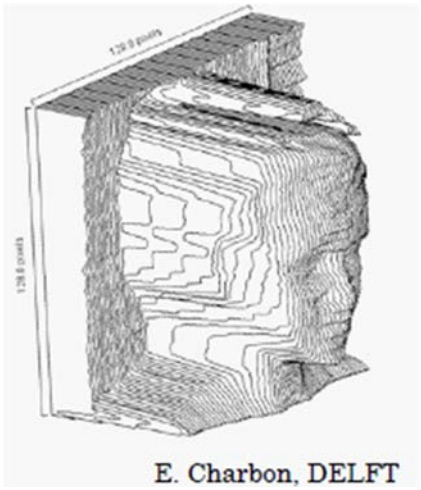

3D image recorded with TOF pixel sensor

Applying high electric field in uniform p-n junction may cause an avalanche multiplication of electrons and holes created by absorbed light…

Linear APD parameters (CMS APD)

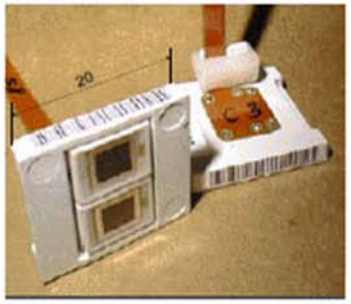

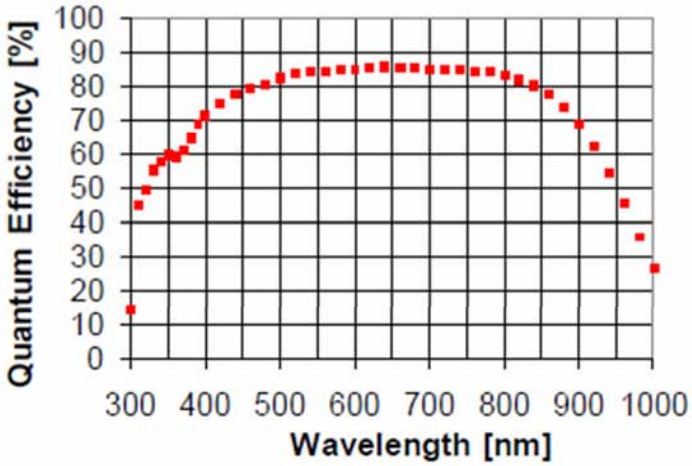

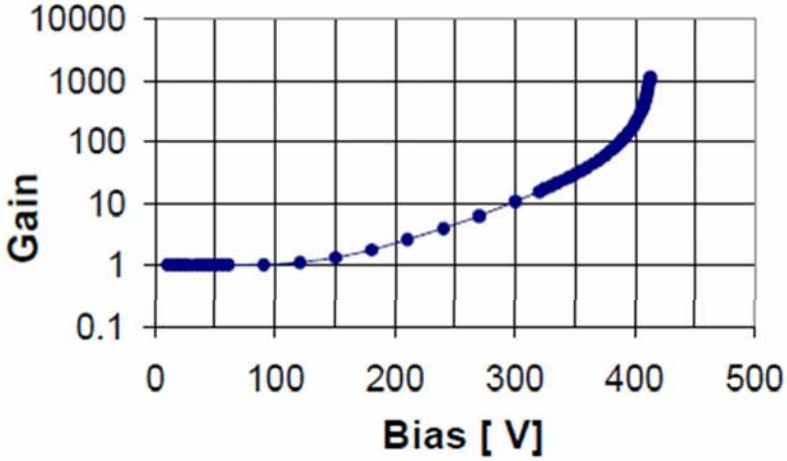

Wojciech.Dulinski@ires.in2p3.fr

APDs operated in Geiger mode

Photon counting with high efficiency → operate APDs over breakdown → Geiger mode APDs

Single pixel Geiger mode APDs were developed a long time ago
(see for example: *R. Haitz et al, J.Appl.Phys. (1963-1965)*
R. McIntyre , J.Appl.Phys. v. 32 (1961))

Planar APD structure

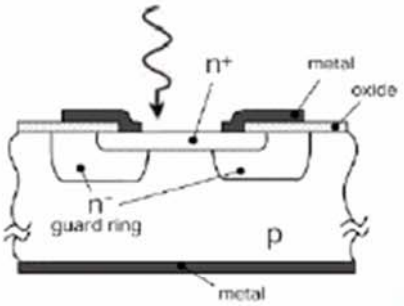

Passive quenching circuit

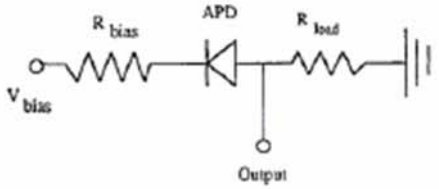

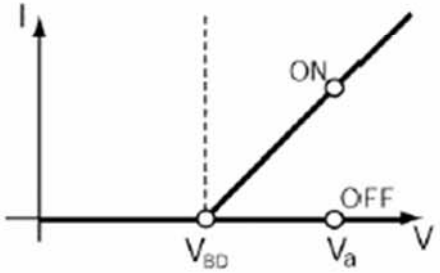

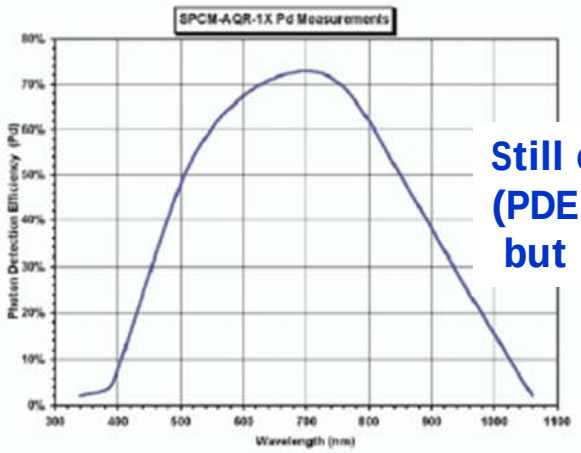

Still excellent Single Photon Detection Eff. (PDE up to 70%) and timing (FWHM ~350 ps) but low temperature operation, linearity…

Wojciech.Dulinski@ires.in2p3.fr

SiPM structure and principles of operation

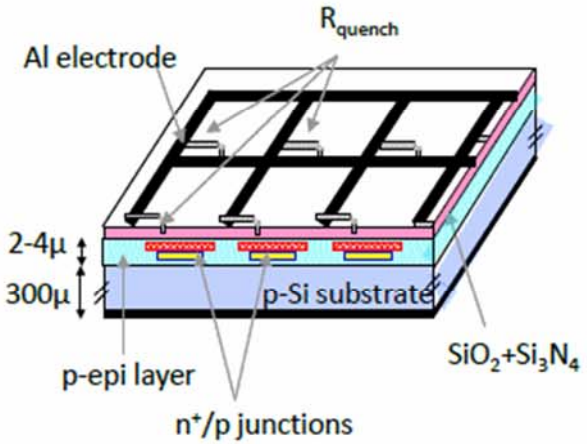

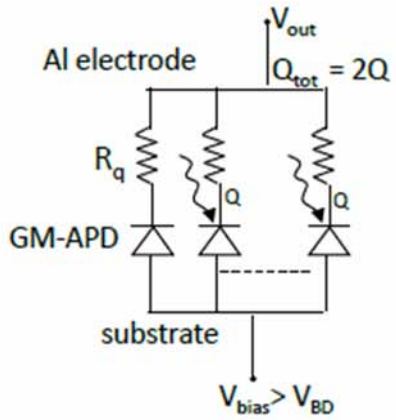

(EDIT-2011, CERN)

- *SiPM is an array of small cells (SPADs) connected in parallel on a common substrate*
- *Each cell has its own quenching resistor (from 100kΩ to several MΩ)*
- *Common bias is applied to all cells (~10-20% over breakdown voltage)*
- *Cells fire independently*
- *The output signal is a sum of signals produced by individual cells*

For small light pulses (N_γ<<N_{pixels}) SiPM works as an analog photon detector

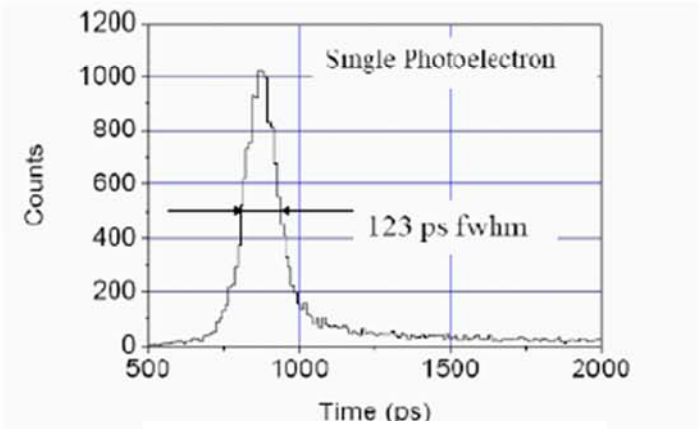

SiPM time resolution

Wojciech.Dulinski@ires.in2p3.fr

Avalanche diodes (SPADs) in CMOS?

dSiPM (Philips)

dSiPM - array of SPADs integrated in a standard CMOS process. Photons are detected and counted as digital signals using a dedicated cell electronics block next to each diode. This block also contains active quenching and recharge circuits, one bit memory for the selective inhibit of detector cells. A trigger network is used to propagate the trigger signal from all cells to the TDC.

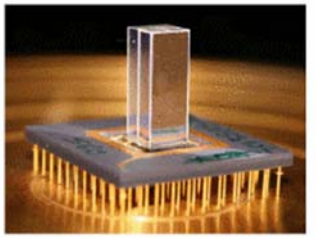

- 2x2 Array of 3x3x15mm³ LYSO
- 1:1 coupling using MeltMount
- Illuminated by ²²Na source
- Corrected only for saturation
- dE/E = 11% (combined)

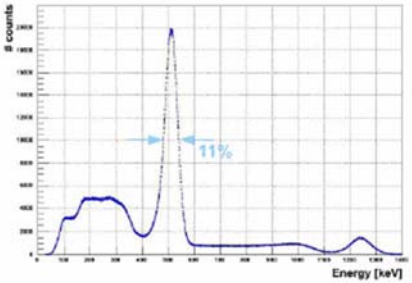

511 keV photon spectrum measured with dSiPM

gital SiPM – The Concept

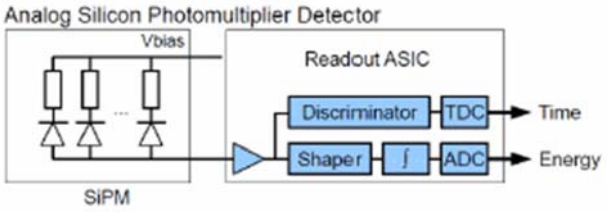

Digital SiPM – Test Chip Architecture

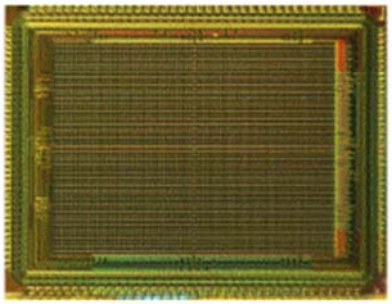

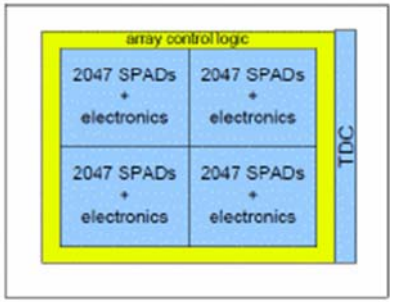

- Pixel composed of 4 identical sub-pixels with 2047 microcells each
- Microcell size 30µmx52µm, 50% fill factor including electronics
- A 1 bit inhibit memory in each microcell to enable/disable faulty diodes
- Active quench & recharge, on-chip memory and array controllers
- Integrated time-to-digital converter with σ = 8ps time resolution
- Variable trigger (1-4 photons) and energy (1-64 photons) thresholds
- Acquisition controller implemented in FPGA for flexibility and testing

(T. Frach, IEEE-NSS/MIC, Orlando, Oct. 2009)

Wojciech.Dulinski@ires.in2p3.fr

Present "hot topic": Vertical Integration (3D electronics)

It is generally referred as a technology to fabricate an electronics device (chip) comprised of 2 or more layers of active semiconductor devices that have been thinned, bonded, and interconnected to form a "monolithic" circuit.

Often the layers (sometimes called tiers) are fabricated in different processes and each layer can be individually optimized for different task (sensor layer, analog processing layer, digital layer, optoelectronics layer).

Industry is moving toward 3D to improve circuit performance (limited by interconnect): speed, power consumption, complexity.

This approach is also extremely promising for a new generation of 'monolithic' sensors…

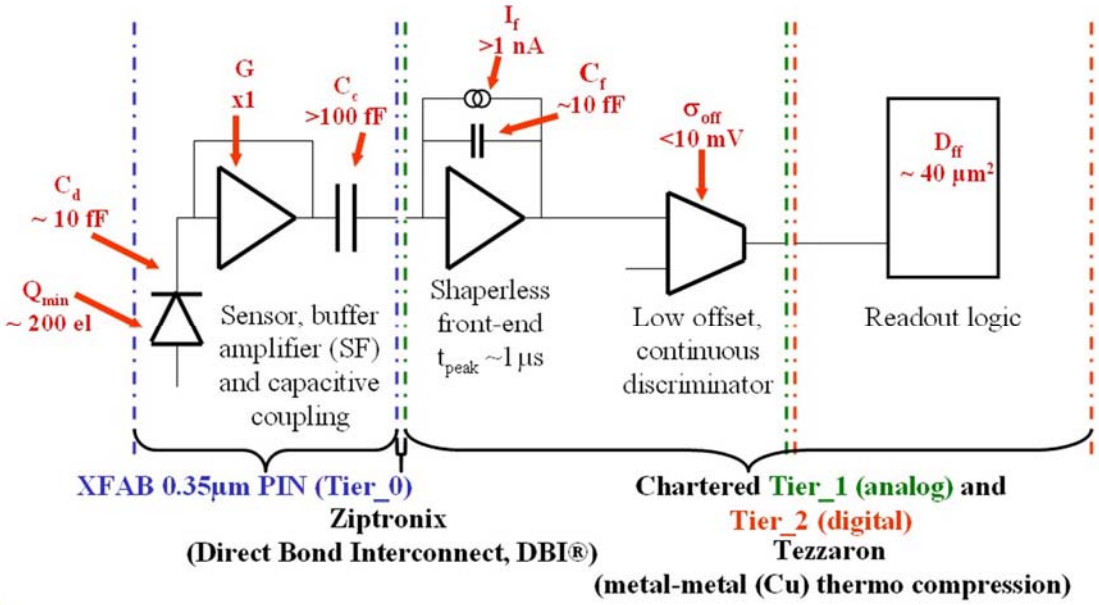

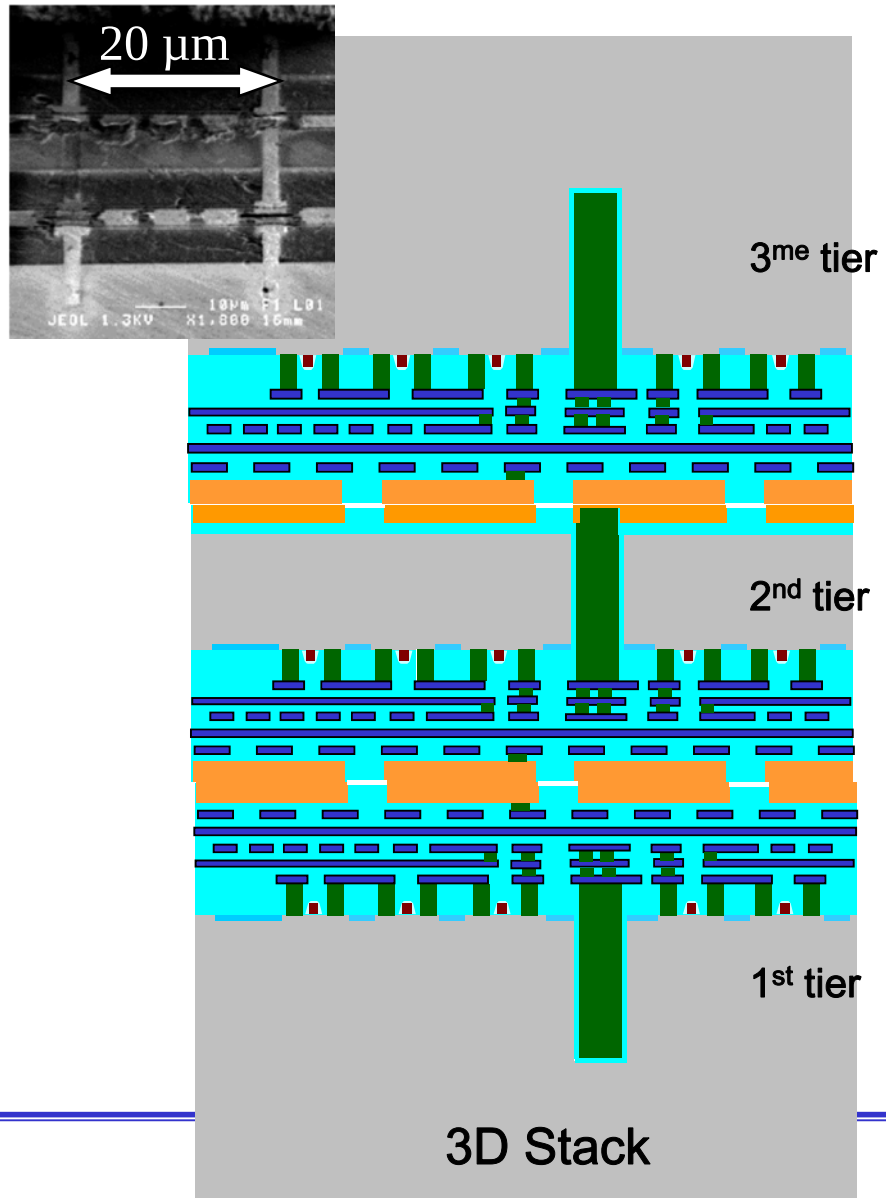

Heterogeneous 3D CMOS sensor (in progress)

Wojciech.Dulinski@ires.in2p3.fr

Another problem: how to construct the system without compromising detection performance? Mechanics, cooling, data transmission…

PLUME concept: double-sided ladder (ILC compatible)

- Array of Mimosa sensors
- Flex PCB: kapton + metal
- SiC foam for spacer between layers

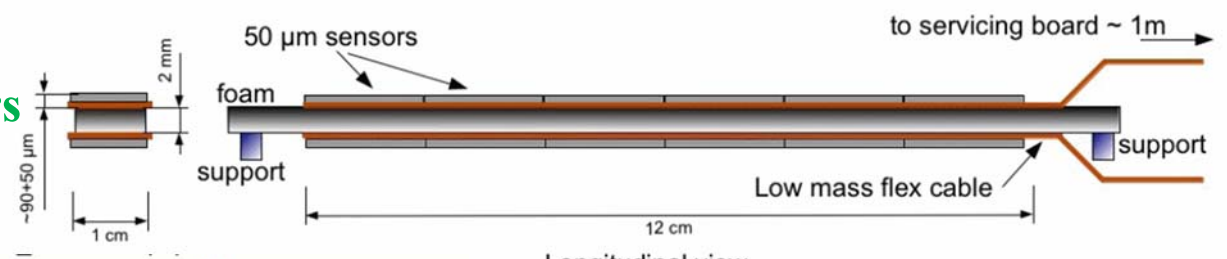

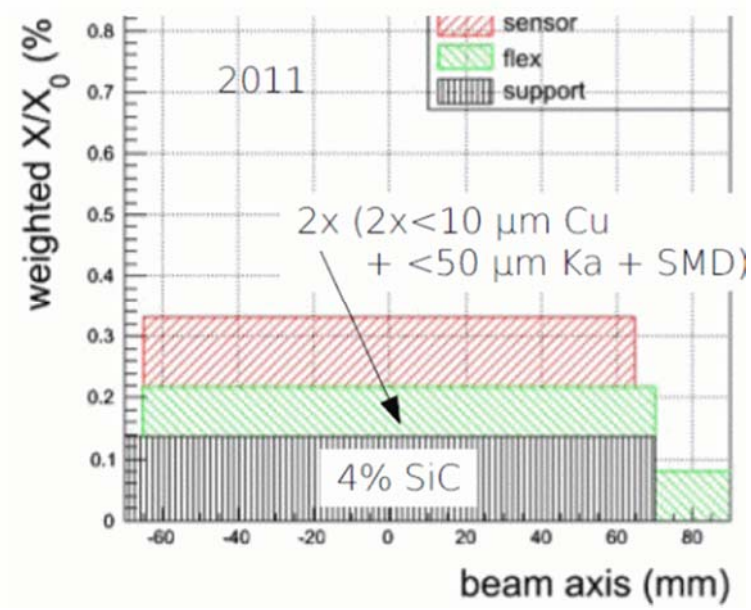

Plume-2011 material budget

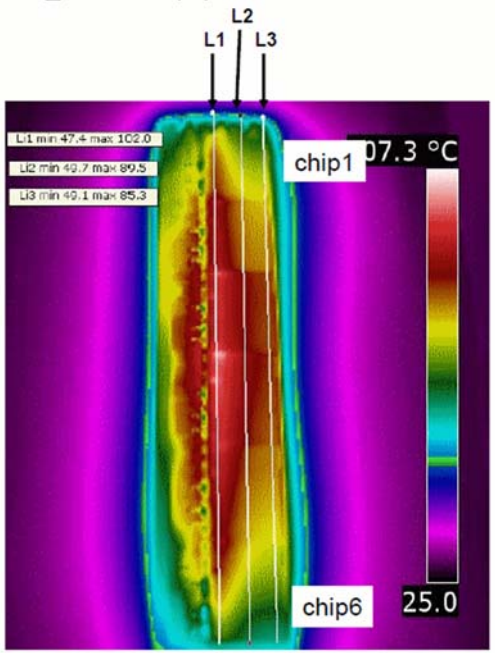

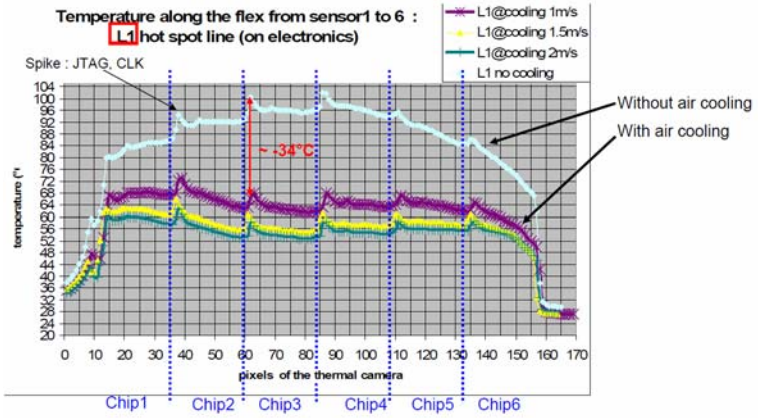

Temperature distribution (Plume-2010, air cooling)

Wojciech.Dulinski@ires.in2p3.fr

Novel packaging methods for ultra-thin monolithic sensors ladders construction: embedding in plastic foils

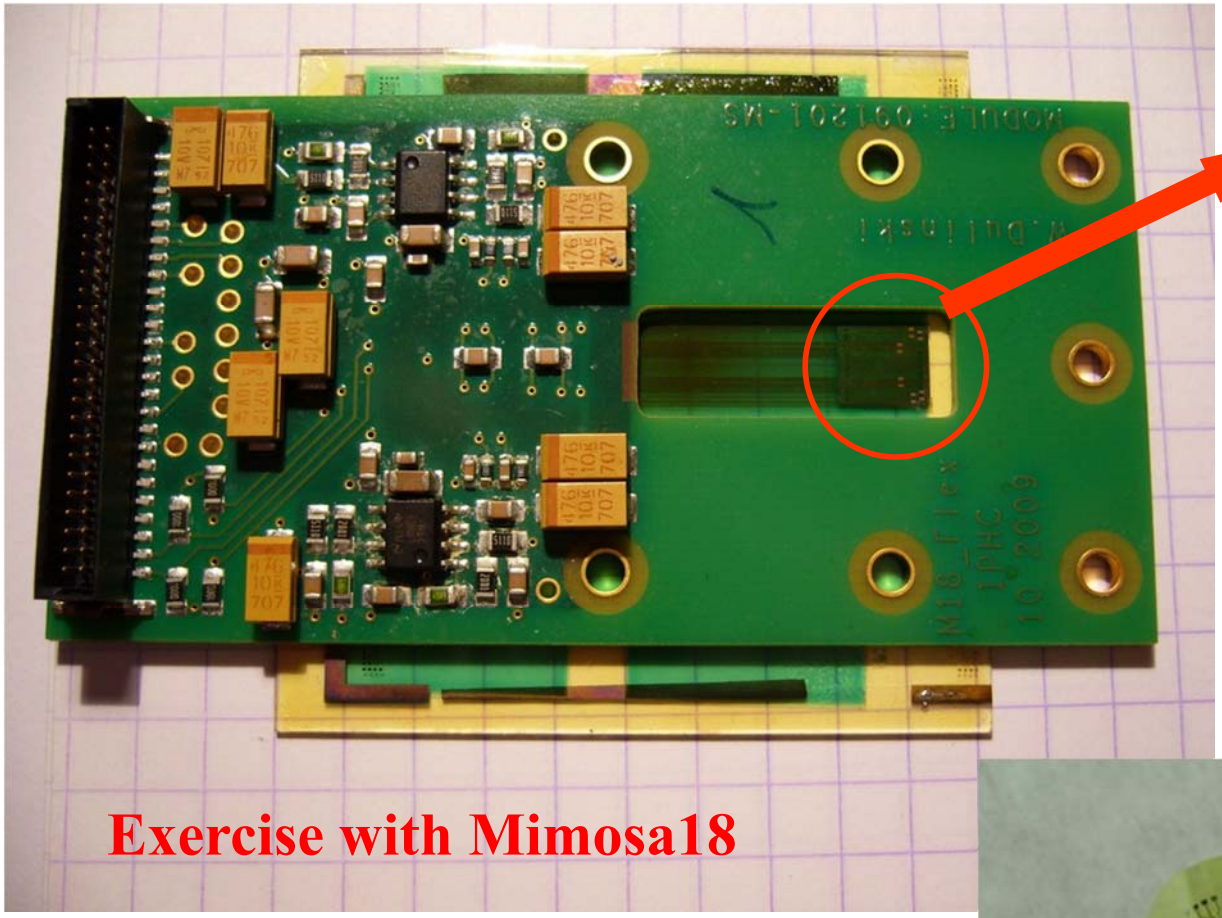

Exercise with Mimosa18

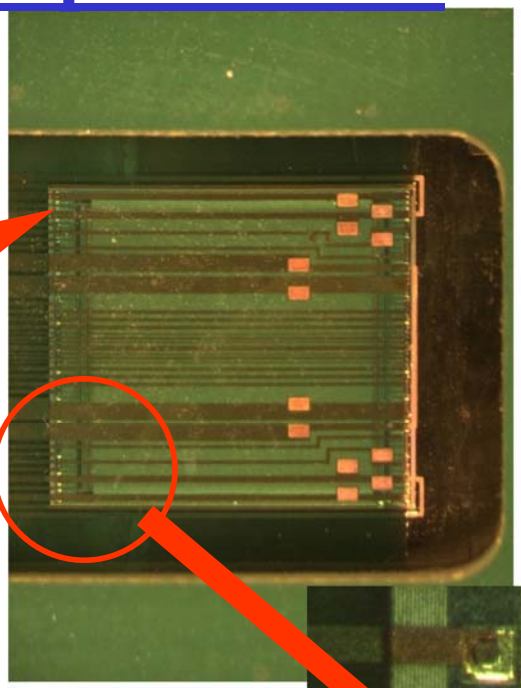

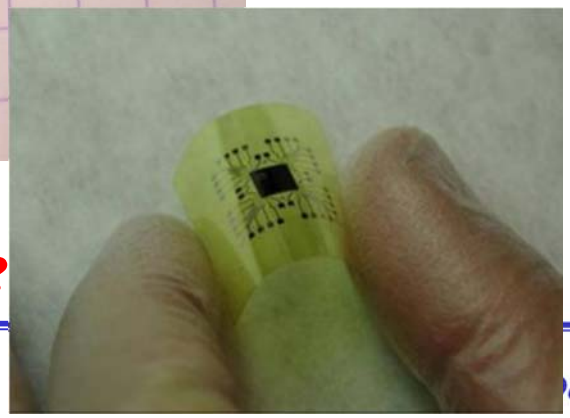

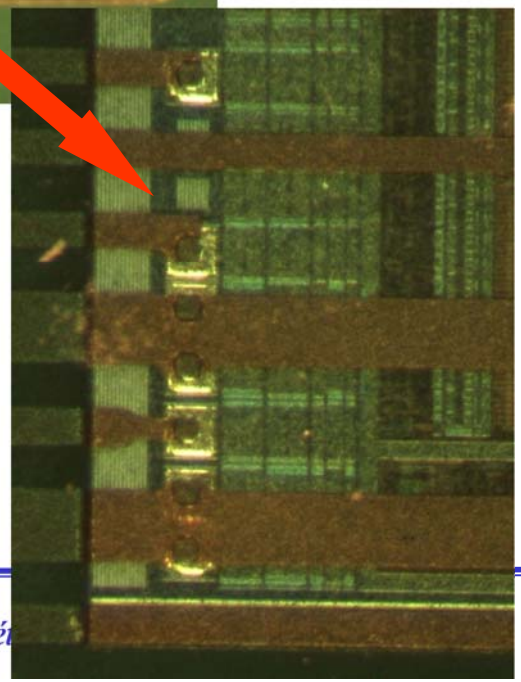

A way to allow tracker cylindrical layers?

Wojciech.Dulinski@ires.in2p3.fr

Conclusions

Les détecteurs à semi-conducteurs sont devenues les éléments incontournables dans les expériences de la physique subatomique, dans l'astrophysique et dans beaucoup des autres domaines…

La Vieille Perrotine

Merci pour votre attention!